

Insulin and Brain Injury: Memory, Metabolism and Microglia

by

Fiona Patricia Brabazon

Dissertation submitted to the Faculty of the
Neuroscience Graduate Program
Uniformed Services University of the Health Sciences
In partial fulfillment of the requirements for the degree of
Doctor of Philosophy 2016



FINAL EXAMINATION/PRIVATE DEFENSE FOR THE DEGREE OF DOCTOR OF PHILOSOPHY
IN THE NEUROSCIENCE GRADUATE PROGRAM

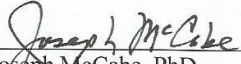
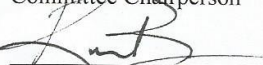
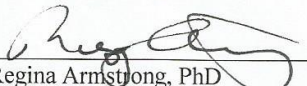
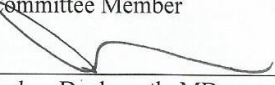
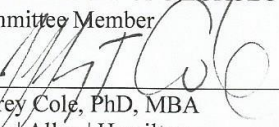
Name of Student: Fiona Brabazon

Date of Examination: April 1, 2016

Time: 1:00 PM

Place: A2074

DECISION OF EXAMINATION COMMITTEE MEMBERS:

	PASS	FAIL
 _____ Joseph McCabe, PhD DEPARTMENT OF ANATOMY, PHYSIOLOGY & GENETICS Committee Chairperson	<input checked="" type="checkbox"/>	<input type="checkbox"/>
 _____ Kimberly R. Byrnes, PhD DEPARTMENT OF ANATOMY, PHYSIOLOGY & GENETICS Dissertation Advisor	<input checked="" type="checkbox"/>	<input type="checkbox"/>
 _____ Regina Armstrong, PhD DEPARTMENT OF ANATOMY, PHYSIOLOGY & GENETICS Committee Member	<input checked="" type="checkbox"/>	<input type="checkbox"/>
 _____ Joshua Duckworth, MD DEPARTMENT OF NEUROLOGY Committee Member	<input checked="" type="checkbox"/>	<input type="checkbox"/>
 _____ Jeffrey Cole, PhD, MBA Booz Allen Hamilton Committee Member	<input checked="" type="checkbox"/>	<input type="checkbox"/>



UNIFORMED SERVICES UNIVERSITY, SCHOOL OF MEDICINE GRADUATE PROGRAMS
Graduate Education Office (A 1045), 4301 Jones Bridge Road, Bethesda, MD 20814

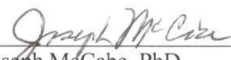


APPROVAL OF THE DOCTORAL DISSERTATION IN THE NEUROSCIENCE GRADUATE PROGRAM

Title of Dissertation: "The Effects of Insulin on Traumatic Brain Injury, Memory, Metabolism and Microglia"
Name of Candidate: Fiona Brabazon
Doctor of Philosophy
April 1, 2016

DISSERTATION AND ABSTRACT APPROVED:

DATE:


Joseph McCabe, PhD
DEPARTMENT OF ANATOMY, PHYSIOLOGY & GENETICS
Committee Chairperson

4-7-16


Kimberly R. Byrnes, PhD
DEPARTMENT OF ANATOMY, PHYSIOLOGY & GENETICS
Dissertation Advisor

4.7.16


Regina Armstrong, PhD
DEPARTMENT OF ANATOMY, PHYSIOLOGY & GENETICS
Committee Member

4-7-16


Joshua Duckworth, MD
DEPARTMENT OF NEUROLOGY
Committee Member

7 APR 16


Jeffrey Cole, PhD, MBA
Booz | Allen | Hamilton
Committee Member

4.7.16

ACKNOWLEDGMENTS

This dissertation is the result of tremendous team work. I am eternally indebted to all of the individuals who assisted me during the course of my graduate career. I would like to extend my gratitude to my extraordinary mentor, Dr. Kimberly Byrnes, for all of the time she spent training me. I am so thankful you agreed to take me on as your first graduate student. Your patience and support have been crucial to my success as a scientist

I would like to thank the members of my dissertation committee Dr. Joseph McCabe, committee chair, Dr. Regina Armstrong, Dr. Jeffery Cole, and Dr. Josh Duckworth. I am extremely appreciative of your time and valuable input into my experimental design.

You have pushed me to produce my best work and for that I am grateful.

I would like to thank the members of the Byrnes Lab past and present Yujia Zhao, Nicole Hockenbury, Sean Cooney, Guzal Khayrullina, Sara Bermudez, Ramona von Leden and John Yauger. I am so fortunate to have found a wonderful, supportive environment to conduct my research in.

I am very grateful for my productive collaboration with Dr. William H. Frey II.

I would like to thank the Graduate Education Office, Dr. Gregory Mueller and Dr. Arthur Kellermann for their role in my success during my time at the Uniformed Services University of the Health Sciences.

I greatly appreciate the assistance of Dr. Aryan Namboodiri and Jishnu Krishnan with the insulin ¹²⁵I study. I would like to thank Amanda Fu, Laura Tucker, and Jessica Ozl for their assistance with the CCI device, Morris water maze experimental set up and data analysis.

I am tremendously appreciative of all of the hard work of the Radiology department past and present including Dr. Reed Selwyn, Colin Wilson, Shalini Jaiswal, and Dr. Bernard Dardzinski.

I would like to thank the Cosmos Club Foundation for their generous grant which helped support this research. I also would like to thank the National Neurotrauma Society for the travel grant and an opportunity to present my data to and receive feedback from some of the best minds in the field.

Finally, I would like to thank my family and friends for their support.

DEDICATION

This dissertation is dedicated to my Mom, Dad and big brother, Dave. Words cannot express my gratitude for your unwavering love and support.

COPYRIGHT STATEMENT

The author hereby certifies that the use of any copyrighted material in the dissertation manuscript entitled: Insulin and Brain Injury: Memory, Metabolism and Microglia is appropriately acknowledged and, beyond brief excerpts, is with the permission of the copyright owner.

Fiona Patricia Brabazon

Fiona Patricia Brabazon

May 20, 2016

DISCLAIMER

The views presented here are those of the author and are not to be construed as official or reflecting the views of the Uniformed Services University of the Health Sciences, the Department of Defense or the U.S. Government.

ABSTRACT

Insulin and Brain Injury: Memory, Metabolism and Microglia

Fiona Patricia Brabazon, Doctor of Philosophy, 2016

Thesis directed by: Kimberly R. Byrnes, PhD

Department of Anatomy, Physiology and Genetics

Professor, Neuroscience Program

Traumatic brain injury (TBI) may result in long term learning and memory dysfunction. The cognitive deficits are the result of cellular and metabolic dysfunction that occurs after injury, including neuronal cell death, decreased cerebral glucose uptake and inflammation. To date, no therapeutic intervention has successfully addressed these post injury deficits. The goals of this study were to provide insight into the mechanism of post-injury cerebral metabolism, assess the ability of intranasal insulin to increase cerebral glucose uptake, memory and learning function after injury, and examine insulin's effect on microglia mediated inflammation.

Adult male Sprague Dawley rats were exposed to a moderate controlled cortical impact (CCI) injury or isoflurane and were sacrificed at 24 hours post procedure. The protein levels of glucose transporters (GLUTs) 1, 3, and 4 as well as insulin receptor (IR) were examined in the cortex, hippocampus, and cerebellum. No significant change in IR

or GLUT expression was observed in the ipsilateral cortex hippocampus, or cerebellum at 24 hours post injury compared to uninjured controls. To further examine the role of insulin after TBI, adult male Sprague Dawley rats were exposed to a moderate controlled cortical impact (CCI) injury followed by intranasal insulin or saline treatment beginning 4 hours post-injury and continuing with daily administration for 14 days. Positron emission tomography (PET) of fluorodeoxyglucose ($[^{18}\text{F}]$ -FDG) uptake was performed prior to injury and at 48 hours and 10 days post-injury. Motor function was tested using the beam and peg board walking test. Learning and memory function was assessed using the Morris water maze. Tissue was collected for assessment of macrophage and astrocyte activity.

Intranasal insulin treatment after CCI significantly improved several outcome measures in comparison to saline treated subjects. Insulin treated animals performed better on the beam walking task and demonstrated significantly improved memory function. In addition, a significant increase in $[^{18}\text{F}]$ -FDG uptake was observed in the hippocampus. Insulin treated animals also had significantly less microglial immunolabeling in the hippocampus after TBI. Microglia are the macrophages of the central nervous system (CNS), which function to monitor and maintain homeostasis. Prolonged microglia activation is detrimental to the CNS as they produce nitric oxide (NO), reactive oxygen species (ROS) and pro-inflammatory cytokines, resulting in neuronal cell dysfunction and death. We subsequently examined the effect of insulin administration on activated microglia *in vitro*.

BV2 microglia were exposed to a pro-inflammatory stimulus, lipopolysaccharide (LPS), and then treated with insulin. Outcome measures were conducted at 24 hours after

treatment. *In vitro* assays quantified NO and ROS production. Western blot and immunocytochemistry further evaluated the effect of insulin on microglia polarization markers. Insulin treatment significantly reduced NO and ROS production following LPS activation. Insulin treatment had no significant effect on any M1 or M2 microglia polarization markers examined. Insulin treatment also resulted in a reduction in two chemoattractants, JE/monocyte chemoattractant protein (MCP)-1 and macrophage inflammatory protein (MIP)-1A.

Together these data suggest that intranasal insulin improves memory, increases cerebral glucose uptake and decreases neuroinflammation, by reducing microglia NO and chemoattractant function. Therefore, intranasal insulin is a promising treatment for TBI.

TABLE OF CONTENTS

LIST OF TABLES	xv
LIST OF FIGURES	xvi
CHAPTER 1: Introduction	1
Brain injury	1
Statistics/demographics.....	1
Diagnosis and Classification.....	1
Imaging methods.....	3
Functional Outcomes of TBI	4
Controlled Cortical Impact	5
Functional outcomes of CCI.....	6
Pathological Outcomes of CCI	6
Glucose in the brain	7
Positron Emission Tomography (PET).....	9
Neurometabolic cascade of concussion	10
Insulin and the CNS.....	11
Neurons	11
Astrocytes	12
Microglia.....	13
Insulin and Brain injury	14
Intranasal Insulin.....	14
Previous Research.....	14
Mechanism of Delivery.....	14
Hypothesis.....	15
Specific Aims.....	15
CHAPTER 2: Intranasal Insulin Treatment of an Experimental Model of Moderate Traumatic Brain Injury	16
Abstract.....	18
Keywords:.....	19
Introduction.....	20
Methods.....	22
Study design.....	22
Moderate traumatic brain injury	24
Intranasal insulin treatment.....	24
Intranasal administration of [¹²⁵ I]-insulin	25
Blood glucose.....	25
Behavioral assays.....	26
Beam walking assay.....	26

Morris water maze	26
PET/CT with [¹⁸ F]-FDG imaging	27
PET/CT image processing	28
Tissue collection and processing	29
Statistics	30
Results.....	31
Moderate controlled cortical impact did not alter insulin receptor or glucose transporter expression	31
Intranasal insulin delivery did not alter blood glucose or weight.....	32
CCI injury does not inhibit intranasal insulin delivery to the central nervous system	32
Intranasal insulin treatment increased glucose uptake in the hippocampus	33
Intranasal insulin improved aspects of motor and cognitive function	34
Intranasal insulin treatment reduced microglia/macrophages in the hippocampus but not astrocytes.	36
Discussion.....	37
Acknowledgements.....	46
Author Disclosure Statement	46
Ethical Research Statement.....	46
Chapter 3: The effects of insulin on the inflammatory action and polarization of BV2 microglia	54
Abstract.....	55
Keywords	55
Introduction.....	56
Methods.....	58
Study Design.....	58
Treatments.....	58
Nitric Oxide measurement	58
Reactive Oxygen Species measurement	59
Immunocytochemistry	59
Protein Quantification.....	60
Oxyblot	60
Cytokine Panel	61
Statistical Analysis.....	61
Results.....	62
Insulin treatment significantly reduced NO and ROS production.....	62
Protein tyrosine nitration or protein carbonylation were not significantly altered by insulin.....	63
Insulin treatment did not significantly alter expression of an M1 markers, iNOS or CD86.....	63
Insulin treatment did not significantly alter M2 polarization marker expression.	64
Insulin treatment reduced the release of microglia chemoattractants.....	65
Discussion.....	66
Acknowledgements.....	70

Chapter 4: Discussion	76
Glucose transporters and Insulin receptor expression after CCI	77
TBI did not inhibit delivery of insulin along the intranasal pathway	79
Intranasal insulin administration improved cognitive function without Significant peripheral effects.....	80
Intranasal insulin treatment did not produce significant motor function improvement after CCI.....	81
Memory function improved with intranasal insulin treatment	82
Intranasal insulin significantly increased [¹⁸ F]-FDG uptake in the hippocampus	85
Cellular response to insulin treatment.....	86
Cellular response to insulin after TBI.....	86
Activated microglia response to insulin <i>in vitro</i>	88
Conclusions and future directions.....	89
Appendix 1: [¹⁸ F]FDG-PET Combined with Diffusion MRI Enhances the Detection of Traumatic Brain Injury in Rats	92
Abstract.....	95
Keywords	96
Introduction.....	97
Materials and Methods.....	99
Study Design.....	99
Moderate Traumatic Brain Injury	99
PET/CT imaging	100
MR Imaging.....	101
PET & MR Image Processing.....	101
Histology.....	102
Statistics	103
Results.....	103
The corpus callosum showed increased [¹⁸ F]-FDG uptake, increased T2, decreased ADC, and increased glial activation.	104
FDG uptake in the hippocampus is bimodal and is accompanied by elevated glial activity, increased T2 and decreased ADC.	106
The amygdala shows a dramatic decrease in [¹⁸ F]-FDG uptake after CCI in addition to small alterations in glial responses.	107
Discussion.....	108
Acknowledgements.....	113
Author Disclosure Statement	113
REFERENCES	120

LIST OF TABLES

Table 1. Animal cohorts and experimental outcomes.	23
Table 2. Experimental groups and timepoints for Appendix 1	99
Table 3. Summary of observations based on region of interest (*p<0.05, **p<0.01, ***p<0.0001, ****p<0.00001).....	104

LIST OF FIGURES

- Figure 1.** The timeline displays times at which animals underwent surgery, behavior training, PET/CT imaging and sacrifice. 47
- Figure 2.** The effect of moderate CCI on GLUT and IR expression. Tissue was collected 24 hours after moderate CCI(n=7) or isoflurane sham(n=7) for western blot quantification. The ipsilateral cortex showed no significant change in GLUT1(A), 3(B), 4(C) or IR(D) expression. There was a trend observed suggesting a decrease in IR that did not reach significance ($p=0.0939$, two-tailed t-test). The ipsilateral cerebellum showed a trend toward depression in GLUT 1(F) and a trend towards increased GLUT 3(G). There was no significant change in GLUT 4(H) or IR (I) expression in the cerebellum at 24 hours post injury compared to control. All proteins are normalized to loading control (GAPDH) and data are represented as mean +/- SEM. 48
- Figure 3.** Intranasal insulin delivery after CCI acts primarily in the CNS. The dose of intranasal insulin given was not sufficient to cause a significant change in blood glucose following CCI in intranasal insulin treated animals (n=4) compared to saline treated injured controls (n=4) as measured by tail vein blood draws at baseline, after injury/immediately prior to treatment and 3 hours after treatment (A). There was also no effect of intranasal insulin on body weight, measured through 21 days post-injury with 14 days of daily administration (n = 7/group injured n=4/group uninjured; B). CCI injury does not inhibit the pathway of intranasal administration to brain regions (C). There was no significant difference between the ipsilateral and contralateral brain region and insulin was detected in the olfactory bulb, cerebellum, brain stem, hippocampus and cortex 45 minutes after administration (n=4). 49
- Figure 4.** PET imaging of [^{18}F]-FDG reveals significant differences in uptake patterns following intranasal insulin treatment compared to intranasal saline treated animals after CCI (n=5/group). PET scans of [^{18}F]-FDG uptake were obtained with a CT for anatomical localization of brain regions. Uptake values from these regions were obtained by aligning a rat atlas to the scans. Regional analysis revealed that at 10 days post injury animals treated with intranasal insulin treatment following CCI had a significantly higher [^{18}F]-FDG uptake in the ipsilateral hippocampus (A) than at baseline ($*p=0.0329$) and 2 days post injury ($p=0.0189$) (2 way ANOVA, Sidak's post-test). 50
- Figure 5.** Intranasal insulin treatment after injury improves some aspects of motor function. After injury, both groups of animals (n=7/group) show a non-significant increase in footfalls indicating a deficit in motor function that recovers over time (A). However, animals treated with intranasal insulin after injury were able to cross the beam significantly faster than saline treated rats ($*p<0.05$; 2 way ANOVA, Sidak's multiple comparison test; B). Data are presented as an average of time and footfalls across the 4 widths of board the animals were trained to cross. Points represent mean +/- SEM. 51
- Figure 6.** Intranasal insulin treatment improved memory function in Morris water maze tests. Animals treated with intranasal insulin or saline did not find the platform more quickly over the course of the learning trials in either the injured or injured

cohorts (A) (n=6/group uninjured, n=10/group injured). However, during the probe trial, the injured animals treated with intranasal insulin (n=7) crossed the island location significantly more times (*p=0.033, 2 way ANOVA, Sidak's multiple comparisons test) than those treated with intranasal saline (n=8) (B). There was no significant difference in island crosses between the uninjured treatment groups (n=6/group). Search strategy utilized by rats during the probe trial was analyzed and categorized into one of 3 major groups (spatial, systematic, and looping) as previously described. (29) Representative patterns are shown (C), and number of animals utilizing each strategy during the probe trial was quantified. Saline and insulin treated uninjured animals (control) showed mostly spatial and systematic search strategies (D). A greater proportion of animals treated with saline after CCI showed a reduction in spatial search strategy and an increase in looping search methods. Likewise, fewer animals that received intranasal insulin for 14 days after injury displayed looping behavior than saline treated rats, and a return of spatial search strategy (p< 0.0001, Chi Square analysis). 52

Figure 7. Treatment with intranasal insulin after CCI reduces macrophage/microglia but does not significantly reduce astrocyte activation. Quantification of Iba1, a marker of microglia and macrophages, revealed a significant reduction (**p=0.0089, two-tailed unpaired t-test) (A) in cells in CA1 of the ipsilateral hippocampus in animals treated with intranasal insulin (C) compared to intranasal saline (B) (n=3 per group). Quantification of GFAP, a cell surface marker of astrocytes, did not show a significant difference (p=0.077, two-tailed unpaired t- test) (D) between insulin treated (n=4) (F) and saline treated animals (n=3) (E). 53

Figure 8. Insulin treatment significantly reduces NO production. BV2 microglia incubated with LPS showed a significant increase in NO production (Fig. 1A; p<0.0001, two way ANOVA) (A). Insulin treatment after LPS was able to significantly reduce NO production in BV2 microglia (p<0.05, one way ANOVA, multiple comparisons, Sidak's multiple comparisons test) (A). Insulin alone did not significantly alter NO release compared to control cells at any dosage. LPS significantly increases the production of ROS in BV2 microglia (p<0.0001, two way ANOVA) and insulin significantly alter ROS production (*p=0.0191, two way ANOVA) (B). Insulin reduced ROS production after LPS at 0.09µM (p=0.0497), 0.18µM (p=0.0319), 0.36µM (p=0.0173), and 0.72µM (p=0.0159). (One way ANOVA, multiple comparisons to LPS alone, Sidak's post test). All experimental conditions were repeated in triplicate. p value indicated by *p < 0.05. Bars are mean +/- SEM. 71

Figure 9. Insulin treatment did not alter protein nitrosylation or carbonylation. Protein tyrosine nitration was quantified using 3-NT antibody. Bands observed were pooled for quantification of total protein nitrosylation then normalized to loading control protein, GAPDH (B). There was no significant difference observed with 3-NT (A) between the treatment groups (n=3 per group). The Oxyblot assay did not detect a significant change in carbonyl groups introduced into proteins (Fig 2 C, n=3 per group). The entire lane was quantified for each protein sample and normalized to GAPDH (Fig. 2D). 72

Figure 10. Insulin treatment does not reduce expression of M1 polarization markers, iNOS and CD86. Insulin treatment did not alter expression of CD86 after LPS or in

controls as measured by western blot (n=3 per group) (A). LPS exposure resulted in a non-significant increase in CD86 expression (A). Representative bands of CD86 and GAPDH are displayed as a stitched image (B). iNOS expression was not altered in cells treated with insulin after LPS compared to LPS alone (C) as measured by immunocytochemistry. A significant effect of iNOS was observed with LPS treatment (p=0.0099, 2 way ANOVA). Bars are mean +/- SEM..... 73

Figure 11. Insulin treatment does not alter expression of M2 polarization markers YM1 and CD206. Insulin treatment did not alter expression of YMI after LPS as measured by western blot (n=3/ per group) (A). LPS exposure resulted in a significant decrease in YM1 expression (p=0.0493, 2 way ANOVA) (A). Representative bands of YM1 and GAPDH are displayed as a stitched image (B). CD206 expression was not altered in cells treated with insulin after LPS compared to LPS alone (C) as measured by immunocytochemistry (D). Bars are mean +/- SEM 74

Figure 12. Insulin treatment reduces the release of microglia chemoattractants. A panel of cytokines show a significant increase in IL-1a (****p<0.0001 LPS vs control; **p<0.01 LPS/Insulin vs. control, 2 way ANOVA, Tukey's post test; A) and IL-1B (**p=0.0027 LPS vs. control and insulin alone, 2 way ANOVA, Tukey's post test) following LPS exposure (B). Insulin significantly reduced the release of JE (C), a microglia chemoattractant, after LPS treatment (*p= 0.0116, 2 way ANOVA, Tukey's post test, n=3 per group). Insulin treatment also significantly reduced the expression of MIP-1A (D) following LPS exposure (*p=0.0131, 2 way ANOVA, Tukey's post test, n=3 per group) as it was also elevated in LPS treated cells compared to controls. Bars represent mean +/- SEM. 75

Figure 13: A graphical representation of the pathways examined in this dissertation. ... 90

Figure 14. Location of regions of interest. Figure A depicts the regions analyzed for histology in a GFAP (green) stained section: 1) corpus callosum, 2) hippocampus, and 3) amygdala. These regions are analogous to those in the atlas produced by VivoQuant (B) for analysis of FDG-PET (C) and MRI (D) scans. 114

Figure 15. FDG uptake, T2, ADC values (A-C), normalized to baseline (1.0 = normal), and histology values (D-E) are presented for the ipsilateral corpus callosum. FDG uptake measurements showed a significant increase on 3 and 11 dpi (A). T2 values were elevated at days 8 and 10 in the ipsilateral corpus callosum (B). ADC values were significantly increased at 8 dpi in the corpus callosum (C). *p<0.05, **p<0.01, ***p<0.0001, ****p<0.00001. Density of GFAP immunostaining was quantified (D), and showed a significant increase in the corpus callosum at 4 days. Representative images of astrocytes, visualized using GFAP antibody, in the corpus callosum in naïve, 2 and 4 dpi tissue. Density of Iba1 immunostaining was quantified (E) and showed no significant elevation after injury due to high variability in tissue. Representative images of microglia, visualized using Iba1 antibody, in the corpus callosum is shown in naïve and at 8 and 12 dpi. Tissue was collected 24 hours after terminal PET scan **p<0.01 vs naïve. Size bar = 300µm. Bars represent mean +/- SEM. 115

Figure 16. FDG uptake, T2, and ADC values (A-C), normalized to baseline (1.0 = normal), and histology values (D-E) in CA1 are presented for the ipsilateral hippocampus. FDG uptakes (A) were significantly increased from baseline at the

acute (3 hours) and chronic stage (20 days) post injury in the ipsilateral hippocampus. In contrast, T2 values (B) were elevated at days 4, 8, 10 and 20 in ipsilateral hippocampus. ADC values (C) were significantly depressed at 2, 4 and 20 dpi in the ipsilateral hippocampus. * $p < 0.05$, ** $p < 0.01$, *** $p < 0.0001$, **** $p < 0.00001$. GFAP density was quantified and showed an overall increase in the hippocampus following CCI injury that did not reach significance (D).

Representative images of astrocytes in CA1 of the hippocampus from naïve, 8 and 21 dpi tissue are shown. Microglia/macrophage activity was quantified and showed a slight but not significant increase in the hippocampus following CCI injury (E). Representative images of microglia in CA1 of the hippocampus are shown from naïve, 1 and 8 dpi tissue. Size bar = 300 μm (D), 200 μm (E). 116

Figure 17. FDG uptake, T2, and ADC values (A-C), normalized to baseline (1.0 = normal), and histology values (D-E) are presented for the ipsilateral amygdala. FDG uptakes were significantly decreased compared to baseline at 3 and 7 dpi in the ipsilateral amygdala (A). T2 values were significantly elevated at 4 and 8 dpi (B). ADC values were significantly reduced at 2, 4, 8 and 21 dpi (C). * $p < 0.05$, ** $p < 0.01$, *** $p < 0.0001$, **** $p < 0.00001$. Density of GFAP immunostaining was quantified (D) and showed no significant change in astrocyte activity at any time point in comparison to naïve tissue. Representative images of astrocytes in the amygdala are shown for naïve, 1 and 21 dpi tissue. Iba1 immunostaining was quantified (E), and showed no significant change in microglia presence at any time point. Representative images of microglia in the amygdala are shown for naïve, 1 and 21 dpi tissue. Size bar = 300 μm 117

Figure 18. Representative images of neurons in the amygdala. NeuN immunolabeling was performed 24 hours after PET imaging at 1, 2, 4, 8, 12, and 21 dpi. NeuN in the amygdala is lost acutely with no change in DAPI staining at any time point but NeuN staining is partially recovered by 8 days. Bar = 50 μm 118

Supplementary Figure 19. FDG uptake, T2 and ADC values normalized to baseline values (post-injury/baseline, normal = 1.0) for the corpus callosum (A), hippocampus (B), and amygdala (C) for whole region as well as ipsilateral and contralateral regions. Statistical significance provided for two-way ANOVA without baseline normalization. * $p < 0.05$, ** $p < 0.01$, *** $p < 0.0001$, **** $p < 0.00001$ 119

CHAPTER 1: Introduction

BRAIN INJURY

Statistics/demographics

Traumatic brain injury (TBI) is a serious public health problem that has gained increased attention in recent years. Each year in the United States, TBI results in about 2.2 million hospital visits and almost 50,000 deaths. (70, 128) The most common causes of TBI emergency room (ER) visits and deaths as reported by the Center for Disease Control and Prevention (CDC) based on data collected from 2002-2010 in the United States were falls, motor vehicle accidents and assaults. The majority of TBI injuries occur in young males ages 15-24. (2) Males are twice as likely to sustain a head injury as females. (2) There are a significant number of documented cases in females and geriatric populations as well. (273) Studies have estimated that TBI care for a mild injury costs more than \$30,000 per case for acute treatment and the cost to treat increases with moderate and severe injury. (110, 158, 212) This results in an estimated annual cost to society of \$30 billion. (108)

Diagnosis and Classification

TBI has been defined by the Brain Injury Association of America (BIAA) as an injury to the brain that results in an alteration in brain function as a result of an external force. (34, 211) The term TBI covers a broad range of injuries. Therefore, several important factors are considered when classifying an injury. (215) The first two major categories are penetrating, a scenario where the skull/brain is penetrated by an object, and

closed, where the skull remains intact. (215) Injuries are typically classified as one of three levels of severity: mild, moderate and severe.

The categorization of an injury with this severity scale typically relies on diagnostic criteria used in the ER. (34) The first tool used for the diagnosis of TBI is the Glasgow coma scale (GCS). The GCS is a non-invasive examination of level of consciousness. The GCS was developed in 1974 and is used as a tool to assess coma and states of impaired consciousness. (248) The scale assigns a score to an individual's level of consciousness based on behavior and responsiveness with a range from 3-15. The GCS examines motor response, verbal response and, eye opening. (248) Diagnosis also depends on a general assessment of loss of consciousness (LOC), post-injury antero- or retrograde amnesia and altered mental state. (211) Altered mental state is a broad term that can include symptoms such as dizziness and confusion. (34, 211)

The classification of TBI based on a GCS score of 13 to 15 is a mild injury, 9 to 12 for a moderate injury, and 8 or less for a severe injury. (128, 147) According to CDC data, more than 75% of TBI are considered mild. (1) Mild TBI is characterized by the loss of consciousness (LOC) not to exceed 30 min, post-injury antero- or retrograde amnesia not exceeding 24 hours, or altered mental state (confusion, dizziness, etc.) not exceeding 24 hours. (211) Patients with a mild TBI generally have a GCS score between 13–15 and no significant findings on MRI or CT. (111) Moderate and severe TBI patients are more likely present with visible abnormalities on CT and MRI scans. Some image abnormalities can be attributed to skull breaks and bleeds which can lead to a significant increase in intracranial pressure. Moderate TBI results in traumatic intracranial hematomas in 5-10% of patients compared to 25-35% of severely injured

patients. (147) Patients presenting with lesions on computerized tomography (CT) had over a 50% chance of high intracranial pressure.(205, 224) Intracranial pressure after TBI can result in ischemia and cerebral herniation. (264) A severe TBI diagnosis based on GCS score alone correlates with a significant likelihood of long term neurological disorders or death as a result of the injury. (160, 197)

Imaging methods

In addition to physical clinical examination, clinicians utilize *in vivo* imaging for diagnosis of brain injury severity. CT is the most widely used and least expensive imaging tool. (125) CT can easily identify contrast between bone and tissue so it is often used to identify damage to the skull following a TBI. Additionally, a CT scan can detect acute subarachnoid or acute parenchymal hemorrhage. (125, 282) A subarachnoid hemorrhage after TBI is the result of blood vessels tearing and leaking into the subarachnoid space (13, 276) whereas, a parenchymal hemorrhage bleeds into the parenchyma. (123, 183)

Magnetic resonance imaging (MRI) is considered superior to CT as it provides more information about the brain's anatomy and vascular function than CT. MRI produces images by magnetic pulses that spin the hydrogen atom of water molecules present in tissue. (61, 277) The machine detects differences in the signal produced and generates images based on this information. There are several types of MRI image acquisition and processing methods that can contribute different types of information about the nature of a TBI. (64) T1 and T2 imaging create anatomical images that can distinguish between fatty composite tissue, such as myelin, and fluid, such as cerebrospinal fluid (CSF). (64, 164) The scans can detect differences in the density of

fatty tissue allowing for detailed images of brain structures. (135) Additionally, T1/T2 MRI images can show blood- brain barrier (BBB) disruption after TBI. (135) Diffusion weighted MRI imaging (DWI) examines the diffusion of water within the tissues. This provides important information in TBI as this movement of water will be altered by changes in the tissue as a result of injury. Diffusion tensor imaging (DTI) MRI is a type of DWI that provides information about white matter connectivity patterns in the brain. (3, 48) This includes the ability to detect diffuse axonal injury (DAI) after TBI. (101) CT and MRI are currently the standard imaging modalities used for diagnosis of TBI. CT and MRI lack sensitivity for the detection of minor injuries. Therefore, current work has shifted toward developing more sensitive, functional imaging methods like positron emission tomography (PET), which is discussed in more detail later in this chapter.

FUNCTIONAL OUTCOMES OF TBI

TBI can result in a variety of cognitive deficits depending on the location and severity of injury. The most common, and most relevant to the research of this dissertation, cognitive deficits after TBI are disturbances in learning and memory function. (145, 175) Up to 15% of individuals with a mild TBI report deficits with cognitive function a year after injury. (210) These cognitive impairments can manifest as retrograde amnesia, resulting from deficits in memory retrieval, or anterograde amnesia, resulting from deficits in task acquisition. (272) Learning and memory function are hippocampal dependent functions. (124, 222) Significant hippocampal atrophy is often observed following severe TBI. (20, 119, 159, 257)

While memory and learning dysfunction after TBI are the primary focus of this dissertation, it is important to briefly mention some additional deficits following injury.

These include alterations in mood, seizures and sleep dysfunction. Depression is observed in 18% of TBI patients of all injury severity levels and anxiety is present in about 22%. (260) The likelihood of presenting with depression or anxiety after TBI increases with injury severity. (260) Sleep dysfunction is a common complaint following TBI and patients can present with a number of issues including insomnia, excessive daytime sleepiness, hypersomnia and circadian rhythm disturbances. (14, 155, 179, 240) TBI induced epilepsy is thought to contribute to about 4-9% of all epilepsy cases. (6, 11, 96, 149) The risk of seizure within the first 6 months after severe TBI is 50 times higher than control and, while lowered over time, patients remain at risk for seizure up to ten years after injury.(11, 149) A number of pre-clinical models of TBI have been developed and successfully replicate the clinical findings following TBI. These model injury systems provide researchers with a valuable tool for the examination of the cellular pathology of TBI and effects of potential therapeutic interventions.

CONTROLLED CORTICAL IMPACT

TBI is studied in a pre-clinical setting using a variety of models. The controlled cortical impact (CCI) injury delivers a direct injury to brain using a piston (59, 188). The CCI model has been well-characterized over the last 20 years and the model has proven to be a valuable research tool for many reasons. The parameters by which the piston strikes the brain (speed, deformation depth, and dwell time) can be easily adjusted and correlate with functional and somatosensory outcomes. (188) Higher levels of injury produce a distinct cavitation (or lesion) at the site of injury along with axonal damage. (59, 161)

Functional outcomes of CCI

CCI replicates a number of behavioral deficits and pathological outcomes observed in human TBI. These deficits include learning and memory dysfunction which are typically studied in rodents with the Morris water maze (MWM) or Barnes maze. CCI causes dysfunction in spatial memory, as measured by MWM, which may persist for up to a year following injury. (60, 271) Similarly, mice tested with the Barnes maze after CCI showed spatial learning impairment after injury compared to sham controls. (74) Motor function performance is also damaged by CCI, particularly when the injury coordinates lie over the supplementary motor and parietal lobe as is the case for data presented in Chapter 2. (199) Motor function can be assessed using a number of experiments, including rotarod and beam walking task. CCI results in motor function deficits that manifest as decreased latency to fall on rotarod and increased time and foot falls on the beam walking task. (199)

Pathological Outcomes of CCI

These observed behavioral deficits following CCI injury are a result of tissue damage and cellular response to injury. Due to the direct impact of the piston to the brain in the CCI model a measurable lesion can develop at the site of impact. This lesion can be measured longitudinally with MRI or in post mortem tissue. (139, 186) Neuronal death occurs after CCI. (47) There is necrotic neuronal cell death as a direct result of the injury. (47, 86) CCI also results in diffuse axonal injury, another common pathology observed in human TBI, (161) with widespread tearing of axons and small vessels by shearing forces. (193)

Neuronal cell death can result from the initial impact and also the prolonged inflammatory response that is triggered by injury and mediated by glial cells, astrocytes and microglia. Astrocytes and microglia primarily function in the maintenance homeostasis of the CNS. CCI injury results in an increased number of microglia and astrocytes. Following injury or infection, astrocytes become activated which results in cellular proliferation. (39, 172) Astrocytes function to clear glutamate after injury but their prolonged activation is detrimental to recovery as they produce excess cytokines and form the glial scar. (172) Prolonged microglia activation is observed after CCI and correlates with neuronal cell death observed after injury. (38) Microglia and their inflammatory response are discussed in greater detail in subsequent sections.

GLUCOSE IN THE BRAIN

The brain is the most metabolically active organ of the body and has the highest glucose demand. It consumes about 60% of the total body glucose intake and makes up only 2% of the total body weight. (66, 162, 198) Glucose enters the brain through glucose transporters. Glucose transporters (GLUTs) are primarily divided into two groups, sodium independent and sodium dependent. (228) The GLUTs of the brain are both sodium independent and sodium dependent. (228) GLUTs can also be characterized by whether they are insulin sensitive/dependent, meaning their expression is increased with insulin, or insulin insensitive/independent, meaning they are constitutively expressed regardless of insulin. (112) The GLUTs present in the brain are GLUT 1, 2, 3, 4 and 5. (27, 157)

The BBB is densely packed with GLUT 1, an insulin insensitive transporter. (192) GLUT1 allows the passage of glucose from the blood to the brain at high volumes using a

facilitated diffusion system. (184) GLUT 1 has been identified on all cell types of the brain. (148) iNOS expression, a marker of inflammation, correlates with significantly decreased cerebral GLUT1 expression suggesting a correlation between glucose and inflammation. (201, 244) GLUT 2 is considered the “glucose sensing” GLUT isoform and is only found in select neuronal populations of the hypothalamus. (130, 157)

GLUT3 has the lowest K_m (Michaelis-Menten constant) of the GLUTs, a property that allows it the highest affinity for available glucose. (32) GLUT3 is most highly expressed on neurons, a pattern observed in both humans and rodents. (126, 152) Extended insulin-induced hypoglycemic episodes result in a significant increase in GLUT3 expression on neurons. (254) These combined facts demonstrate the evolutionary traits that allow for preferential distribution to neurons in times of low glucose availability. In addition, knockout studies have shown that homozygous mutants for GLUT 1 and 3 are embryonic lethal, but heterozygous mutants survive and present with significant CNS deficits, including reduced brain size and significant cognitive deficits. (81, 266) GLUT4 is the insulin sensitive transporter of the brain. (261) Insulin causes the translocation of GLUT4 transporters from their basal, intracellular location to the plasma membrane which allows for increased glucose transport into cells. (230, 261) GLUT4 expression has been identified on neurons, microglia and astrocytes. (7, 171) Studies of GLUT4 also provide insight into the relationship between insulin and inflammation. Previous work has shown that treatment of macrophages with TNF- α produced a significant reduction in GLUT4 protein and a minor reduction in insulin receptor (IR). (146, 237) GLUT5 is primarily a transporter of fructose and exclusively expressed on microglia. (195)

Positron Emission Tomography (PET)

Positron emission tomography (PET) uses a radiation detection machine to generate images based on the location of a systemically administered radioactively labeled compound. (34) PET has a broad range of uses because it can non-invasively image any biological compound that can be radioactively labeled. This allows for longitudinal scans and more specific information about biological processes. There are a number of different PET tracers. Fluorodeoxyglucose (^{18}F)-FDG is one of the most commonly used PET tracers. ^{18}F -FDG is a radioactive glucose analog that is manufactured by replacing the hydroxyl group on the 2-carbon of a glucose molecule with a fluoride atom. (285) It circulates throughout the body and is processed in a similar way to glucose once it enters the cell. (208) The important difference between glucose and ^{18}F -FDG is that once the deoxyglucose (DG) is phosphorylated by hexokinase it is not further metabolized, becoming trapped in the cell with a slow clearance rate. (208, 285) This allows for quantification of the ^{18}F -FDG accumulation in brain tissue in proportion to glucose uptake using PET imaging.

PET is not widely used in the diagnosis of TBI, as it is cost prohibitive, but it is increasingly used in clinical and pre-clinical studies. (for review: (34)) ^{18}F -FDG PET imaging has provided important information about the neurometabolic crisis following TBI. Animal studies using 2-DG autoradiography identified specific regions of reduced glucose uptake but these are terminal studies. (202) 2-DG autoradiography provides higher resolution than PET but PET can be used for longitudinal studies and autoradiography cannot. This allows one to monitor the effects of treatment using a clinically relevant tool.

Neurometabolic cascade of concussion

Glucose plays a crucial role in normal brain function and any disruption in delivery can be detrimental. A number of neurological conditions result in decreased brain glucose perturbations, including Alzheimer's disease and TBI. The neurometabolic cascade of concussion, a phrase coined by Hovda and Giza (83), refers to the cellular metabolic response that persists for days to years after brain injury. Acutely after injury, hyperglycolysis is observed as cells utilize ATP-requiring membrane ionic pumps in an effort to restore ionic and cellular homeostasis. (84, 283) Following this initial burst of energy, the brain enters a hypometabolic state that can last for days to weeks after injury in pre-clinical models. (283) Regional cerebral hypometabolism has been observed in patients up to years after injury and is associated with cognitive and behavioral deficits. (34, 88) One pre-clinical study provides evidence that glucose plays a crucial role in facilitating repair after brain injury. The period of cerebral hypometabolism is also a period of increased vulnerability to injury. (202, 227)

Animal models of TBI appropriately replicate the neurometabolic cascade of concussion. A mild lateral fluid percussion (LFP) injury results in global cerebral hypometabolism that persists from three hours to nine days post injury. (226) Appendix 1 contains a manuscript describing the [¹⁸F]-FDG uptake profile after moderate CCI that provided the preliminary data for the data presented in this dissertation. These data show, similarly to the LFP model, CCI results in a significant hypermetabolic response in the hippocampus at 3 hours post injury which returns to baseline by one to ten days post injury (Appendix 1 Fig. 16A). Additionally, a significant decrease in glucose uptake is observed in the amygdala from days three to seven post injury and returning to baseline

by day ten (Appendix 1 Fig.17A). These data show that CCI is a good model to test therapeutic interventions targeting the metabolic crisis following TBI.

INSULIN AND THE CNS

Insulin is a large molecule (5808 Da) and its passage into the brain is tightly regulated by saturable insulin transporters on the BBB. Insulin receptors (IR) are expressed on neurons, microglia and astrocytes. (44, 235, 256) While it has been shown that select neurons can produce insulin de novo (216, 217) the majority of insulin in the brain is from the blood. The ability of neurons to synthesize insulin in the absence of insulin suggests a necessary role of insulin in normal function and development. This idea is exemplified by Alzheimer's disease pathology. Alzheimer's disease results, most notably, in memory and learning dysfunction as a result of an accumulation of insoluble beta amyloid plaques in the brain. (225) Additionally, studies have shown that Alzheimer's disease presents with its own neurometabolic response prompting some researchers to refer to Alzheimer's disease as "type 3 diabetes". (54) This term refers to the cerebral insulin resistance and reduction in glucose metabolism observed in Alzheimer's disease. (107) These data have lent themselves to a more in depth examination of the effect of insulin on cell populations of the CNS beyond the GLUT response.

Neurons

The ability of neurons to synthesize insulin when deprived of it suggests it plays a crucial role in normal neuronal function. The role of insulin in neuronal function has been reasonably well studied. Insulin increases neuronal glucose uptake by increasing the translocation of GLUT 3 from the cytosol to the membrane. (255) Insulin promotes

neurite growth and formation by promoting α and β tubulin production, suggesting a crucial role in neurodevelopment and maintenance. (163, 259) Insulin essentially acts as a neurotrophic factor as it has been repeatedly shown to support neuronal survival in a manner separate from its metabolic influence. (214, 245, 259) There is an increase in insulin receptors in synapses of the hippocampus following a short term memory task. (288) Insulin's role in memory function is supported by its ability to regulate the endocytosis of AMPA receptors, thus playing a role in synaptic function and long term depression (LTD). (109, 151) Together, this shows that neurons respond to insulin not only with increased GLUT expression but also with increased markers of survival and function including neurite outgrowth, tubulin formation and synaptic function.

Astrocytes

The role of insulin in glial populations is significantly less studied than the neuron-insulin relationship. This may be attributed to the significantly higher expression of IR on neurons than on glia. (16, 78) Nevertheless, an understanding of glial activity in response to insulin is crucial. Astrocytes are glial cells that outnumber neurons in the brain. (196) Astrocytes play a crucial role in neural transmission by clearing glutamate from the synaptic cleft. (5, 196) After injury, they adopt an activated phenotype which produces reactive oxygen species (ROS), excess cytokines and forms the glial scar. (172)

The relationship between insulin and astrocytes has predominantly been studied in the context of metabolism and appetitive behavior. (30) Insulin promotes glycogen storage in astrocytes. (98) Glycogen is a repository for stored glucose. (30) Neurons lack glycogen stores so this characteristic of astrocytes lends itself to a cooperative metabolic relationship between astrocytes and neurons. (for review: (68)) Astrocytes

have been shown *in vitro* to respond to insulin at low doses (1nM) with increased production of IL-6 and IL-8, pro-inflammatory cytokines, but this effect dissipates at higher doses (100 nM), suggesting that insulin plays a role in astrocyte inflammatory response as well as glycogen storage. (235)

Microglia

Microglia are the resident macrophage of the CNS. (187) Microglia comprise about 10-15% of the cells of the CNS. (36) Microglia are different from the macrophage of the periphery because they are derived from the yolk sac as opposed to the bone marrow. (187, 194) This developmental source suggests some differences in functions but there are a number of conserved properties across the two cell types. Microglia are responsible for sensing and maintaining homeostasis in the CNS. (120, 180, 253) Following an environmental stimulus, microglia adopt a series of different physical phenotypes ranging from pro-inflammatory (M1) classical activation to anti-inflammatory (M2) alternative activation. (87, 140, 187) M1 activated microglia produce nitric oxide (NO), reactive oxygen species (ROS) and a number of pro-inflammatory cytokines. (173) Additionally, microglia release chemoattractants, such as monocyte chemoattractant protein (MCP-1), that draw more microglia to the site, increasing the inflammatory response. (56, 102, 281) The M2 phenotype produces anti-inflammatory cytokines and can be neuroprotective. (41, 236)

The effect of insulin on peripheral macrophages has been studied extensively, particularly in the context of obesity and diabetes. (185) Individuals with insulin resistance and diabetes have high levels of the pro-inflammatory cytokines produced by macrophages, TNF α and IL-6. (185, 243) Insulin treatment can significantly reduce

inducible nitric oxide synthase (iNOS) expression and NO production in peripheral macrophages. (238) One study has specifically examined the effects of insulin on microglia and showed reduced production of MCP-1 but increased interleukin-8 (IL-8) with insulin treatment of activated microglia. (235)

Insulin and Brain injury

Hyperglycemia is a common occurrence after TBI and a predictor of poor neurological outcome. (249, 284) Additionally, diabetic patients have a significantly higher risk of mortality after TBI. (131) Markers of insulin resistance are associated with higher rates of mortality in TBI patients. (170) This has led to some examination of insulin treatment after TBI. Hyperglycemia after TBI is typically treated with intravenous insulin in an effort to maintain tight glycemic control. (258) This typically results in more favorable outcome than loose glycemic control. (21, 279)

Intranasal Insulin

Previous Research

As previously mentioned, Alzheimer's disease also presents with cerebral hypometabolism, memory dysfunction and cerebral insulin resistance. (54, 107) Clinical trials have presented a promising treatment that addressed these three issues; intranasal insulin. Intranasal insulin administration increases cerebral glucose uptake, cognitive function and verbal memory in memory impaired adults. (207) In pre-clinical studies intranasal insulin has also been shown to reverse age-related cognitive deficits. (150)

Mechanism of Delivery

Intranasal delivery of insulin allows insulin to bypass the saturable BBB insulin delivery system and reach the brain directly via the olfactory and trigeminal nerve pathways and distribution into the CSF. (251) Insulin delivered intranasally comes into direct contact first with the olfactory sensory neurons dendritic processes, which are present in the upper nasal passage, and their axons, which are present in the spaces of the cribriform plate. (251, 252) Free nerve endings of branches from the trigeminal nerve are also present in the nasal epithelium. (72, 143) Insulin is transported along the olfactory and trigeminal nerves by intracellular pathways, via endocytosis by the nerve and then anterograde transport, or extracellular pathways, via paracellular diffusion. (10, 143, 250) Additionally, compounds delivered by intranasal administration have been detected in the CSF suggesting another route of distribution through the CNS. (25, 207).

HYPOTHESIS

This literature review and preliminary research has led to the development of the following hypothesis: We hypothesize that TBI results in reductions in GLUT expression and that intranasal insulin will increase cerebral glucose uptake after TBI and reduce glial mediated inflammation, leading to a reduction in TBI-related pathology and functional impairment. This hypothesis was tested with the three subsequent specific aims.

SPECIFIC AIMS

- Demonstrate that TBI results in a reduction in glucose transporters and insulin receptors in the brain. (Chapter 2)
- Examine the effects of insulin administration following TBI. (Chapter 2)
- Determine the anti-inflammatory effect of insulin on activated microglia. (Chapter 3)

CHAPTER 2: Intranasal Insulin Treatment of an Experimental Model of Moderate Traumatic Brain Injury

Fiona Brabazon B.A.¹, Colin M Wilson, M.A.^{2,3}, Shalini Jaiswal, M.S.^{2,3}, William H. Frey 2nd, Ph.D.⁴, Kimberly R. Byrnes, Ph.D.^{1,3,5}

¹Neuroscience Program, Uniformed Services University of the Health Sciences, 4301 Jones Bridge Road, Bethesda, MD 20814

² Department of Radiology, Uniformed Services University of the Health Sciences, 4301 Jones Bridge Road, Bethesda, MD 20814

³ Center for Neuroscience and Regenerative Medicine, Uniformed Services University of the Health Sciences, 4301 Jones Bridge Road, Bethesda, MD 20814

⁴ HealthPartners Neuroscience Research, 640 Jackson Street, St. Paul, MN 55101

⁵Department of Anatomy, Physiology and Genetics, Uniformed Services University of the Health Sciences, 4301 Jones Bridge Road, Bethesda, MD 20814

*Corresponding Author: Kimberly R. Byrnes, Ph.D.

Department of Anatomy, Physiology and Genetics

Room C2115

4301 Jones Bridge Road

Bethesda, MD 20814

Phone: 301-295-3217

Fax: 301-295-1786

kimberly.byrnes@usuhs.edu

Fiona Brabazon B.A.
Department of Anatomy, Physiology and Genetics
Uniformed Services University of the Health Sciences,
4301 Jones Bridge Road
Bethesda, MD 20814
Phone: 301-295-3217, Fax: 301-295-1786
Fiona.brabazon@usuhs.edu

Colin Wilson M.A.
Department of Radiology
Uniformed Services University of the Health Sciences,
4301 Jones Bridge Road, Bethesda, MD 20814
Phone: 301-295-0557, Fax: 301-295-3893
colin.wilson.ctr@usuhs.edu

Shalini Jaiswal M.S.
Department of Radiology
Uniformed Services University of the Health Sciences,
4301 Jones Bridge Road, Bethesda, MD 20814
Phone: 301-295-5674, Fax: 301-295-3893
shalini.jaiswal.ctr@usuhs.edu

William H. Frey II, PhD
Center for Memory & Aging (Alzheimer's Research Center)
Regions Hospital, 640 Jackson St., St. Paul, MN 55101
Professor of Pharmaceutics, Neurology and Neuroscience
University of Minnesota
Phone: 651-261-1998, Fax: (651)-254-3661
alzheimer@umn.edu

ABSTRACT

Traumatic brain injury (TBI) may result in long term learning and memory dysfunction. The cognitive deficits are the result of cellular and metabolic dysfunction that occurs after injury, including neuronal cell death, decreased cerebral glucose uptake and inflammation. To date, no therapeutic intervention has successfully addressed these post injury deficits. The goal of this study was to assess the ability of intranasal insulin to increase cerebral glucose uptake after injury, improve memory and learning function and reduce inflammation.

Adult male Sprague Dawley rats were exposed to a moderate controlled cortical impact (CCI) injury followed by intranasal insulin or saline treatment beginning 4 hours post-injury and continuing with daily administration for 14 days. Positron emission tomography (PET) of fluorodeoxyglucose ($[^{18}\text{F}]$ -FDG) uptake was performed prior to injury and at 48 hours and 10 days post-injury. Motor function was tested using the beam and peg board walking test. Learning and memory function was assessed using the Morris water maze. Tissue was collected for assessment of macrophage and astrocyte activity.

Intranasal insulin treatment after CCI significantly improved several outcome measures in comparison to saline treated subjects. Insulin treated animals performed better on the beam walking task and demonstrated significantly improved memory function. In addition, a significant increase in $[^{18}\text{F}]$ -FDG uptake was observed in the hippocampus. Insulin treated animals also had significantly less microglial immunolabeling in the hippocampus. Together these data suggest that intranasal insulin improves memory, increases cerebral glucose uptake and decreases neuroinflammation, and may therefore be a viable therapeutic for TBI.

KEYWORDS:

Traumatic brain injury (TBI), Intranasal insulin, Positron emission tomography (PET),

Glucose uptake, Microglia

INTRODUCTION

TBI is a serious public health concern that results in long term cognitive deficits for which there is no current treatment. (206) TBI results in a triphasic metabolic response: an initial hypermetabolic state, a significant reduction in cerebral glucose uptake and a slow increase over time back to normal glycemic uptake values. (84) A chronic state of reduced cerebral glucose uptake is directly correlated with negative long term patient outcome. (77, 84, 133)

This metabolic response has been examined in animal studies using several methods including microdialysis of metabolic byproducts and *in vivo* positron emission tomography (PET) imaging. (181, 263) Byproducts of metabolism include lactate and pyruvate, which can give information about cerebral metabolic rate of glucose (CMR_{glc}); fluorodeoxyglucose ([¹⁸F]-FDG) PET imaging shows the accumulation of glucose in specific regions of the brain. These methodologies contribute to the body of knowledge that shows a period of hypermetabolism acutely after injury followed by a significant reduction in metabolic function which is not solely a product of ischemia. (263) Additionally, studies have shown that the period of hypometabolism following an injury results in increased neuronal vulnerability and an additional injury during this time period can have longer lasting and more severe outcome. (202)

The brain consumes 60% of the body's total glucose and it is thought that this is primarily used to maintain membrane potential and for neurotransmitter production. (18) As glucose is a polar molecule, it does not passively diffuse into cells but instead relies on the presence of glucose transporters (GLUTs) for membrane facilitated diffusion into cells. (162, 184) GLUT expression is important for normal brain development and function. (228) There is a high density of GLUT 1 on the BBB, which is primarily

responsible for movement of glucose into the brain. (148, 166) Knockout studies have shown that homozygous mutants for GLUT 1 and 3 are embryonic lethal, but heterozygous mutants survive and present with significant CNS deficits, including reduced brain size and significant cognitive deficits. (81, 266) Hamlin et al. (92) examined the effect of a severe diffuse brain injury on GLUT expression and showed a significant increase in GLUT 3, the neuronal specific transporter, in the acute stage (4 to 48 hours) post injury in the cortex and cerebellum. This increase in GLUT expression likely mimics the hyperglycolytic state in the acute stages after injury, which is then followed by a significant reduction in cerebral metabolic function.

GLUT membrane translocation in the periphery is primarily dictated by the presence of insulin; insulin in the brain promotes metabolism, glycogen synthesis, neurotransmitter synthesis, cell survival and proliferation (for review, see (200, 221)). The movement of insulin into the brain, like many substrates, is limited and tightly regulated by transporter expression on the BBB. (37) Therefore, systemic insulin administration with the goal of increasing glucose uptake in the brain is limited by its ability to pass the BBB, and carries the risk of inducing hypoglycemia. Intranasal administration of insulin to the brain bypasses the BBB by using olfactory and trigeminal neurons that pass through the cribriform plate. (57, 144, 252) Intranasal insulin administration has been shown to promote glucose uptake, cognitive function and verbal memory in memory impaired adults. (207) Intranasal insulin has also been shown to reverse age-related cognitive deficits in the Morris water maze task, a test of memory. (150) Taken together, these data suggest that intranasal insulin is an appropriate therapy

to increase glucose uptake after brain injury and improve cognitive function and neuronal survival.

This study therefore examined the effect of brain injury, using the controlled cortical impact (CCI) injury model, on GLUT and insulin receptor (IR) expression in the brain in an effort to expand on the knowledge base provided by Hamlin et al. (92) No previous study has assessed the density of IR or GLUT4, the primary insulin sensitive GLUT, after brain injury. Furthermore, this study examined the efficacy of intranasal insulin to increase cerebral glucose uptake after injury, improve motor and cognitive function and reduce the pathological effects of CCI injury in adult male Sprague Dawley rats.

METHODS

Study design

The study includes four cohorts of adult male Sprague Dawley rats (Taconic, 250-400g). The first cohort (n=7 per group) was euthanized 24 hours after the surgical procedure for western blot analysis of GLUT and IR in cortex, hippocampus and cerebellum. This cohort contained two groups: CCI injured and uninjured isoflurane controls. The second cohort (see Figure 1 for a timeline) received a moderate CCI or no injury and intranasal insulin or vehicle treatment followed by motor and cognitive testing and assessment of tissue at 21 days post injury. This cohort included four groups: 1) moderate CCI with intranasal insulin treatment (n=9), 2) moderate CCI with saline treatment (n=10), 3) uninjured with insulin treatment (n=6), and 4) uninjured with saline treatment (n=6). Two animals in the uninjured saline cohort received only isoflurane exposure without intranasal saline but their results were grouped with the rest of the

group. A sub-group of this cohort (n=10; n=5/group moderate CCI with intranasal insulin or saline) received PET/CT scans with [¹⁸F]-FDG at baseline, 2 days and 10 days post injury. The third cohort (n =4) received a moderate CCI and was treated with intranasal insulin-¹²⁵I 4 hours after injury. This group was euthanized 15 minutes after the conclusion of treatment. The fourth cohort (n=4/per group) received a moderate CCI and intranasal insulin or saline treatment with blood glucose testing at baseline, four hours after injury/immediately before treatment and three hours after treatment. This group was euthanized after the final blood glucose sample. For all studies, animals were given free access to food and water and a 12h light/12h dark cycle. Animal baseline weight was obtained prior to injury and weight was monitored throughout the course of the study. All animal procedures were approved by the Uniformed Services University IACUC.

Table 1. Animal cohorts and experimental outcomes.

Cohort	Groups	Experimental Outcomes
1	1) CCI injury (n=7) 2) Uninjured isoflurane control(n=7)	Western Blot analysis of GLUTs and IR 24 hours after injury.
2	1) CCI with intranasal insulin (n=9) 2) CCI with intranasal saline (n=10)	Morris water maze Beam walking/peg board task Lesion volume IBA1 and GFAP PET with [¹⁸ F]-FDG
2	3) Uninjured with intranasal insulin (n=6) 4) Uninjured with intranasal saline (n=6)	Morris water maze Beam walking/peg board task
3	1) CCI with intranasal [¹²⁵ I] insulin (n=4)	Quantification of [¹²⁵ I] -insulin distribution in brain
4	1) CCI with intranasal insulin (n=4) 2) CCI intranasal saline (n=4)	Blood glucose testing at baseline, post-injury and 3 hours after treatment

Moderate traumatic brain injury

Moderate CCI was performed as previously described (59). Briefly, rats were anesthetized with isoflurane (4% induction, 2.5% maintenance) and temperature was measured rectally and maintained at 36.5 – 37.5°C. The animal was placed in a standard rodent stereotaxic frame and positioned using ear and incisor bars. A 5mm circular craniotomy was performed over the left motor cortex at -2.5 mm lateral and -3.0 mm posterior from Bregma. Following the craniotomy, the CCI device (Impact One™, Leica Microsystems, Buffalo Grove, IL) with a 3mm impactor tip was placed in the center of the craniotomy site and a moderate injury was induced with 5 m/s speed, 200 msec dwell time and 2 mm deformation depth. The skull flap removed in the craniotomy was not replaced after injury. The incision site was closed with surgical staples or sutures if the animal was receiving a PET/CT scan. Animals were placed in a heated chamber and monitored after injury until anesthesia effects had worn off and the animal was returned to home cage.

Intranasal insulin treatment

Humulin R- 100 insulin (0.06IU per daily treatment, Eli Lilly, Indianapolis, IN) or an equal volume of saline (60 µL) was administered to the nasal cavity using a 10 µL pipettor. Animals were placed in a supine position in an anesthesia chamber while drug was administered in 6 µL increments to alternating nares with each dose occurring 2 minutes apart. The first dose was administered 4 hours post-injury and continued daily for up to 14 days. Animals were anesthetized during treatment with 2.5% isoflurane.

Intranasal administration of [¹²⁵I]-insulin

Four hours after injury, rats were anesthetized with 2.5% isoflurane and received approximately 10 μ Ci of insulin intranasally. A 50 μ Ci lot of [¹²⁵I]-insulin (Perkin Elmer, specific activity=2200 Ci/mmol 378.8 μ Ci/ μ g, molecular weight = 5931.6) powder was aliquoted in equal volumes (125 μ L) Humulin R (Eli Lilly) and sterile saline. This dilution allowed for the delivery of approximately 10 μ Ci of insulin in 50 μ L (10, 5 μ L drops administered to alternating nares, 2 minutes apart). Following the final dose, the animal remained in a supine position for 15 minutes under anesthesia before euthanasia (sodium pentobarbital Euthasol solution, 0.1ml/g) followed by transcardial perfusion with 1X PBS. The brain was then divided into the ipsilateral and contralateral hemispheres and the following regions were collected: cortex, hippocampus, olfactory bulb, brainstem and cerebellum. A gamma counter (Perkin Elmer, Model WALLAC Wizard 3" 1480-011) was used to calculate total radioactive content of each brain region. Samples were weighed and radioactivity was calculated by normalization to sample weight, calculation of specific activity of control and gamma counter efficiency (82%).

Blood glucose

Blood glucose levels were obtained via tail vein blood using an Accu Chek Aviva Plus blood glucose system (Roche Diagnostics, USA) in non-fasted rats anesthetized with 2.5% isoflurane. A baseline blood glucose level was obtained prior to injury. Animals received a moderate CCI and one treatment of intranasal insulin 4 hours after injury. Blood glucose was collected immediately before beginning treatment. Three hours after treatment a final blood glucose level was obtained and animals were euthanized.

Behavioral assays

Beam walking assay

Animals were trained for 3 days prior to injury on a beam /peg board walking motor function test as previously described. (226) Briefly, rats were trained to walk across beams of decreasing width (4, 3, 2, and 1 cm) and a pegboard, a 2cm wide board with circular pegs projecting from the top, to return to their home cage. Time to cross the beam/peg board and number of footfalls were measured at baseline and at 1, 7, 14 and 21 days post injury by an investigator blinded to group. The post-injury measurements were averaged for each trial and compared to baseline values collected.

Morris water maze

Animals (n=31) in the second cohort underwent testing in the Morris water maze with minor modifications to the protocol as described by Morris et al. (168) The testing paradigm included 4 training sessions on 4 consecutive days during which the animal was placed in each of the 4 quadrants of the pool and had 60 seconds to locate a hidden platform located in the Northwest quadrant of the pool. Four large visual cues were posted outside of the pool to guide the subject to the correct quadrant. Animals that did not find the platform within the 60 second window were directed to it at the end of the trial. One to 3 hours after the training session on the fourth day, animals underwent the probe trial. In this trial, the platform was removed from the pool and animals were placed in the pool for 60 s. Data was collected using AnyMaze™ Video Tracking System version 4.70 (Stoelting Co. Wood Dale IL). Swim speed and latency to platform were collected. Island crosses during the probe trial were counted by a blinded

investigator with the requirement that the head of the rat must pass through the island region to count as a cross. Search strategy analysis was conducted on traces collected during the probe trial by 2 blinded experimenters using a scoring method previously described.(29)

PET/CT with [¹⁸F]-FDG imaging

Serial [¹⁸F]-FDG PET/CT scans were obtained in 10 rats (n = 5/group; CCI with intranasal insulin or saline) prior to injury (baseline) and at 2 and 10 days post injury. PET and CT images were acquired using an Inveon multimodality preclinical scanner (Siemens Medical Solutions, Erlangen, Germany) in the small-animal PET/CT facility of the Translational Imaging Core, Center for Neuroscience and Regenerative Medicine, Uniformed Services University. Under 1-2% isoflurane anesthesia in oxygen at 2L/min, rats were injected with 1.5 - 2 mCi [¹⁸F]-FDG via the lateral tail vein. Rats were maintained under anesthesia for a 45-minute uptake period and for the duration of the imaging session. Physiologic monitoring included measurements of temperature, respiration rate, heart rate and oxygen saturation. A brief CT scan was acquired for attenuation correction and anatomical localization (80 kVp, 500 μ As, 420 msec, 195° rotation in 120° steps) and reconstructed in real time using a modified-Feldkamp algorithm (down sample 2, bin 4) with a Shepp-Logan filter and beam hardening correction applied. The CT image matrix was 352 x 352 x 592 with isotropic voxel dimensions of 0.23 mm³. A 30-minute static PET scan was acquired in list mode (350-650 keV, 3.432 ns) with an axial field of view of 12.7 cm.

PET data were reconstructed with Inveon Acquisition Workplace software, version 1.5 (Siemens Medical Solutions, Erlangen, Germany). Corrections were applied

for dead-time, decay, attenuation and scatter and a requested resolution smoothing setting of 0.5 mm was used. The reconstruction algorithm was a three dimensional ordered-subset expectation maximization/maximum a posteriori (OSEM 3D/MAP) iterative protocol (2 OSEM3D iterations and 18 MAP iterations). The image matrix was 256 x 256 with final voxel dimensions of 0.39 x 0.39 x 0.80 mm³. The intrinsic resolution of the system was 1.4 mm full width half maximum at the center of the field of view.

PET/CT image processing

Processing and analysis of FDG-PET data was performed using Vivoquant software version 1.22 (inviCRO, LLC Boston, MA). PET data were resampled to match reference CT voxel size (0.23 mm³ isotropic) and dimensions (352x352x536). Pre-processing of image data, including PET unit conversion, PET to CT image registration, and image cropping, was achieved via a scripted process. PET data were converted to units of activity (μCi) and registered to the CT image using an automatic algorithm (6 parameter, rigid-fast). The coregistered PET/CT image was cropped to a region surrounding the brain (170x170x240) and an additional automatic registration (6 parameter, rigid-fine) was applied post-cropping. The coregistered, cropped dataset was manually reoriented (Z-axis rotation) and saved as a DICOM file.

Pre-processed PET/CT data were registered to a 13-region rat brain atlas by way of the CT, using an automatic algorithm that combines a rigid transformation of the data and scaling of the atlas. A manual correction process was required to improve Data-Atlas co-registration for select subjects. Briefly, CT data was manually translated and rotated (six parameters with linear interpolation) to better fit the skull to the brain atlas. The transformation matrix was applied to the PET data and the data was reprocessed to

generate a new quantitative output. The inviCRO rat brain atlas provides the following 13 regions of interest (ROIs): basal ganglia, thalamus, amygdala, cerebellum, cortex, hypothalamus, midbrain, corpus callosum, olfactory, hippocampus, septal area, white matter and other (ventricles). Quantitative output was obtained for left, right and combined hemispheres for a total of 41 ROIs. The uptake concentration for each ROI was normalized to the uptake concentration of the entire atlas (whole brain normalization) for inter-subject comparison.

Tissue collection and processing

Rats were deeply anesthetized with a pentobarbital solution (Euthasol, 0.3 mg/kg) and perfused with saline followed by 10% formalin before the 5mm region surrounding the lesion site of the brain was dissected for histology (n=4 per group). Brain tissue was sectioned at 20 μ m for histological analysis.

For protein analysis, rats were deeply anesthetized with a pentobarbital solution (Euthasol, 0.3 mg/kg) and perfused with saline. Brain tissue was then divided and the entire ipsilateral cortex (including the perilesional region), hippocampus and cerebellum were collected. Samples were placed immediately on dry ice before being stored at -80°C.

Standard hematoxylin and eosin (H&E) stain was used for lesion volume quantification. Brain tissue was immunolabeled for microglia (Iba1 1:100, Wako Chemicals USA, Richmond, VA) and astrocytes (GFAP, 2.5:1000 Abcam, Cambridge, MA). Fluorescent secondary antibodies (Alexa-Fluor Secondaries, Invitrogen, Grand Island, NY) were used to visualize primary antibodies. Images were then collected with an Olympus BX43 microscope (Olympus America) with Olympus cellSens microscopy

software (Olympus, Center Valley, PA, USA) or the NanoZoomer Digital Pathology System. Scion Image Analysis (<http://rsb.info.nih.gov/nih-image>) was used to quantify pixel density of immunolabeling using stain intensity as threshold. Measurement was performed on a minimum of 4 equally spaced images with a random start within the ipsilateral hippocampus in CA1. All images were obtained at 20x magnification therefore; the size of the region of interest was maintained for all quantification of images. (50)

For protein analysis, tissue was collected from the ipsilateral cortex, cerebellum and hippocampus and homogenized for quantification of GLUT 1 (1:100, Abcam, Cambridge, MA, USA), GLUT3 (1:50, Abcam, Cambridge, MA, USA), GLUT 4 (1:100, Abcam, Cambridge, MA, USA), IR (1:50, Abcam, Cambridge, MA). Western blots were performed as previously described. (50) Briefly, 25 µg protein was run on an SDS polyacrylamide gel and then transferred to nitrocellulose sheet (Trans-Blot Turbo Transfer System, Biorad, Hercules, CA, USA). Membranes were stripped with Reblot plus mild antibody stripping solution (Millipore, Billerica, MA, USA) prior to probing for GAPDH. Resultant bands were quantified with Image J densitometry and normalized to a loading control protein, GAPDH (1:5000, Millipore, Billerica, MA, USA).

Statistics

All data were collected by an investigator blinded to treatment group. Beam and peg board walking data were compared to baseline values and statistical significance was determined by a 2 way ANOVA, using Sidak's multiple comparisons. Morris water maze island crosses during the probe trial were analyzed using a 2 way ANOVA, using Sidak's multiple comparisons. Morris water maze trace analysis was conducted by two

blinded investigators and a Chi Square analysis of the four groups was conducted. A student's two-tailed t-test was performed to compare western blot protein content between groups. Pixel density was measured for histological comparison and a two tailed unpaired t-test was conducted and reported. Uptake values obtained from PET data were logged and statistical analysis changes over time in a group using 2 way ANOVA with Sidak's post test for family wise correction. All statistical analysis was conducted using Graphpad Prism Software version 6.01. (GraphPad Software, San Diego, CA). A p value < 0.05 was considered statistically significant.

RESULTS

Moderate controlled cortical impact did not alter insulin receptor or glucose transporter expression

To examine the effect of moderate CCI on GLUT and IR protein expression, we examined tissue at 24 hours post injury, a time point where significant changes to expression have been observed previously. (92) Injured animals were compared to uninjured controls who received an equal amount of isoflurane exposure. Our data showed no significant difference in GLUT 1 (Fig.2A), GLUT 3 (Fig 2B) or GLUT 4 (Fig. 2C) expression in the ipsilateral cortex between the injured and uninjured groups. While no significant change in IR was observed, a trend in depression after injury ($p=0.094$) was observed in the ipsilateral cortex at 24 hours (Fig. 2D). In addition, there was no significant difference in GLUT 1 (Fig. 2F), GLUT 4 (Fig. 2H) or IR (Fig. 2I) in the ipsilateral cerebellum after injury. However, a trend was observed that suggests an increase in GLUT 3 (Fig. 2G) in the ipsilateral cerebellum after injury, but did not reach significance ($p=0.4$). Finally, no significant difference in GLUTs or IR was detected in the hippocampus (data not shown).

Intranasal insulin delivery did not alter blood glucose or weight

In order to demonstrate that the intranasal insulin at the dose delivered would have no or limited negative peripheral effects, blood glucose and body weight were assessed. Blood glucose was measured at three timepoints: prior to CCI, prior to treatment at four hours post-injury, and at three hours post treatment with intranasal insulin (Fig. 3A). While some variability was observed at baseline in animals, attributable to the animals not being fasted prior to assessment, there was no pre-injury difference between groups (Repeated measures 2 way ANOVA with Sidak's multiple comparisons, adjusted p value=0.2523). There was no significant variation as a result of interaction (p=0.28), time (p=0.0626), or injury (p=0.3929; repeated measures 2 way ANOVA). This demonstrated that neither injury nor insulin administration altered systemic glucose concentration.

The weight of the animals in the second cohort was monitored over the course of the 21 day study (Fig. 3B). The uninjured cohorts treated with intranasal insulin or saline showed a steady increase in weight over time but no significant difference between treatment groups. The injured groups showed an acute decrease in weight after injury that recovered over time and remained consistent between the two groups. There was no significant difference in weight between the intranasal insulin or intranasal saline-treated groups at any time point.

CCI injury does not inhibit intranasal insulin delivery to the central nervous system

To verify that CCI does not disrupt the pathways of intranasal drug delivery to the brain and to confirm targeted delivery of insulin, we traced the delivery of iodinated insulin after injury. After a moderate CCI, animals were treated with intranasal [¹²⁵I]-

insulin combined with Humulin I-100. The total iodinated dose administered was approximately 10 μ Ci per animal. [¹²⁵I]-insulin was detected in all regions investigated (Fig. 3C). The highest concentration of tagged insulin was found in the olfactory bulb, with amounts exceeding 5 nM of [¹²⁵I]-insulin. The next highest regions were the cerebellum, brain stem, hippocampus and cortex, respectively. There was no significant difference between the ipsilateral and contralateral sides of any of these brain regions, indicating that the injury does not significantly hinder delivery along the intranasal pathway.

Intranasal insulin treatment increased glucose uptake in the hippocampus

In order to determine the effect of intranasal insulin administration on cerebral glucose uptake in a moderate CCI, we conducted a longitudinal PET [¹⁸F]-FDG study. [¹⁸F]-FDG uptake was visualized as a heat map and aligned with CT scan. The Vivoquant V1.22 atlas was then aligned to the scan for detailed regional uptake data. Uptake is presented as a quantifiable heat map with blue indicating regions of low uptake, red is higher uptake and white as the highest uptake. Baseline values were consistent with no significant difference detected between treatment groups (Fig. 4A, B). There was no significant difference in [¹⁸F]-FDG uptake in any region between the groups at 2 days post injury. However, at 10 days post injury, animals treated with intranasal insulin had significantly higher [¹⁸F]-FDG uptake in the ipsilateral hippocampus compared to baseline values ($p=0.0329$) and uptake at 2 days post injury ($p=0.0189$) (Fig.4A; repeated measures 2 way ANOVA). There was no significant difference in [¹⁸F]-FDG uptake in animals treated with saline at 2 or 10 days post injury compared to uptake at baseline.

Time was a significant source of variation ($p=0.0033$) but there was not a significant interaction effect ($p=0.4586$) (2 way ANOVA, Sidak's post test).

The ipsilateral and contralateral portion of the remaining atlas regions: basal ganglia, thalamus, amygdala, cerebellum, cortex, hypothalamus, midbrain, corpus callosum, olfactory, hippocampus, septal area, other (ventricles), white matter, entire atlas were examined as well, but no other regions showed significant changes in [^{18}F]-FDG uptake as a result of treatment (data not shown).

Intranasal insulin improved aspects of motor and cognitive function

Rats were trained on two motor function tasks, beam and peg board walking, prior to injury and tested at 1, 7, 14 and 21 days post injury. The injury to the motor cortex increased the number of footfalls in both the insulin treated and saline treated groups but there was no significant difference in number of footfalls between the groups at any time point (Fig. 5A). Time was a significant source of variation in footfalls on the beam walk ($p<0.0001$) but there was no significant interaction or effect of treatment. (2 way ANOVA, Sidak's post test) However, animals treated with intranasal insulin demonstrated a significant decrease in time to cross the beam walk in comparison to animals treated with intranasal saline after CCI (Fig. 5B, $p=0.0209$, 2 way ANOVA, Sidak's multiple comparison test). This difference was observed by day 1 after injury, suggesting that a single dose of intranasal insulin resulted in the improved behavior. This effect in the intranasal insulin treated group was sustained for the 21 day testing period. There was no source of variation from interaction ($p=0.2014$), time ($p=0.0523$) or treatment ($p=0.1104$) in time to cross the beam walk. (2 way ANOVA, Sidak's post test)

There was no significant difference between intranasal insulin treated and intranasal saline treated in time to cross the beam at 7, 14 and 21 days post injury,

Cognitive function, including learning and memory, was assessed in animals from cohort 2 using the Morris water maze task from days 11-14 post injury. There was a significant effect of time ($p < 0.0001$) and treatment ($p = 0.0032$) but no significant interaction ($p = 0.4462$) in latency to platform. (2 way ANOVA, repeated measures, Sidak's post test) Uninjured rats treated with insulin learned the location of the hidden platform slightly faster (3.70 ± 0.6 seconds) than uninjured rats treated with saline (6.51 ± 1.9 seconds) by day 4 of training (Fig. 6A). In addition, injured insulin-treated rats, reached the platform slightly faster (within 15.1 ± 3.1 seconds) by day 4 of training compared to saline treated animals (20.4 ± 4.9 seconds). Although the interaction effect was not significant, injured animals treated with saline were significantly slower to find the platform on trial day 3 than uninjured treated with saline ($p = 0.0078$) and uninjured treated with insulin ($p = 0.0031$). (2 way repeated measures ANOVA, Sidak's post-test) Injured animals treated with saline also performed worse on trial day 4 than uninjured treated with saline ($p = 0.0247$) or insulin ($p = 0.0065$). There was no significant difference between injured animals treated with insulin and uninjured cohorts in latency to platform.

However, treatment with intranasal insulin did result in a significant increase in target region (island) crosses during the probe trial, suggesting an influence of insulin on memory rather than learning behavior (Fig. 6B). In this probe trial assessment, in which the hidden platform is removed, saline and insulin treated naïve animals showed no difference from insulin-treated injured rats, while saline-treated injured rats showed significantly fewer crosses than those that received insulin (Fig. 6B; $p = 0.033$, 2 way

ANOVA, Sidak's multiple comparisons test). Additionally, there was a significant interaction effect observed ($p=0.0182$, 2 way ANOVA).

To further evaluate this data, the search strategy utilized by animals during the Morris water maze was assessed as previously described. (29) Data is presented as a percentage of rats in each group that displayed the search behavior (Fig. 6C). Analysis of traces obtained during the probe trial showed a significant difference between all of the groups (Fig. 6D; $p < 0.0001$, Chi Square analysis). Neither the insulin nor saline treated group of uninjured animals displayed looping behavior. Uninjured animals treated with saline displayed equal (50%) amounts of spatial and systematic search strategy. Interestingly, uninjured insulin treated animals displayed more systematic (84%) search strategy than uninjured saline treated animals (50%). In contrast, both injured groups demonstrated looping search strategy, although injured animals treated with intranasal insulin showed less looping behavior (14%) than injured animals treated with saline (50%). The injured group treated with intranasal saline also showed equal amounts of spatial and systematic search strategy (43%), whereas looping behavior was the dominant search strategy for the saline treated injured animals (50%) and spatial was the least used for this treatment group (14%).

Intranasal insulin treatment reduced microglia/macrophages in the hippocampus but not astrocytes.

Immunohistochemical and histological assessment of tissue was conducted to examine the effects of injury and treatment on specific cellular populations and overall tissue health. H&E staining confirmed that the lesion was within the cortex and did not penetrate into the hippocampus. However, despite improved behavioral outcome, intranasal insulin did not reduce lesion volume in the cortex (data not shown).

Analysis of immunohistochemistry for the inflammatory marker Iba1, a marker for both macrophages and microglia, demonstrated a significant reduction ($p=0.0089$, two-tailed unpaired t-test) in Iba1 immunoreactivity in the CA1 region of the hippocampus (Fig. 7A) in intranasal insulin treated animals (7C) compared to intranasal saline treated (7B). In addition, quantification of GFAP (Fig. 7D), a marker of astrocytes, showed no significant difference between intranasal insulin (Fig. 7F) and intranasal saline (Fig. 7E) treatment after injury ($p=0.077$, two-tailed unpaired t-test).

DISCUSSION

This study expands the body of knowledge relevant to the neurometabolic crisis that occurs after brain injury. Our data now shows that there no significant effect on IR or GLUTs in the ipsilateral cortex, cerebellum or hippocampus at 24 hours post injury as a result of a moderate CCI. This study also shows the potential of a novel therapeutic treatment, intranasal insulin. Our findings show that treatment with intranasal insulin beginning at 4 hours post-injury significantly improves several outcome measures, including beam walk function, memory recall, [^{18}F]-FDG uptake at 10 days post injury, and decreases neuroinflammation in the hippocampus. Further, these improvements in functional outcome were not complicated by peripheral side effects as intranasal insulin did not alter blood glucose or weight.

Only one previous study has examined GLUT expression after injury; (92) however, it was conducted in a severe, diffuse, closed head model of injury so the pathological outcome is very different from the open skull moderate CCI model used in our current work. Therefore, it is not entirely surprising that our data yielded different results. Most notably, where Hamlin et al. showed a significant increase in GLUT3 at 24

hours post injury in the cerebellum, we showed no significant difference. However, we did observe a trend toward an increase in GLUT3 expression in the cerebellum compared to uninjured controls, although it did not reach statistical significance. We also observed no significant difference in expression of GLUTs in the hippocampus, and no significant difference in GLUT expression in the cerebellum or cortex. It is important to note that there was considerable variability within groups in cerebellum and cortex measures. This may be attributed to the size of the region of interest examined for protein quantification, as the entire region (cortex, hippocampus, and cerebellum) was extracted, including the lesion epicenter, the perilesion and potentially normal distal regions, in order to be as similar as possible to the PET atlas. This may have resulted in a wash out effect on significance in the lesioned area by the lack of change in expression in non-lesioned tissue. Future studies will examine smaller regions of interest near the lesion for more precise measures. In addition, as the effect of the weight drop model on glucose uptake has not been established, it is possible that the different models of injury result in a different time course of the metabolic crisis.

Despite the lack of a significant effect on the cortex, intranasal insulin did have significant effects on other aspects of recovery after TBI. Intranasal delivery of peptides and other drugs using a pipette has been shown to be successful in previous rodent studies. (150, 209, 250) However, to date, no previous study has attempted to deliver intranasal insulin to rats following CCI or any other model of brain injury. In order to confirm appropriate delivery and lack of peripheral effects, we performed a number of control analyses and showed that both the expected route of delivery was intact after CCI, leading to appropriate delivery of insulin to the brain, and that there was no change in

peripheral glucose or weight. Quantification of [¹²⁵I]-insulin showed that there was no significant difference between ipsilateral and contralateral brain regions indicating that injury did not inhibit pathways necessary to deliver drug. Previous studies have shown that both the olfactory and trigeminal neural pathways deliver therapeutic proteins from the nasal mucosa to a variety of brain regions. (209) Our data shows that while insulin reaches the highest concentration in the olfactory bulb, it also distributes to the cortex, cerebellum, hippocampus and brainstem.

We and others have shown that TBI can significantly change glucose uptake, as measured with [¹⁸F]-FDG PET, and CMRglc, in the brain. (226, 234, 283) Clinical studies have also shown a correlation between increased [¹⁸F]-FDG uptake and memory function in normal controls and Alzheimer's patients. (52) Our study showed a significant increase in [¹⁸F]-FDG uptake in the ipsilateral hippocampus at 10 days post injury compared to baseline and 2 days post injury in the intranasal insulin treated group. This increase at 10 days is interesting as it correlates with the beginning of the Morris water maze training, in which insulin treated animals performed significantly better. Morris water maze is a test of learning and memory, which are primarily functions of the hippocampus. Our findings suggest that the increase in glucose uptake in the hippocampus may contribute to improved functional performance. Human studies have shown a significant acute increase in ATP (adenosine triphosphate) and phosphocreatine, which represent the brains energy reserve levels, after intranasal insulin administration. (114) These data suggest that intranasal insulin administration may facilitate the brain's energy supply and thus influence appetitive behavior. It is also important to note that the

dose administered in this study, 40IU, also did not alter blood glucose suggesting this is a focused CNS treatment with little peripheral confounding effects. (114)

Examination of insulin action on a cellular level has shown that insulin acts on neurons to increase GLUT 3 expression on the membrane, directly increasing glucose uptake and the energy available to maintain cellular homeostasis and produce neurotransmitters necessary for memory function. (255) This metabolic response and insulin's direct effect on promoting survival in neurons may be responsible for improving memory function. (8) Insulin also increases dendritic function, leading to long lasting effects observable as changes in memory. (43) However, these are not immediately manifested as an improvement in learning response (43, 63), which may explain the lack of effect on latency in the Morris water maze, but improved performance in the probe trial in our own findings.

Intranasal insulin treatment significantly improved time to cross the beam walk after injury in comparison to saline treated animals. There was a significant increase in time to cross at one day post injury observed in the saline treated animals that was not observed in insulin treated animals. There was a marked increase in foot falls after injury in both groups verifying that the injury equally affected this component of motor function. Intranasal insulin treatment did not improve foot falls after injury. The difference in these two outcomes suggests that while the injury has occurred within proximity to the motor cortex, our histological analysis shows that the lesion primarily extends to the parietal cortex. Further, this difference suggests that treatment did not have a significant effect in the cortex. This is supported by data showing no significant difference in lesion volume between saline and insulin treated animals, which may be due

to the low insulin receptor density of the neurons of the cortex. (154) Second, there is the suggestion that animals treated with insulin showed increased recall of how to accomplish the task. It should be noted that while we did not observe a difference in foot falls we did not count total steps taken. Future studies should take into account that a faster moving animal is more likely to make errors whereas an animal that truly has a motor deficit will both take more steps and make more errors in its effort to cross the beam. One previous study by LeMay et al. examined the effect of pre-treatment with peripherally administered insulin on motor function recovery after an ischemic event. A significant improvement in motor function was observed in animals pre-treated with an intraparietal injection of insulin prior to an aortic occlusion at 24 hours post occlusion. (127) The difference in motor function observed in the previous study compared to our findings may be attributed to a number of factors. First, the previous study uses several different motor function assays to quantify outcome which may have greater sensitivity to detecting differences than our beam and peg walking tasks. Second, the injury models are drastically different. The previous study uses the aortic occlusion model induces injury by disrupting blood flow whereas CCI induces injury by direct impact on the brain. Third, the authors attribute the difference to the hypoglycemia induced by their treatment which was not observed in our treatment model due to the mode of administration, intraparietal insulin injection versus intranasal insulin.

While IR density is low in the cortex, its expression in the hippocampus, the region of the brain responsible for memory formation, is one of the highest in the brain. (97) It is well documented that TBI inhibits both learning and memory recall. (35, 232) The animal's ability to locate the platform during the probe trial is primarily a test of

memory. (26, 233) Alternatively, the animal's ability to find the platform in a shorter amount of time as measured by latency to platform over the training days is a measurement of learning. (26) Therefore, the Morris water maze allows us to examine both learning and memory in one paradigm in both our injured and uninjured cohorts. While there was a slight increase in latency between non-injured and injured groups, both the injured and uninjured treatment groups showed the ability to learn over the course of the trials as they found the platform more quickly each day. This was an unexpected finding, as we and others have previously observed impaired learning in the Morris water maze with moderate CCI. (218) This finding suggests that the repeated isoflurane exposure may contribute to overall improvement in learning; previous studies have demonstrated a neuroprotective component of isoflurane. (134, 241)

Despite similar learning ability, we did find a significant difference in island crosses between our intranasal saline and intranasal insulin treated injured animals. Animals treated with intranasal insulin after CCI crossed the island location significantly more times during the probe trial, indicating that this group showed improved recall of the location of the platform. Insulin resistance, caused by reduced sensitivity of the receptor to ligand, is observed in Alzheimer's patients and is correlated with decreased memory function and learning. (58) The function of insulin has been tested in healthy adults and the improvement observed in memory function in the presented study is analogous to human trials where a significant improvement in long term but not immediate recall of a word list was observed in intranasal insulin treated individuals compared to placebo treated. (17) Further, there was no difference in attention or

concentration observed between the two treatment groups in the clinical study, supporting our findings that this treatment improves memory recall rather than overall learning.

In addition to platform crosses, we also examined search strategy. The three major sub categories of Morris water maze search strategy analysis are spatial, systematic, and looping; each correlates with familiarity with the task, level of injury and general intelligence. (113) Looping behavior is typically observed in rodents on the first day of training or in those with moderate to severe TBI, and is defined by the animal remaining primarily in the outer quadrant, swimming the perimeter. Systematic behavior is defined by the animal primarily scanning the central four quadrants, indicating recall of the location of the platform. Spatial search strategy is considered the most efficient and is defined by the animal searching primarily within the platform quadrant. Our data shows that a greater proportion of injured animals treated with intranasal insulin employed a spatial search strategy compared to the injured animal group that was treated with intranasal saline. We also show that a significantly greater number of the injured animals treated with intranasal saline employed the looping search strategy than injured animals treated with intranasal insulin. Looping behavior is typically observed in animals naïve to the task and injured animals, suggesting that insulin treatment reduces injury and improves performance. As an animal learns the location of the platform in the inner quadrant, they are more likely to explore the center of the pool. In contrast, the naïve animal will remain in the outer quadrant close to the wall, where they are less exposed. Additionally, looping behavior has been observed in rats with neurotoxic hippocampal lesions, supporting the idea that decreased looping is indicative of hippocampal damage and is measurable using this analysis. (80)

Additionally, a significant difference in search strategy was observed in the uninjured cohorts. Uninjured rats treated with intranasal insulin showed significantly more systematic search strategy than those treated with intranasal saline. Neither of the uninjured groups exhibited looping search strategy behavior. No other significant differences in Morris water maze were observed in uninjured cohorts; therefore this increase in systematic search strategy is a point of interest and will be the subject of future experiments as it suggests that intranasal insulin alter learning strategies.

Despite a lack of change in lesion volume, a significant alteration in neuroinflammation within the hippocampus was observed. Microglia are the resident macrophages of the brain. These cells serve an important purpose in the acute stages following injury of clearing cellular debris but prolonged activation can be detrimental. (140) Pro-inflammatory microglia, produce reactive oxygen species and cytokines that can result in neuronal cell death. (153) Intranasal insulin treatment significantly reduced the amount of Iba1, a marker of microglia and macrophages, in the hippocampus at 21 days post injury. The density of Iba1 was assessed in order to evaluate not just cell number but also take into account cell size and processes, as activated, pro-inflammatory microglia have an enlarged cell body compared to quiescent microglia. (42) Previous studies have shown that intranasal insulin administration can simultaneously restore insulin signaling pathway while reducing microglia activation in a mouse model of Alzheimer's disease. (40) This reduction in microglia activation may decrease the amount of pro-inflammatory cytokines, nitric oxide and reactive oxygen species produced by microglia in their activated state following injury. These compounds result in neuronal cell death, thus a decrease would promote neuronal viability which manifests

as improved behavioral outcome. Recently, *in vitro* studies have supported the *in vivo* findings by showing that insulin treatment can significantly reduce the production of monocyte chemoattractant protein-1 (MCP-1) from activated microglia. (235) This cytokine plays a role in recruiting additional macrophage and microglia to the site of injury. (56) The reduction in this molecule would explain the observed reduction in Iba1 following intranasal insulin treatment. Together, these data suggest that insulin acts directly on microglia to reduce activation.

We found no significant reduction in astrocyte activity as a result of intranasal insulin after CCI injury. Similar to microglia, astrocytes can play a role in healing after brain injury. (172) but prolonged astrocyte activity also contributes to neuronal cell death after TBI. (278) It is important to note that while there was no significant difference in number of astrocytes, intranasal insulin may have had a direct effect on their action. Insulin treatment has been shown to reduce the production of nitric oxide from activated astrocytes *in vitro*. (132)

In summary, intranasal insulin treatment improves memory function and glucose uptake in the ipsilateral hippocampus and hypothalamus after CCI. Intranasal insulin was successfully delivered to the cortex, hippocampus, brain stem and cerebellum after CCI injury using a pipet method. This delivery and dosage did not negatively impact blood glucose or weight gain in injured or uninjured animals. Additionally, intranasal insulin treatment significantly reduced Iba1 staining in CA1 of the hippocampus. Together, the data from this study suggest that intranasal insulin treatment is a promising method of treating the metabolic crisis following TBI, as well as improving memory function and reduces microglia mediated inflammation.

ACKNOWLEDGEMENTS

This study was funded by the Cosmos Club Foundation, with support for FB by NIH grant number 1R01NS073667-01A1. The authors would like to thank Dr. Aryan Namboodirri, Jishnu Krishnan, Guzal Khayrullina, Laura Tucker, and Dr. Reed Selwyn for their technical assistance and consultation on this project

AUTHOR DISCLOSURE STATEMENT

Fiona Brabazon, Kimberly R. Byrnes and William H. Frey 2nd are listed as inventors for a patent from the Uniformed Services University/Health Partners Institute for Education and Research for intranasal insulin in the treatment of traumatic brain injury. William H. Frey 2nd is an inventor on a patent owned by Health Partners Institute for Education and Research regarding the use of intranasal insulin. Colin Wilson and Shalini Jaiswal have no competing financial interests to report.

ETHICAL RESEARCH STATEMENT

All animal procedures were conducted as approved by the Uniformed Services University IACUC.

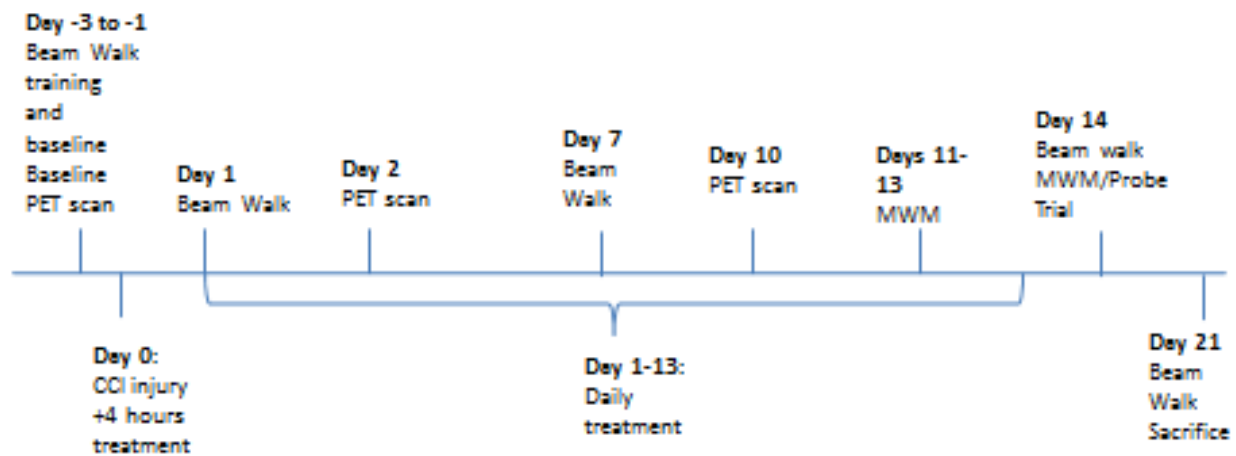


Figure 1. The timeline displays times at which animals underwent surgery, behavior training, PET/CT imaging and sacrifice.

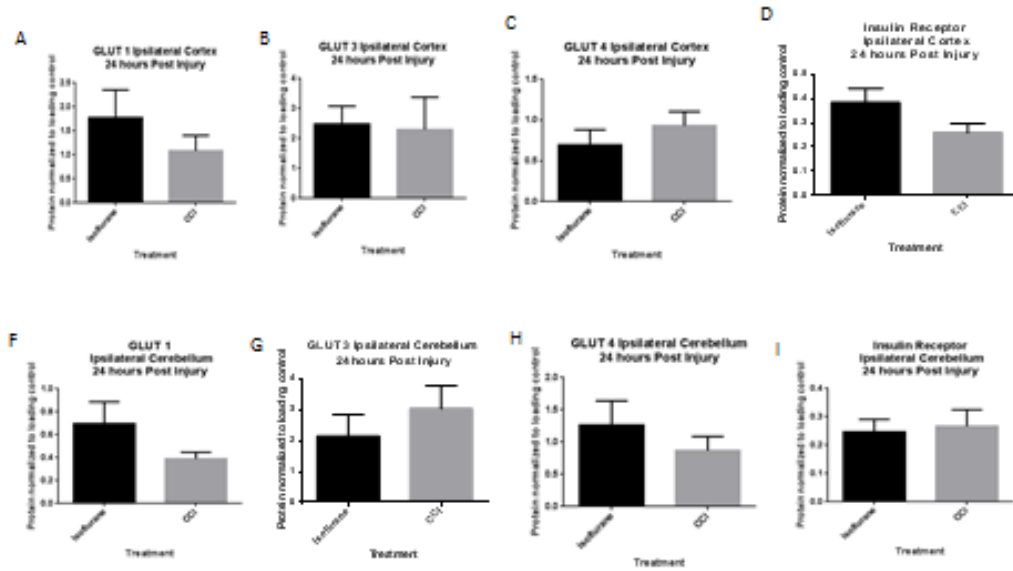


Figure 2. The effect of moderate CCI on GLUT and IR expression. Tissue was collected 24 hours after moderate CCI (n=7) or isoflurane sham (n=7) for western blot quantification. The ipsilateral cortex showed no significant change in GLUT1(A), 3(B), 4(C) or IR(D) expression. There was a trend observed suggesting a decrease in IR that did not reach significance ($p=0.0939$, two-tailed t-test). The ipsilateral cerebellum showed a trend toward depression in GLUT 1(F) and a trend towards increased GLUT 3(G). There was no significant change in GLUT 4(H) or IR (I) expression in the cerebellum at 24 hours post injury compared to control. All proteins are normalized to loading control (GAPDH) and data are represented as mean \pm SEM.

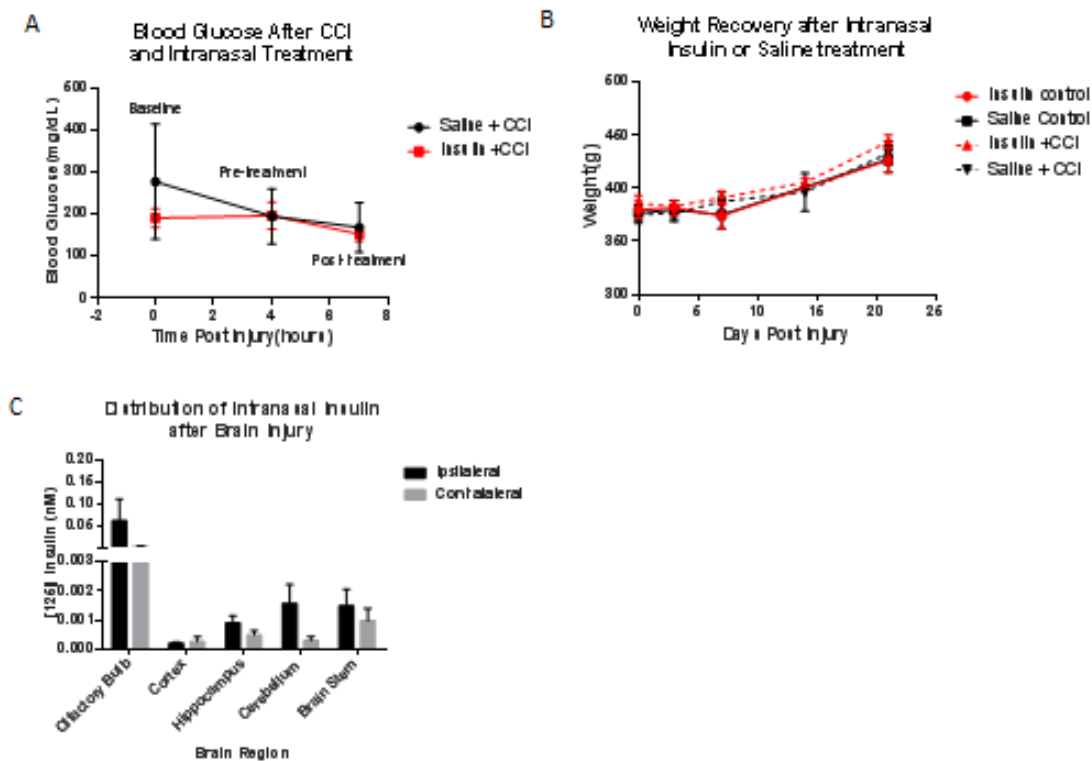


Figure 3. Intranasal insulin delivery after CCI acts primarily in the CNS. The dose of intranasal insulin given was not sufficient to cause a significant change in blood glucose following CCI in intranasal insulin treated animals (n=4) compared to saline treated injured controls (n=4) as measured by tail vein blood draws at baseline, after injury/immediately prior to treatment and 3 hours after treatment (A). There was also no effect of intranasal insulin on body weight, measured through 21 days post-injury with 14 days of daily administration (n = 7/group injured n=4/group uninjured; B). CCI injury does not inhibit the pathway of intranasal administration to brain regions (C). There was no significant difference between the ipsilateral and contralateral brain region and insulin was detected in the olfactory bulb, cerebellum, brain stem, hippocampus and cortex 45 minutes after administration (n=4).

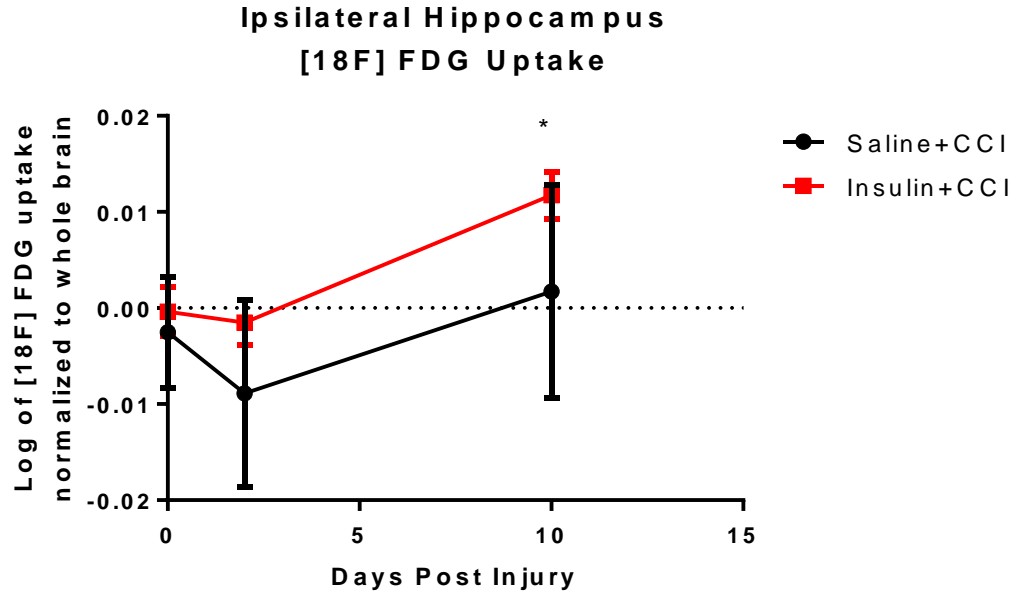


Figure 4. PET imaging of [¹⁸F]-FDG reveals significant differences in uptake patterns following intranasal insulin treatment compared to intranasal saline treated animals after CCI (n=5/group). PET scans of [¹⁸F]-FDG uptake were obtained with a CT for anatomical localization of brain regions. Uptake values from these regions were obtained by aligning a rat atlas to the scans. Regional analysis revealed that at 10 days post injury animals treated with intranasal insulin treatment following CCI had a significantly higher [¹⁸F]-FDG uptake in the ipsilateral hippocampus (A) than at baseline (*p=0.0329) and 2 days post injury (p=0.0189) (2 way ANOVA, Sidak's post-test).

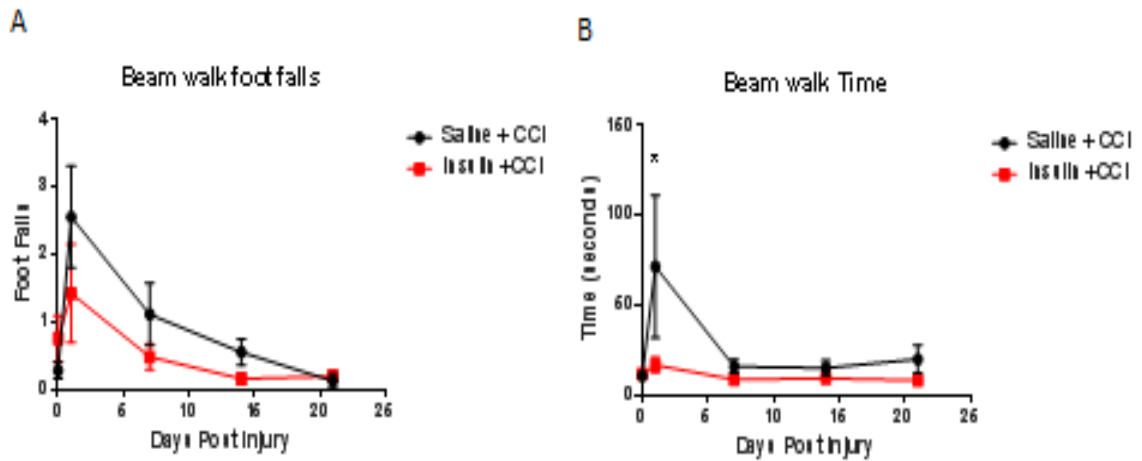


Figure 5. Intranasal insulin treatment after injury improves some aspects of motor function. After injury, both groups of animals (n=7/group) show a non-significant increase in footfalls indicating a deficit in motor function that recovers over time (A). However, animals treated with intranasal insulin after injury were able to cross the beam significantly faster than saline treated rats (*p<0.05; 2 way ANOVA, Sidak's multiple comparison test; B). Data are presented as an average of time and footfalls across the 4 widths of board the animals were trained to cross. Points represent mean +/- SEM.

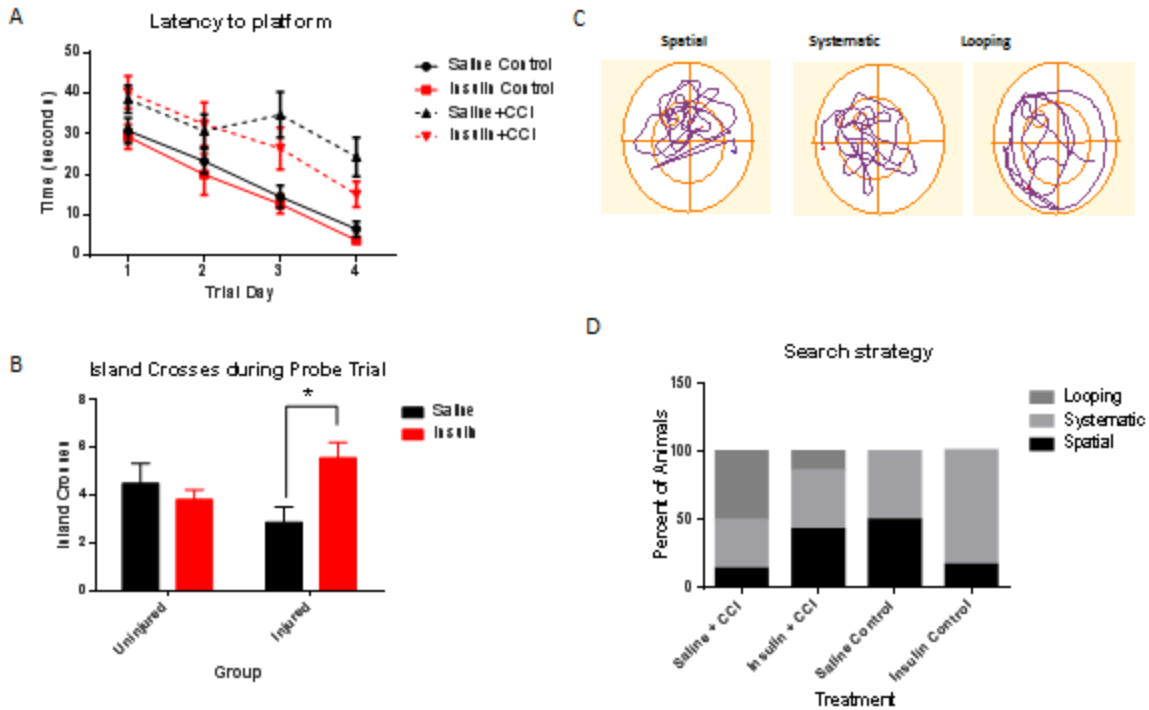


Figure 6. Intrasal insulin treatment improved memory function in Morris water maze tests. Animals treated with intranasal insulin or saline did not find the platform more quickly over the course of the learning trials in either the injured or uninjured cohorts (A) ($n=6/\text{group}$ uninjured, $n=10/\text{group}$ injured). However, during the probe trial, the injured animals treated with intranasal insulin ($n=7$) crossed the island location significantly more times ($*p=0.033$, 2 way ANOVA, Sidak's multiple comparisons test) than those treated with intranasal saline ($n=8$) (B). There was no significant difference in island crosses between the uninjured treatment groups ($n=6/\text{group}$). Search strategy utilized by rats during the probe trial was analyzed and categorized into one of 3 major groups (spatial, systematic, and looping) as previously described. (29) Representative patterns are shown (C), and number of animals utilizing each strategy during the probe trial was quantified. Saline and insulin treated uninjured animals (control) showed mostly spatial and systematic search strategies (D). A greater proportion of animals treated with saline after CCI showed a reduction in spatial search strategy and an increase in looping search methods. Likewise, fewer animals that received intranasal insulin for 14 days after injury displayed looping behavior than saline treated rats, and a return of spatial search strategy ($p < 0.0001$, Chi Square analysis).

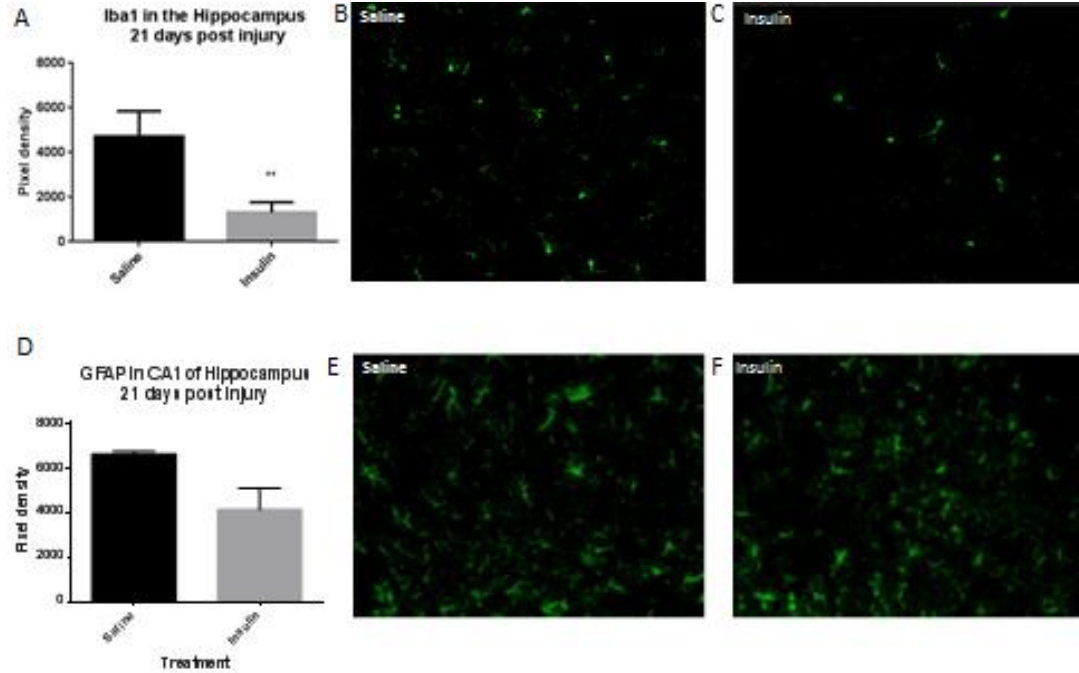


Figure 7. Treatment with intranasal insulin after CCI reduces macrophage/microglia but does not significantly reduce astrocyte activation. Quantification of Iba1, a marker of microglia and macrophages, revealed a significant reduction (** $p=0.0089$, two-tailed unpaired t-test) (A) in cells in CA1 of the ipsilateral hippocampus in animals treated with intranasal insulin (C) compared to intranasal saline (B) ($n=3$ per group). Quantification of GFAP, a cell surface marker of astrocytes, did not show a significant difference ($p=0.077$, two-tailed unpaired t-test) (D) between insulin treated ($n=4$) (F) and saline treated animals ($n=3$) (E).

Chapter 3: The effects of insulin on the inflammatory action and polarization of BV2 microglia

Fiona Brabazon B.A.¹, Sara Bermudez, M.S.², Guzal Khayrullina B.S.², Kimberly R. Byrnes, Ph.D.^{1,2,3}

¹ Neuroscience Program, Uniformed Services University of the Health Sciences, 4301 Jones Bridge Road, Bethesda, MD 20814

² Department of Anatomy, Physiology and Genetics, Uniformed Services University of the Health Sciences, 4301 Jones Bridge Road, Bethesda, MD 20814

³ Center for Neuroscience and Regenerative Medicine, Uniformed Services University of the Health Sciences, 4301 Jones Bridge Road, Bethesda, MD 20814

*Corresponding Author: Kimberly R. Byrnes, Ph.D.

Department of Anatomy, Physiology and Genetics

Room C2115

4301 Jones Bridge Road

Bethesda, MD 20814

Phone: 301-295-3217

Fax: 301-295-1786

kimberly.byrnes@usuhs.edu

ABSTRACT

Microglia are the macrophages of the central nervous system (CNS), which function to monitor and maintain homeostasis. Microglia activation occurs after CNS injury, infection or disease. Prolonged microglia activation is detrimental to the CNS as they produce nitric oxide (NO), reactive oxygen species (ROS) and pro-inflammatory cytokines, resulting in neuronal cell dysfunction and death. Microglia activation is implicated in the neurological deficits following traumatic brain injury (TBI) and Alzheimer's disease. Intranasal insulin administration is a promising treatment of Alzheimer's disease and TBI. The goal of this study was to specifically examine the effect of insulin administration on activated microglia. BV2 microglia were exposed to a pro-inflammatory stimulus, lipopolysaccharide (LPS), and then treated with insulin. Outcome measures were conducted at 24 hours after treatment. *In vitro* assays were used to evaluate NO and ROS production and, western blot and immunocytochemistry examined the effect of insulin on microglia polarization markers. Insulin treatment significantly reduced NO and ROS production following LPS activation. Insulin treatment had no significant effect on any M1 or M2 macrophage polarization markers examined. Insulin treatment also resulted in a reduction in two chemoattractants, JE/monocyte chemoattractant protein (MCP)-1 and macrophage inflammatory protein (MIP)-1A. These data suggest that insulin acts on microglia to reduce NO, ROS, and chemoattractant production. Therefore, administration of insulin to the CNS is a promising anti-inflammatory treatment.

KEYWORDS

Insulin, Microglia, Inflammation, Cytokines, Nitric Oxide

INTRODUCTION

Microglia are resident immune cells of the brain responsible for sensing and maintaining homeostasis. (120, 180, 253) In their quiescent state, microglia sample the surrounding environment with their long processes. (180) Microglial activation occurs in response to infection, injury, inflammation, neuronal cell death and cytokine release. (23) Microglia respond to a broad spectrum of stimuli including tumor necrosis factor α (TNF α), interleukin 6 (IL-6), and interleukin 1 β (IL-1 β) as well as lipopolysaccharide (LPS), a bacterial cell wall product. (140) Regardless of the source of stimulus, microglial activation results in a series of well-documented outcomes, including changes to cellular morphology including shortened processes and enlarged cell body. (239)

Microglial activation occurs along a spectrum that ranges from pro-inflammatory (M1) classical activation to anti-inflammatory (M2) alternative activation. (87, 140, 187) M1 activated microglia produce nitric oxide (NO), reactive oxygen species (ROS) and a number of pro-inflammatory cytokines. (173) NO plays an important role as a messenger but its prolonged release from microglia can be detrimental. NO and its degradation products are highly reactive and cause DNA deamination and neuronal cell death. (24, 204, 274) NO release is mediated by the expression of inducible NO synthase (iNOS). (138, 176) Intracellular microglia production of ROS promotes inflammation, and increased extracellular release over time overwhelms the antioxidant systems of neurons resulting in lipid peroxidation, oxidative protein modifications and cell death. (22, 65) Additionally, microglia release chemoattractants, such as monocyte chemoattractant protein (MCP-1), that draw more microglia to the site, increasing the inflammatory response. (56, 102, 281) The M2 phenotype produces anti-inflammatory cytokines and can be neuroprotective. (41, 236)

Microglial activation is an important aspect of the pathology of trauma and neurodegenerative diseases, such as traumatic brain injury and Alzheimer's disease. Additionally, dysfunction of the insulin receptor has been implicated in the pathology of Alzheimer's disease. (79, 165) Recent studies have shown that insulin administered directly to the brain via intranasal drug delivery can improve cognitive deficits associated with Alzheimer's disease and aging. (45, 150) A significant reduction in microglia was observed following intranasal insulin treatment in a mouse model of Alzheimer's disease. (40) Our lab has shown a significant improvement in memory function after moderate brain injury with intranasal insulin treatment (Brabazon et al, in review). Interestingly, this improvement in memory function was correlated with a significant reduction in microglial activation in the brain after intranasal insulin treatment similar to that observed by Chen et al. (40)

One recent study examined the effect of insulin on a primary human microglia and astrocyte cell line. (235) This work showed that insulin administration significantly reduced the production of monocyte chemoattractant protein-1 (MCP-1) but increased interleukin-8 (IL-8) release in human microglia cultures stimulated with a combination of IL-6, TNF- α and IL-1 β . This resulted in a significant reduction in microglial-induced toxicity to neuronal cells. However, the effect of insulin on microglial polarization and oxidative stress has not yet been established. Therefore, the purpose of this study was to examine the effect of insulin on activated microglia *in vitro*. This study verifies that insulin has an anti-inflammatory effect on the BV2 microglial cell line, reducing NO and chemokine production, which provides further support for the use of insulin in the treatment of Alzheimer's disease and neurotrauma.

METHODS

Study Design

The BV2 microglia cell line (a gift from Carol Colton, Duke University) was cultured in a humidified incubator at 37°C 5% CO₂/95% oxygen. BV2s are an excellent model of primary microglia inflammatory response following LPS stimulation. (100) The cells were maintained with Dulbecco's Modified Eagle Media (DMEM, Invitrogen) with 10% fetal bovine serum (FBS, Hyclone, Logan, UT, USA) and 1% penicillin/streptavidin (Fisher, Pittsburgh, PA, USA). BV2s were extracted from flasks with Accutase (Innovative Cell Technologies, San Diego, CA) after reaching confluency and plated at 1X10⁵/ml density for all experiments. Each outcome measure was repeated in triplicate.

Treatments

BV2 cells were treated with 125ng/ml of lipopolysaccharide (LPS) one hour prior to insulin treatment. Commercially available human recombinant insulin (Humulin R, Eli Lilly, Indianapolis, IN) was administered to BV2 cells with a dose range of 0.09μM, 0.18μM, 0.36μM, 0.72μM, and 1.45μM for 24 hours.

Nitric Oxide measurement

NO was measured in BV2s treated with insulin after LPS activation and a 24 hour incubation period. NO content in the media was quantified using a Griess reagent assay kit (Invitrogen, Grand Island, NY). The assay was performed per manufacturer's recommendations and as previously described. (33, 49) Colorimetric changes in 96-well plates were quantified with a Chroma Plate Reader (Midwest Scientific, St. Louis, MO, USA) at 545 nm.

Reactive Oxygen Species measurement

ROS production following each treatment paradigm was quantified per the manufacturer's recommendations and as previously described. (49) The assay measures the oxidation of 5 (and 6)-chloromethyl-20,70-dichlorodihydro-fluorescein diacetate-acetyl ester (CM-H2DCFDA; Molecular Probes, Eugene, OR). Briefly, media from microglia plated into 96-well plates was removed and replaced with warmed PBS. CM-H2DCFDA (10 μ M) was added to the plate wells and incubated for 45 minutes. Fluorescence was measured using excitation wavelengths of 492-495 nm and emission wavelength of 517-527nm.

Immunocytochemistry

Cells were plated on coverslips and fixed with 4% paraformaldehyde at 24 hours for immunocytochemistry analysis. Cells were incubated with blocking agent for 15 minutes then incubated overnight with primary antibody. The primary antibodies for analysis of microglia polarization state were CD206 (1:500, Abcam, Cambridge, MA, USA) and iNOS (1:500, Cell Signaling, Danvers, MA, USA). Slides were incubated for one hour with a secondary fluorescent antibody (Alexa-Fluor Secondaries, Invitrogen, Grand Island, NY, USA) for one hour then coverslipped with hard set DAPI mounting media (Vectashield, Vector Laboratories, Inc., Burlingame, CA, USA). Five randomly chosen images at 20X magnification were collected from each coverslip for quantification using Scion Image Analysis (<http://rsb.info.nih.gov/nih-image>). Density of immunolabeled protein above a threshold standardized between coverslips was normalized to number of DAPI positive cells, obtained using ImageJ (<http://imagej.nih.gov/ij/>, NIH, Bethesda, MD). (220)

Protein Quantification

Protein was collected from cells 24 hours post treatment. Cells were lysed, treated with protein inhibitor (Halt Protease Inhibitor single use cocktail, Thermo Scientific) then centrifuged. The supernatant was collected and western blot analysis was performed as previously described. (50) Briefly, 25 µg of protein sample was run on a Mini-protean TGX precast gel then transferred to a nitrocellulose sheet (Trans-Blot Turbo Transfer System, Biorad, Hercules, CA, USA). The nitrocellulose sheet was blocked for one hour then incubated overnight with the following antibodies: CD86 (1:5000, Abcam, Cambridge, MA, USA), YM1 (1:1000, Cell Signaling, Danvers, MA, USA), 3-NT (1:500, Abcam, Cambridge, MA, USA). Resultant bands were quantified with Image J densitometry and normalized to a loading control protein, GAPDH (1:5000, Millipore, Billerica, MA, USA).

Oxyblot

The OxyBlot Protein Oxidation Detection Kit (Millipore) was conducted per the manufacturer's instructions. Briefly, protein samples were treated with 1X 2,4-dinitrophenylhydrazine (DNPH) Solution followed by a neutralization solution for derivatization reaction. A protein sample for each specimen was not subjected to derivatization reaction and thus served as a control. Samples were then run on a mini-protean TGX precast gel and then transferred to a nitrocellulose sheet (Trans-Blot Turbo Transfer System, Biorad, Hercules, CA, USA). After one hour blocking at room temperature, the nitrocellulose sheet was incubated for one hour with the primary antibody, after which it was washed and incubated with secondary antibody. The sheet was developed and the entire row was taken per sample for quantification using Image J

densitometry. Samples were normalized to the GAPDH loading control protein (1:5000, Millipore, Billerica, MA, USA.)

Cytokine Panel

Cytokines expressed by BV2 microglia were quantified using the Proteome Profiler Mouse Cytokine Array Panel (R&D Systems, Minneapolis, MN, USA). The assay was conducted per the manufacturer's instructions on 1000 µg of protein collected from the cell supernatant (n=3 per group). Quantification of the resultant array was conducted using the density slice function of Scion Image. All measurements were normalized to the average of three control spots provided by the manufacturer on the array.

Statistical Analysis

Statistical analysis was conducted using Graphpad Prism Software version 6.01 (GraphPad Software, San Diego, CA, USA). NO and ROS assays were conducted in triplicate for each trial, and the trials were replicated 3 times to generate a sample size of n=3 per group. A one way ANOVA, Dunnett's multiple comparisons test was conducted on the averages of each trial for NO and ROS assay measures. Immunocytochemistry and western blot measurements were analyzed with a one way ANOVA, Dunnett's multiple comparisons test. Proteome profiler results were analyzed using a two way ANOVA, with Tukey's post test. For all statistical tests described, a p value < 0.05 was considered statistically significant. Data is presented as mean +/- standard error of the mean (SEM).

RESULTS

Insulin treatment significantly reduced NO and ROS production.

To examine the effects of insulin treatment on activated microglia, BV2 microglia were activated with LPS (125 μ g) for one hour. Following this incubation, cells were treated with insulin (0.09 μ M, 0.18 μ M, 0.36 μ M, 0.72 μ M, or 1.45 μ M). NO and ROS assays were conducted 24 hours after the addition of insulin. Control cells not treated with LPS were treated with insulin at the same time with the same doses. There was a significant effect of LPS ($p < 0.0001$; 2 way ANOVA, no multiple comparisons) but no significant interaction ($p = 0.9460$) or effect of insulin ($p = 0.3644$). Insulin alone did not significantly affect NO release (Fig. 8A, one way ANOVA). LPS treatment significantly increased NO release compared to control (Fig. 8A; $p = 0.0467$, one way ANOVA, multiple comparisons, Sidak's multiple comparisons test). However, insulin was able to significantly reduce NO production in BV2 microglia following LPS activation at 0.36 μ M ($p = 0.0401$), 0.72 μ M ($p = 0.0374$), or 1.45 μ M ($p = 0.0487$; one way ANOVA, multiple comparisons to LPS as control, Sidak's multiple comparisons test).

LPS treatment also significantly increased the production of ROS in BV2 microglia compared to control (Fig. 8B; $p < 0.0001$, one way ANOVA, multiple comparisons, Dunnett's multiple comparisons test). BV2 microglia treated only with insulin did not show any significant difference in ROS production compared to control. There was a significant interaction ($p = 0.1185$) but there was a significant LPS factor ($p < 0.0001$) and insulin factor ($p = 0.0191$). (2 way ANOVA, no multiple comparisons). There was a significant reduction in ROS production with insulin treatment at 0.09 μ M

($p=0.0497$), $0.18\mu\text{M}$ ($p=0.0319$), $0.36\mu\text{M}$ ($p=0.0173$), and $0.72\mu\text{M}$ ($p=0.0159$; one way ANOVA, multiple comparisons to LPS alone, Sidak's post test).

Protein tyrosine nitration or protein carbonylation were not significantly altered by insulin.

Protein tyrosine nitration was quantified using 3-NT antibody. Protein samples ($n=3$ per group) were prepared for Western blot at 24 hours after treatment. Bands observed were pooled for quantification of total protein nitrosylation (Fig. 2B). There was no significant difference observed in 3-NT expression observed between the treatment groups (Fig. 9A). There was no significant effect of interaction ($p=0.9055$), LPS ($p=0.8367$) or insulin ($p=0.9726$; 2 way ANOVA). The Oxyblot assay (Millipore) was used for the detection of carbonyl groups introduced into proteins. The entire lane was quantified for each protein sample and normalized to GAPDH (Fig. 9D). There was no significant difference in protein carbonylation detected between groups (Fig. 9C). There was no significant effect of interaction ($p=0.6448$), LPS ($p=0.5983$) or insulin ($p=0.8410$; 2 way ANOVA).

Insulin treatment did not significantly alter expression of an M1 markers, iNOS or CD86.

Microglial polarization was assessed by the quantification of well-established polarization markers. iNOS and CD86 are associated with M1, or classically activated microglia. Following one hour LPS activation, BV2 microglia were treated with insulin. The expression of CD86 was quantified using western blot and normalized to GAPDH (Fig. 10A, B). There was no significant interaction ($p=0.2478$) or effect of LPS ($p=0.4727$) or insulin ($p=0.3641$) on CD86 expression. LPS treatment resulted in a non-

significant increase in CD86 expression (Fig.10A). Insulin treatment did not affect CD86 expression in either LPS treated or control cells.

iNOS expression was quantified following a 24 hour incubation by immunocytochemistry. The density of expression was quantified (n=5 for control and insulin alone, n=6 for LPS and LPS+insulin, representative images shown in Fig. 3D). The density of iNOS positive pixels was normalized to the number of DAPI positive nuclei (Fig. 10D). There was no significant interaction (p=0.8775) or insulin effect (p=0.0099) but there was an LPS effect (p=0.5239; 2 way ANOVA). LPS alone resulted in a non-significant increase iNOS expression in BV2 cells compared to control (p=0.1663, one way ANOVA, multiple comparisons, Dunnett's multiple comparisons test) and insulin alone (p=0.571, one way ANOVA, multiple comparisons, Dunnett's multiple comparisons test) (Fig. 10C). 0.36 μ M insulin did not significantly alter iNOS expression compared to control (Fig. 10C). iNOS expression was not significantly decreased in cells treated with 0.36 μ M insulin after LPS compared to LPS alone (Fig. 10C).

Insulin treatment did not significantly alter M2 polarization marker expression.

The expression of two markers of the anti-inflammatory (M2) microglia phenotype, CD206 and YM1, were quantified following insulin and LPS treatment. YM1 expression was quantified using western blot (n=3 per group). There was no significant interaction (p=0.7092) or effect of insulin (p=0.6685) but LPS treatment did result in a significant reduction in YM1 expression (p=0.0493; 2 way ANOVA).

CD206 expression was measured following 24 hour incubation by immunocytochemistry. Expression was quantified (n=5 per group for control, insulin

alone and LPS, n= 4per group for LPS+insulin, representative images shown in Fig. 11D). There was no significant interaction ($p=0.6770$) or effect of insulin ($p=0.4058$) or LPS ($p=0.7084$) on CD206 expression (Fig 11 C). (2 way ANOVA)

Insulin treatment reduced the release of microglia chemoattractants.

A panel of cytokines was quantified using a mouse Proteome Profiler cytokine array. Samples were collected following a 24 hour incubation (n=3 per group). Significant changes were observed in IL-1 α , IL-1 β , JE/MCP-1 and MIP-1A. IL-1 α and IL-1 β , cytokines released by pro-inflammatory microglia, were significantly increased with LPS treatment, verifying the validity of the assay and LPS dose. There was a significant increase in IL-1 α in LPS treated samples compared to control ($p<0.0001$, 2 way ANOVA, Tukey's post test; Fig. 12A). Insulin did not significantly alter IL-1 α expression after LPS exposure, although there was a trend toward reduction, IL-1 α in this group remained significantly elevated above control ($p=0.019$, 2 way ANOVA, Tukey's post test). There was no detectable IL-1 β in insulin alone samples and a significant increase in IL-1 β in controls compared to LPS treated ($p=0.0027$, 2 way ANOVA, Tukey's post test, Fig. 12B). There was no significant difference in IL-1 α or IL-1 β between insulin alone and control (Fig.12 A, B). LPS produced a non-significant increase in JE/MCP-1 and MIP-1A production compared to controls (Fig. 12 C). Insulin significantly reduced the release of JE/MCP-1 (Fig. 12 C), a microglia chemoattractant, after LPS treatment ($p= 0.0116$, 2 way ANOVA, Tukey's post test). Insulin treatment also significantly reduced the expression of MIP-1A (Fig. 12 D) following LPS exposure ($p= 0.0131$, 2 way ANOVA, Tukey's post test).

DISCUSSION

This study provides important information on the inflammatory response and polarization of BV2 microglia in response to insulin. This research is relevant to both brain trauma and Alzheimer's disease research as microglia activation and insulin dysregulation have been implicated in their pathology. Our data shows that insulin treatment can reduce NO and ROS production in activated microglia. However, insulin treatment did not significantly alter expression of markers of M1, iNOS and CD86, or M2, CD206 and YM1, microglia polarization. Furthermore, treatment with insulin significantly reduced the production of JE/MCP and MIP-1A, both of which function as chemoattractants.

Previous studies have examined the effect of insulin on the inflammatory response and polarization of cells in the periphery. Insulin treatment has been shown to reduce the production of NO and iNOS expression in peripherally circulating macrophages in a rodent model of diabetes. (238) Our study shows that insulin treatment has a similar effect on microglia, the macrophages of the CNS. We show a significant decrease in NO production following LPS stimulation with 0.36 μ M dose of insulin (Fig. 8 A). The observed reduction in NO expression did not correlate with a reduction in iNOS production. Our study does not show a significant reduction in iNOS expression in LPS stimulated BV2 microglia after a 24 hour treatment with insulin. It is important to establish the similarities and differences in responses of microglia and peripheral circulating macrophages as they differ in their origin and in some activities.

NO plays an important role in normal function but the excess amount produced as a result of prolonged microglia activation can be detrimental. (203) This is the result of protein tyrosine nitration, a post translational modification that damages protein

function. Excess NO production can result in the nitration of heat shock protein (HSP) 90, which results in cell death. (75, 122) 3-NT staining was used to assess the amount of protein tyrosine nitration. While our study shows a significant increase in NO production (Fig. 8A), there was no significant difference observed in 3-NT at 24 hours. Previous studies that have shown an increase in protein tyrosine nitration in BV2 cells at 24 hours used LPS doses 5-10 times higher than our study. (122) Additionally, protein tyrosine nitration is an accumulating effect that requires time, and therefore protein samples collected at 48 hours post-treatment or with a higher LPS concentration may show the downstream effects of increased NO.

There was a significant reduction in ROS production in LPS stimulated BV2 microglia treated with insulin (Fig. 8 B). Oxidative stress damage was also measured by the use of Oxyblot (Fig. 9 D). We did not detect a significant difference in the carbonylation of proteins as measured (Fig. 9 C). While we did detect a significant increase in ROS production in LPS treated cells compared to control this did not result in a significant change in protein carbonylation. This may be attributed to the time at which protein was collected. Later time points may allow for accumulated ROS to damage proteins in a more significant manner.

It is worthwhile to note that LPS is a particularly strong activator of microglia that resulted in a significant increase in ROS production compared to controls (Fig 8 B). Different activators of microglia like tumor necrosis factor alpha (TNF- α) or IL-6 may produce an activity level that is more amenable to insulin treatment. This was reported in the work of Spielman et al, which showed a significant reduction in IL-8 production as well as MCP-1, but ROS were not measured. (235)

M1 and M2 polarization states are a useful way to identify the overall activity of a cell, but it is important to note that polarization state is neither permanent nor finite. CD86 and iNOS are markers of M1 microglia/macrophage polarization. The M1 phenotype is pro-inflammatory and over time causes neuronal cell death. CD206, or mannose receptor, and YM1, or chitinase 3-like 3, are markers of M2 microglia polarization. It is also important to note that the shift between these two states in response to stimuli may result in the expression of both M1 and M2 markers. (121) This is why measures of cellular response, such as NO, ROS, and cytokine release, are important to analyze in addition to these M1 and M2 markers. We observed a significant reduction in NO and ROS, indicating that treatment with insulin promoted anti-inflammatory activity, even though we did not observe a robust change in polarization markers. Insulin's role in peripheral macrophage polarization and inflammation has been studied in the context of metabolic disorders including obesity and diabetes. Obesity and insulin resistance often present with an increase in pro-inflammatory M1 macrophages in the periphery. (268, 278) Specifically, previous work has shown a significant increase in IL-10, a marker of M2 polarization, in lean animals compared to obese. (146) This protects them from the detrimental effects of TNF- α . and IL-6, which can block insulin action in adipocytes. (95, 146)

Additional insight about polarization was gained from the cytokine panel used to examine the effect of insulin on microglia activation. Insulin alone did not significantly alter the expression of cytokines compared to control (data not shown). The assay verified that LPS administered at 125 ug/mL significantly increased classical markers of microglia activation including IL-1a (Fig. 12 A) and IL-1b (Fig. 12 B). (67) There was

no significant reduction in other pro-inflammatory cytokines. Our assay did not detect IL-10, an anti-inflammatory cytokine, production in any of the experimental paradigms tested. The broad cytokine panel may limit the sensitivity of the assay. Previous studies have shown a link between IL-10 production and insulin resistance in peripheral macrophages so future studies may address this specific cytokine. (104)

Despite a lack of significant effects on cytokines, our data shows a significant decrease in two major microglia chemoattractants. Insulin treatment following a one hour activation period with LPS significantly reduced the expression of JE/MCP-1 from BV2 cells. JE is a gene identical to monocyte chemoattractant 1 (MCP-1). (46, 56) MCP-1 is responsible for recruiting pro-inflammatory macrophages to the site. (116, 182) Additionally our cytokine array panel showed a significant reduction in MIP-1A in BV2 cells treated with insulin after LPS exposure. MIP-1A is a β -chemokine that binds to the chemokine receptor CCR5 and is also involved in the recruitment of macrophages. (85, 269) Previous *in vitro* work showed a significant reduction in MCP-1 in human microglia with insulin treatment following activation with IL-6, TNF- α , and IL-1 β . (235) These data support previous *in vivo* work in our lab that showed a significant reduction in microglia in the brain following TBI with intranasal insulin treatment (Brabazon et al 2016). Intranasal administration allows insulin to act directly on the brain and therefore likely directly reduced microglia chemoattractant production thus the lower numbers observed.

In conclusion, much of our study serves to validate findings observed in other models showing a correlation between insulin treatment and a reduction in NO, ROS, and chemokines in macrophages/microglia. Our study further examines the effect of insulin

treatment on ROS production, a panel of cytokines and microglia polarization. Our study is also novel as it expands on the new field examining the effect of insulin on the CNS, which was previously thought to be insulin insensitive. This work is also important due to the increased use of intranasal insulin as a treatment of CNS disorders including Alzheimer's disease and TBI. (52, 167) Together these data validates the use of BV2 microglia as a model of insulin effects on inflammation as these cells behaved similarly to responses observed in studies of human microglia.

ACKNOWLEDGEMENTS

This study was funded by the Uniformed Services University of the Health Sciences Student Grant T0-70-3278, with support for FB, SB and GK by NIH grant number 1R01NS073667-01A1. The authors would like to thank Dr. Josh Duckworth, Dr. Barrington G. Burnett and Young Yauger for their technical assistance and consultation on this project.

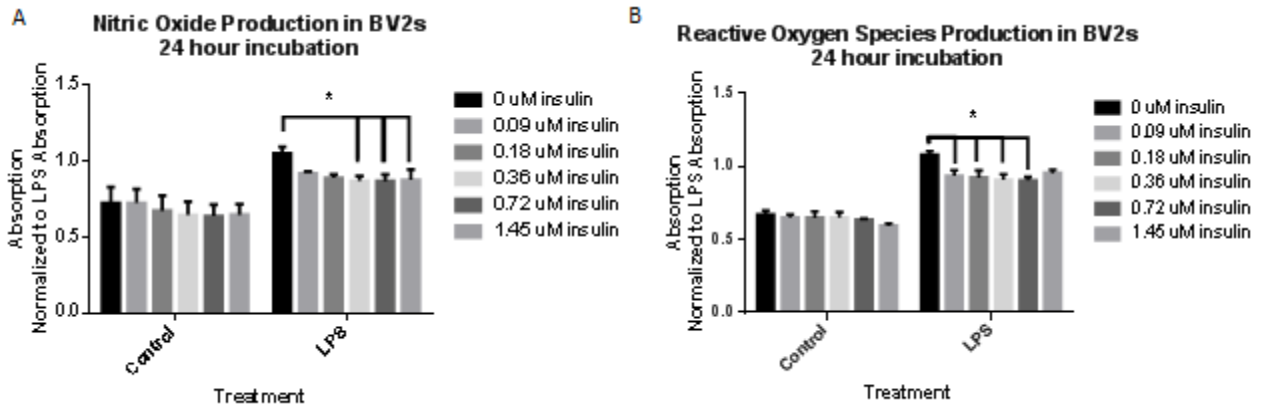


Figure 8. Insulin treatment significantly reduces NO production. BV2 microglia incubated with LPS showed a significant increase in NO production (Fig. 1A; $p < 0.0001$, two way ANOVA) (A). Insulin treatment after LPS was able to significantly reduce NO production in BV2 microglia ($p < 0.05$, one way ANOVA, multiple comparisons, Sidak's multiple comparisons test) (A). Insulin alone did not significantly alter NO release compared to control cells at any dosage. LPS significantly increases the production of ROS in BV2 microglia ($p < 0.0001$, two way ANOVA) and insulin significantly alter ROS production ($*p = 0.0191$, two way ANOVA) (B). Insulin reduced ROS production after LPS at $0.09 \mu\text{M}$ ($p = 0.0497$), $0.18 \mu\text{M}$ ($p = 0.0319$), $0.36 \mu\text{M}$ ($p = 0.0173$), and $0.72 \mu\text{M}$ ($p = 0.0159$). (One way ANOVA, multiple comparisons to LPS alone, Sidak's post test). All experimental conditions were repeated in triplicate. p value indicated by $*p < 0.05$. Bars are mean \pm SEM.

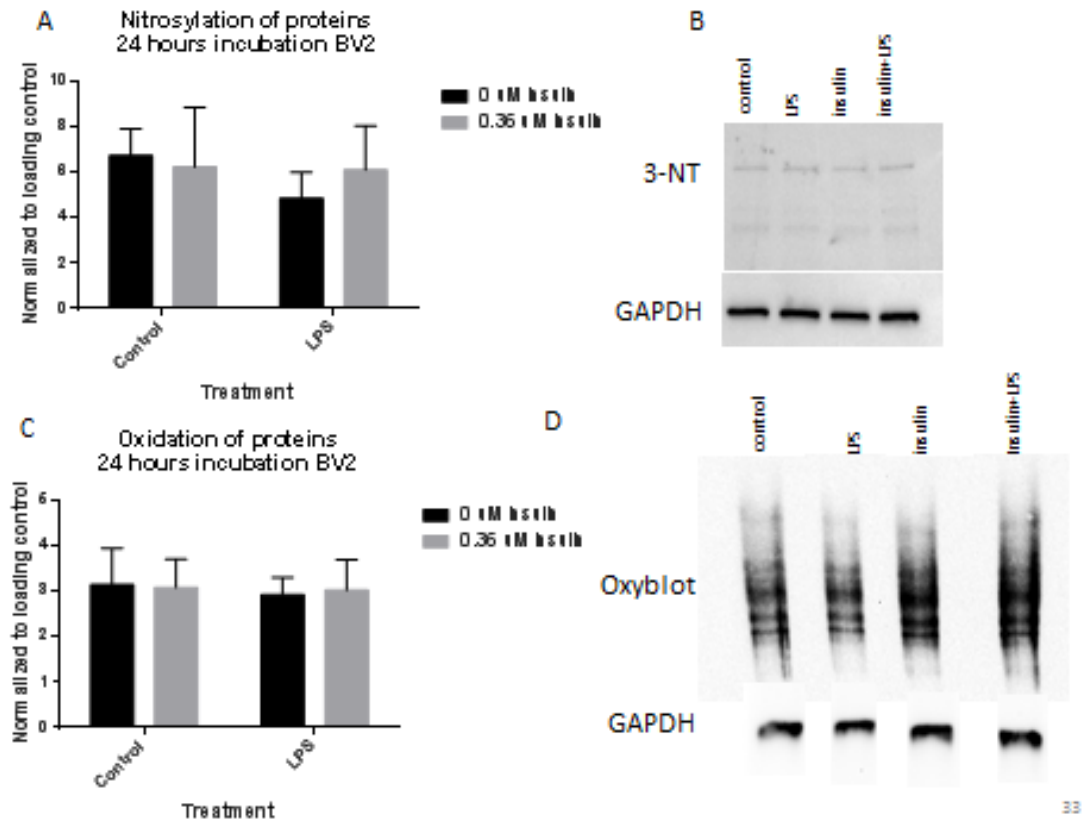


Figure 9. Insulin treatment did not alter protein nitrosylation or carbonylation. Protein tyrosine nitration was quantified using 3-NT antibody. Bands observed were pooled for quantification of total protein nitrosylation then normalized to loading control protein, GAPDH (B). There was no significant difference observed with 3-NT (A) between the treatment groups (n=3 per group). The Oxyblot assay did not detect a significant change in carbonyl groups introduced into proteins (Fig 2 C, n=3 per group). The entire lane was quantified for each protein sample and normalized to GAPDH (Fig. 2D).

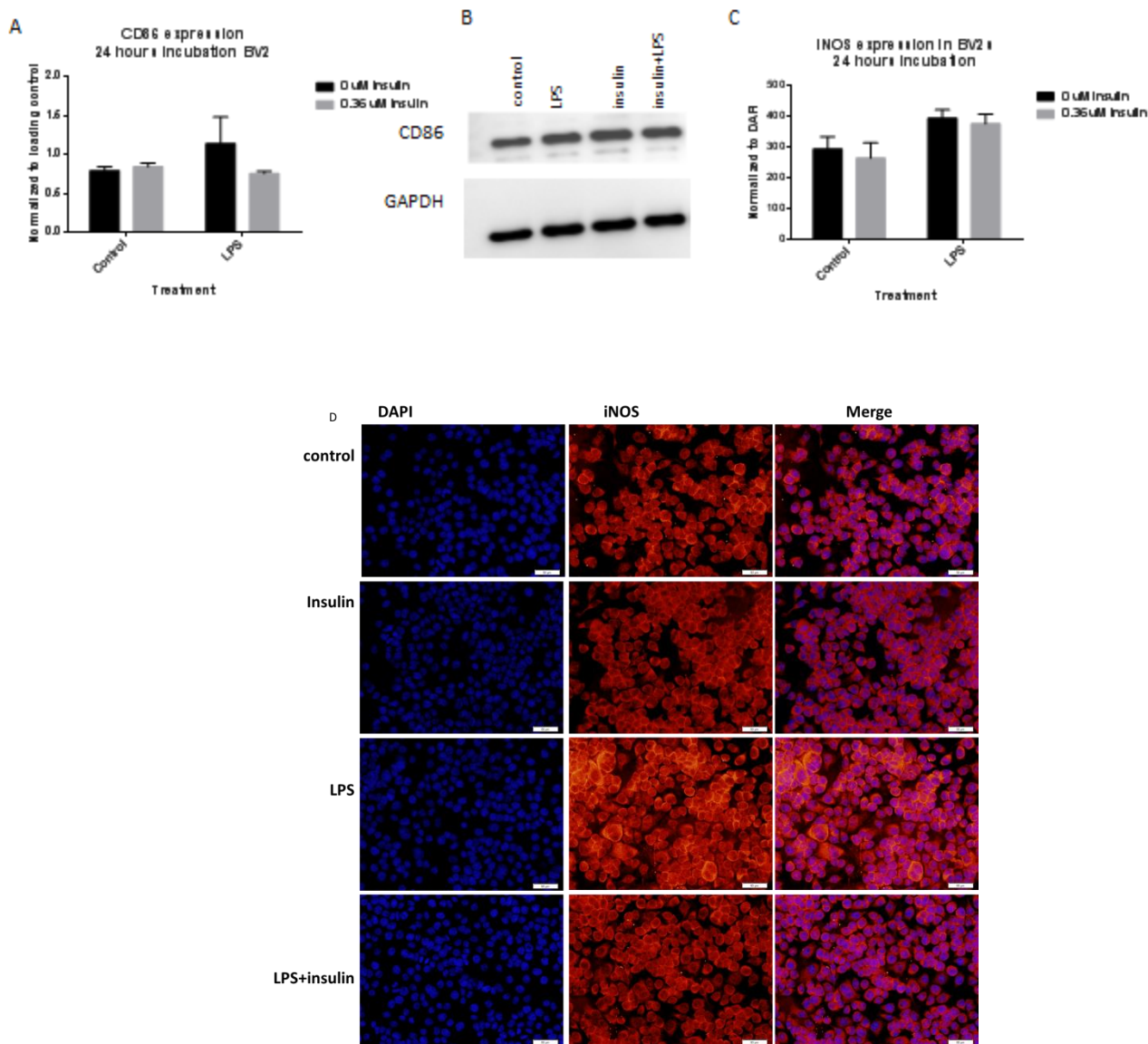


Figure 10. Insulin treatment does not reduce expression of M1 polarization markers, iNOS and CD86. Insulin treatment did not alter expression of CD86 after LPS or in controls as measured by western blot (n=3 per group) (A). LPS exposure resulted in a non-significant increase in CD86 expression (A). Representative bands of CD86 and GAPDH are displayed as a stitched image (B). iNOS expression was not altered in cells treated with insulin after LPS compared to LPS alone (C) as measured by immunocytochemistry. A significant effect of iNOS was observed with LPS treatment (p=0.0099, 2 way ANOVA). Bars are mean +/- SEM.

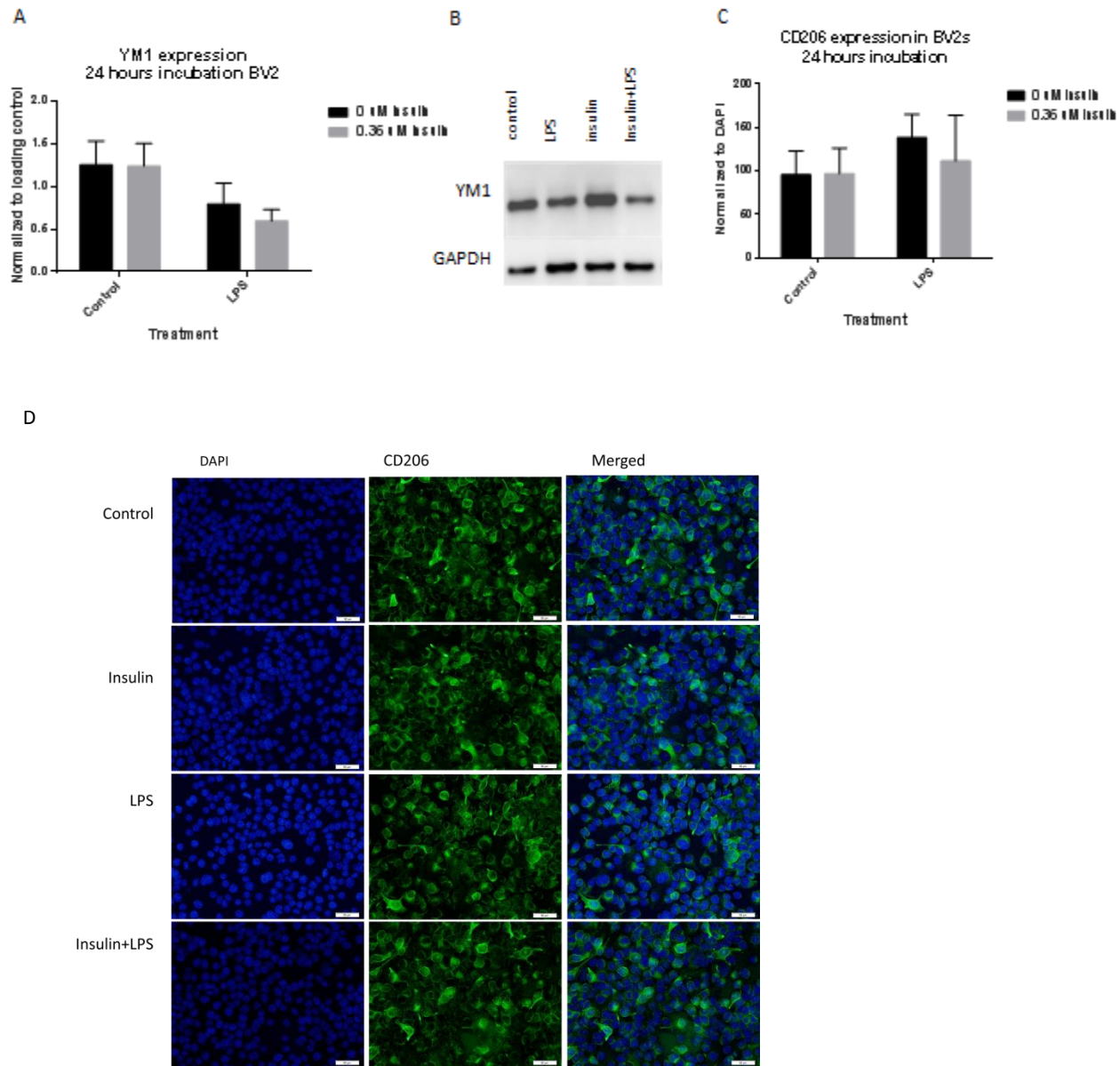


Figure 11. Insulin treatment does not alter expression of M2 polarization markers YM1 and CD206. Insulin treatment did not alter expression of YM1 after LPS as measured by western blot (n=3/ per group) (A). LPS exposure resulted in a significant decrease in YM1 expression (p=0.0493, 2 way ANOVA) (A). Representative bands of YM1 and GAPDH are displayed as a stitched image (B). CD206 expression was not altered in cells treated with insulin after LPS compared to LPS alone (C) as measured by immunocytochemistry (D). Bars are mean \pm SEM

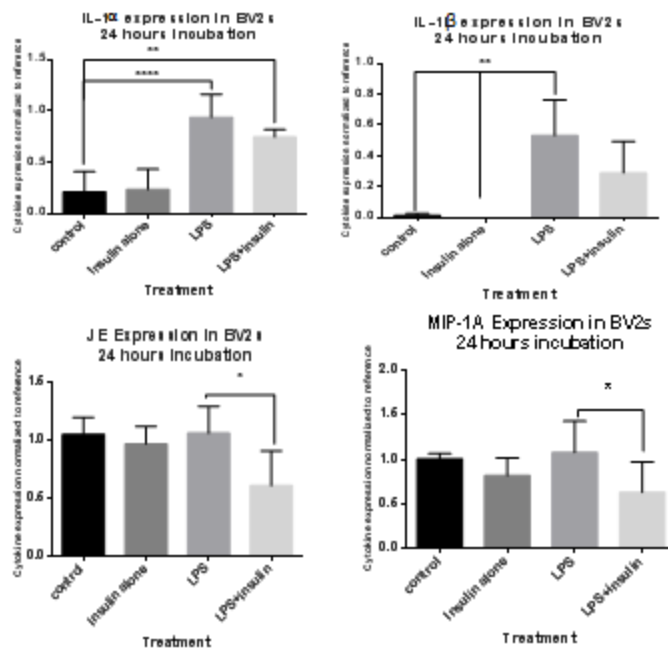


Figure 12. Insulin treatment reduces the release of microglia chemoattractants. A panel of cytokines show a significant increase in IL-1 α (**** p <0.0001 LPS vs control; ** p <0.01 LPS/Insulin vs. control, 2 way ANOVA, Tukey's post test; A) and IL-1 β (** p =0.0027 LPS vs. control and insulin alone, 2 way ANOVA, Tukey's post test) following LPS exposure (B). Insulin significantly reduced the release of JE (C), a microglia chemoattractant, after LPS treatment (* p =0.0116, 2 way ANOVA, Tukey's post test, n =3 per group). Insulin treatment also significantly reduced the expression of MIP-1A (D) following LPS exposure (* p =0.0131, 2 way ANOVA, Tukey's post test, n =3 per group) as it was also elevated in LPS treated cells compared to controls. Bars represent mean \pm SEM.

Chapter 4: Discussion

The development of a treatment for TBI is an important public health effort. The pathology of TBI is not fully understood. This study provides further insight into the mechanism of the metabolic crisis observed in humans and verified in animal models by quantifying GLUTs and IR after injury. Further, the data presented in Chapter 2 of this manuscript provides a potential treatment option that addresses the neurometabolic crisis observed after TBI. Additionally, the work presented in Chapter 3 examines the potential anti-inflammatory effect of insulin by characterizing the response of activated microglia to insulin treatment in an *in vitro* model.

The primary objective of this dissertation was to investigate the treatment of TBI with intranasal insulin. The examination of the role of insulin after TBI is not, in itself, novel. Previous work has examined peripheral insulin administration to control post-injury hyperglycemia after TBI with promising results. (21, 286) Clinical research has shown that diabetic patients with TBI have a greater risk of mortality primarily due to insulin deficiency, instead of elevated blood glucose, suggesting that insulin plays a crucial role in recovery. (131)

The administration method, intranasal, however, is novel and provides significant advantages over traditional peripheral administration as it allows for direct treatment of the brain. (94) This therapeutic approach was developed based on similarities between TBI and Alzheimer's disease: cerebral hypometabolism and impaired memory function. (19, 169, 263) These deficits in Alzheimer's disease are proposed to be a result of cerebral insulin resistance and a reduction in insulin receptor density. (79, 267) While

our study did not find a significant reduction in IR density after injury, we did find that with intranasal insulin treatment, we observed significant improvement in memory function and increased [¹⁸F]-FDG uptake in the hippocampus. These findings (increased [¹⁸F]-FDG uptake with improved memory function) are analogous to the response observed in Alzheimer's disease patients treated with intranasal insulin. (17, 52)

Additionally, we found a significant reduction in Iba1 in the hippocampus, in research presented in Chapter 2. Only one previous study has documented a reduction in microglia following intranasal insulin in 3xTg-AD mice, a model of Alzheimer's disease. (40) The final objective of this dissertation was to therefore expand upon this finding and examine the effect of insulin on activated microglia using an in vitro model. Previous work has primarily focused on the effect of intranasal delivery on neuronal health. (150, 280, 287) It is important to examine the effect of insulin on glial populations as their responses directly affect neuronal viability and function. The in vitro model allowed us to identify a potential pathway by which insulin reduced microglia activation in the hippocampus. The data presented in Chapter 3 shows that activated microglia respond to insulin by reducing production of NO, ROS, and two chemokines, JE/MCP-1 and MIP-1A. These reductions suggest that with intranasal insulin treatment, fewer microglia are recruited to the site and those present produce less NO and ROS. Collectively our data suggests that intranasal insulin treatment alters the metabolic and inflammatory pathways following TBI to improve cognitive performance.

GLUCOSE TRANSPORTERS AND INSULIN RECEPTOR EXPRESSION AFTER CCI

CCI did not cause a significant reduction in GLUTs or IR at 24 hours post injury. This data lends insight into the mechanism of hypometabolism after TBI. This study

suggests that significant GLUT reduction is not necessary to result in decreased cerebral glucose uptake after TBI. Our study examined the expression of GLUTs 1, 3, and 4 and IR at 24 hours after a CCI injury in an effort to expand previous studies on GLUTs after TBI (51, 92) and correlate receptor expression with [¹⁸F]-FDG PET uptake patterns previously observed in our lab at this time point. Previous work in a rodent model of TBI showed a significant decrease in GLUT 3 in the cerebellum after TBI, (92) which was not detected in our study. A trend toward decreased GLUT 3, the primary neuronal GLUT, was observed in our study but did not reach significance. These differences can be attributed to differences in the models and the size of the region examined. The large sample region may have resulted in a wash out effect on significance in the lesioned area by the lack of change in expression in non-lesioned tissue. Future studies will examine smaller regions of interest near the lesion for more precise measures. In addition, as the effect of the weight drop model on glucose uptake has not been established, it is possible that the different models of injury result in a different time course of the metabolic crisis.

While we did not observe a significant decrease in IR expression, we did observe a trend ($p=0.0939$). No previous study has examined IR expression after TBI; one recent study has examined insulin receptor sensitivity. (117) This study was conducted in a mouse model of closed head injury and showed a decrease in phosphorylation of AKT, a downstream mediator of the insulin pathway, following insulin exposure. Presence of a receptor is not a definitive marker of functionality. Our study provided important data to move the field forward but future studies could enhance the current experimental design. This could be achieved by examining downstream targets such as the phosphorylation of AKT or insulin receptor substrate-1 (IRS-1). Further insight about the functionality of

the GLUTs following TBI could be obtained from cerebral metabolic rate of glucose consumption (CMRGlc) assays and PET imaging of [¹⁸F]-FDG. These assays do not provide detail on which specific GLUT is active, so data collected could be analyzed in tandem with protein analysis. Additionally, an immunohistochemical analysis of the co-localization of GLUTs with markers of CNS cell type would provide additional valuable information about metabolic activity of specific cell populations after injury.

TBI DID NOT INHIBIT DELIVERY OF INSULIN ALONG THE INTRANASAL PATHWAY

This is the first study to show successful delivery of insulin to the CNS via intranasal administration in a rodent model of TBI. [¹²⁵I] Insulin was detected in all regions examined with the highest concentration in the olfactory bulb, followed by the cerebellum, brain stem, hippocampus and cortex, respectively. This distribution of [¹²⁵I] insulin is strongly supported by previous work showing that insulin receptors are most abundant in the olfactory bulb, followed by the cerebellum, pyriform cortex, hippocampus, choroid plexus and hypothalamus in the rodent brain. (154) Localization and density of insulin receptor is well conserved across species, including humans, and there is a wide spread distribution of receptors suggesting that efficient delivery of intranasal insulin to the brain in human patients after TBI. (105)

There was no significant difference between the ipsilateral and contralateral sides of any of the brain regions examined and delivery was confirmed in all brain regions examined. This indicates that the injury does not significantly hinder delivery of insulin along the previously shown intranasal pathway. (28, 250) Intranasal insulin drug delivery has been widely studied in the context of Alzheimer's disease, in both pre-clinical and clinical studies. Intranasal administration allows insulin to bypass the blood-

brain barrier, which typically regulates the flow of insulin into the brain by a saturable receptor transport system. (12, 15) The pathway of insulin following intranasal delivery is to pass through the olfactory mucosa then the cribriform plate where it enters the anterior layers of olfactory bulbs by the olfactory nerve pathway. (209) We examined insulin localization at one time point after administration. Earlier time points may provide verification of drug delivery along the previously described pathway and the time it takes for the drug to reach the target brain regions. Later time points would provide valuable information about the degradation of insulin after intranasal administration. An additional alternative method would be the use of a pressurized olfactory delivery system as opposed to a traditional pipettor approach, as this system improves brain penetrance. (103)

INTRANASAL INSULIN ADMINISTRATION IMPROVED COGNITIVE FUNCTION WITHOUT SIGNIFICANT PERIPHERAL EFFECTS

Our study examined the effect of intranasal insulin on two systemic outcome measures, weight and blood glucose, to verify intranasal insulin action was focused in the CNS. These outcome measures have been previously used in studies that examined intranasal insulin treatment of Alzheimer's disease, diabetes, and weight loss but not in TBI. We found no significant difference in weight between insulin and saline treated rats at any time point in both the injured and uninjured cohorts. One clinical study showed that intranasal insulin can significantly reduce body weight and body fat in lean male, but not female, subjects. (91) Subjects in this study received about 0.5 IU per kg 4 times a day, or 2 IU per kg total a day, for 8 weeks, based on average subject start weight. Our dose, considering the average weight of the rats, was about 0.15 IU per kg only once a

day. This means that a dose 13 times higher than used in our study was necessary to reduce weight.

We also measured blood glucose and found no significant difference between the groups treated with intranasal insulin or saline after brain injury, demonstrating that neither injury nor insulin administration altered systemic glucose concentration. Previous work has proposed intranasal insulin as an appropriate glycemic control for diabetics. (189) This study administered insulin intranasally every 15 minutes and a dose of 30 IU significantly reduced blood glucose. (189) In clinical trials of intranasal insulin treatment of Alzheimer's disease in unfasted individuals, a single dose of 40 IU resulted in improved memory recall but did not significantly alter blood glucose. (52) These data, and ours, show that in order to elicit a peripheral response (weight loss or hypoglycemia) to intranasal insulin, dosing must be administered frequently and significantly higher than that needed to improve cognitive function.

INTRANASAL INSULIN TREATMENT DID NOT PRODUCE SIGNIFICANT MOTOR FUNCTION IMPROVEMENT AFTER CCI

Motor deficits are observed after TBI if the motor cortex is damaged. The location of the injury in this study targeted the parietal lobe and supplementary motor cortex. This results in some disturbances in lower limb function. Our study measured motor function using the beam walking task and peg board as previously described. (71) An increase in foot falls compared to baseline verified that the injury had caused some damage to motor function and this behavior is typical of what is seen after CCI. (118, 188) Few studies have examined the effect of insulin on improved motor function. Notably, one study showed minor improvements in motor function with peripheral insulin treatment prior to cerebral ischemia in rats. (127) The researchers noted that

hypoglycemia was necessary for functional improvements. (28) Intranasal insulin treatment has been shown to improve motor function in a mouse model of Parkinson's disease. (191) This motor function improvement can be attributed to differences in the mechanism of disease as it targets a specific subset of neurons and is not a result of direct tissue damage as seen in CCI. Our study showed no significant reduction in foot falls as a result of insulin treatment. Interestingly, a significant difference was detected in time to cross the beam one day after injury. Saline treated animals took significantly longer to cross the beam. Insulin treated animals crossed the beam at the same pace as they did pre-injury. This suggests that while their motor skills are inhibited after injury, as shown by increased foot falls, insulin treated rats remember how to accomplish the task better than saline treated. Injured animals returned to baseline motor function by 14 days post injury. Additionally, motor function was characterized in Morris water maze, conducted on days 11 to 14 post injury, by examining the average swim speed of subjects. There was no significant difference in swim speed in injured animals treated with intranasal insulin or intranasal saline.

Overall, we found that treatment with intranasal insulin in the acute stages of injury did not alleviate motor deficit as measured by the beam walking task. We also saw no significant reduction in lesion volume. Our PET data also did not show a significant increase in [¹⁸F]-FDG uptake in the cortex. The lack of insulin action in the cortex may be attributed to a normally low concentration of IR, compared to the rest of the brain, which is decreased further following CCI injury. This is supported by the low distribution of insulin ¹²⁵I in the cortex and [¹⁸F]-FDG PET results. (71, 118, 188)

MEMORY FUNCTION IMPROVED WITH INTRANASAL INSULIN TREATMENT

The ability of intranasal insulin to improve cognitive function after CCI was measured with the Morris water maze test. Impaired memory and learning function is often observed in patients with TBI (106, 156) and CCI is an excellent pre-clinical paradigm of these deficits. (60, 188) After CCI, rats take more time to find the location of the hidden platform compared to uninjured controls. (93) The animal's ability to locate the platform during the probe trial is primarily a test of memory. (26, 233) We observed a slight increase in latency between non-injured and injured groups, but both the injured and uninjured groups showed the ability to learn over the course of the trials as they found the platform more quickly each day. While there was no significant improvement in latency to platform following intranasal insulin, we did observe a significant increase in island crosses during the probe trial. This indicates that the intranasal insulin treated group with CCI showed improved recall of the location of the platform. Brain insulin resistance, caused by reduced sensitivity of the receptor to ligand, is observed in Alzheimer's patients and is correlated with decreased memory function and learning. (58) In clinical trials, Alzheimer's disease patients treated with intranasal insulin displayed a significant improvement in the ability to recall a list of words compared to vehicle treated controls.(45, 207) It is important to note that there was no difference in the ability to learn the list of words initially. This is analogous to our findings; we saw an improvement in memory recall, as measured by island crosses during probe trial, but no difference in learning, as measured by latency to platform.

A third data set analysis, search strategy, was used to more closely examine cognitive function during the Morris water maze. The 3 major sub categories of Morris water maze search strategy analysis are spatial, systematic, and looping; each correlates

with familiarity with the task, level of injury and general intelligence. (113) Looping behavior was only observed in the injured cohort. Looping behavior is typically observed in rodents on the first day of training or in those with moderate to severe TBI. (265) Additionally, looping behavior has been observed in rats with neurotoxic hippocampal lesions, supporting the idea that increased looping is indicative of hippocampal damage and is measurable using this analysis. (80) Rats treated with intranasal insulin displayed significantly less looping and more spatial search strategy behavior than those treated with intranasal saline. This behavioral outcome further supports our data suggesting that intranasal insulin has a primarily hippocampal effect. Importantly, this is in agreement with our other data, which demonstrated an accumulation of insulin in the hippocampus and an increase in [¹⁸F]-FDG uptake in the hippocampus.

Interestingly, a significant difference in search strategy was observed in the uninjured cohorts. Neither treatment group displayed looping behavior but uninjured rats treated with intranasal insulin showed significantly more systematic search strategy than those treated with intranasal saline. Systematic behavior is defined by the animal primarily scanning the central four quadrants, indicating recall of the location of the platform. This suggests that intranasal insulin alters learning strategies. One study comparing search strategies of animals treated with peripubertal stress with controls showed that stressed animals stayed near to the walls more than un-stressed. (82) This suggests that scanning the central quadrants more may be an indicator of reduced stress and anxiety in the insulin treated group. Intranasal insulin has been proposed as a treatment of posttraumatic stress disorder (PTSD), and the potential anxiolytic effect of intranasal insulin could be better examined in with open field testing. (76)

Morris water maze is an excellent tool for the study of hippocampal function after CCI as there are a number of alternative paradigms that can be conducted to examine different aspects of learning and memory.(218) Our study conducted the probe trial one hour after the final training session. This timepoint has been previously identified as sensitive enough to detect changes in short term spatial recall after TBI. (73, 179, 265) One alternative experiment would be to run the probe trial one day after the final training session. This would provide an examination of the effect of intranasal insulin on long term memory. Both our current paradigm and this suggested paradigm examine the ability of the animal to recall new information acquired following an injury. Another alternative Morris water maze paradigm could examine the ability of the subject to recall information learned prior to injury. This can be achieved by conducting the training prior to injury and the probe trial after treatment. Motor function deficits after injury may provide a technical challenge for conduction this paradigm. Overall, Morris water maze is sensitive to damage after CCI and supports our data showing hippocampal recovery with intranasal insulin treatment.

INTRANASAL INSULIN SIGNIFICANTLY INCREASED [¹⁸F]-FDG UPTAKE IN THE HIPPOCAMPUS

Intranasal insulin treatment significantly increased [¹⁸F]-FDG uptake in the ipsilateral hippocampus at 10 days post injury compared to baseline. We also observed a significant accumulation of [¹²⁵I] insulin in the hippocampus which has been previously identified as a region of the brain dense in insulin receptors. (154) Decreased [¹⁸F]-FDG uptake has been documented in individuals with mild cognitive impairment (MCI) and Alzheimer's disease. (136) This same study showed global hypometabolism in Alzheimer's disease patients but only focal hippocampal hypometabolism in MCI. (136)

Additionally, human studies have shown a significant acute increase in ATP (adenosine triphosphate) and phosphocreatine, which represents the brains energy reserve levels after intranasal insulin administration. (114) These data and our findings suggest that intranasal insulin increases [¹⁸F]-FDG uptake in the hippocampus and results in improved memory function. While previous studies have examined this in Alzheimer's disease our shows that this system is conserved and applicable to the treatment of TBI.

Some potential pitfalls have been identified in our study design. We observed significant variability in our post injury saline uptake values. This may be attributed to a lag in time to scan following isoflurane which can be easily corrected in future studies.

CELLULAR RESPONSE TO INSULIN TREATMENT

Cellular response to insulin after TBI

Our analysis of tissue provided additional support to our hypothesis that intranasal insulin improves functional outcome by reducing neuropathological deficits after TBI. We did not find a significant reduction in lesion volume with intranasal insulin treatment compared to intranasal saline treatment. This may be attributed to a minimal action of insulin in the cortex. This is supported by comparatively low [¹²⁵I] insulin in the cortex compared to other regions, no significant changes in [¹⁸F]-FDG uptake in the cortex, and no change in foot falls in the beam walking task with intranasal insulin compared to saline.

We found a significant reduction in Iba1, a marker of microglia and macrophages, in the hippocampus of animals treated with intranasal insulin compared to intranasal saline after CCI. Cellular quantification was based on fluorescent intensity and not simple cell count as this takes into account the significant increase in size and number of

processes upon activation in both microglia and astrocytes. (62) Prolonged microglial activation after TBI results in neuronal cell death due to ROS, NO and cytokine release. (for review: (141)) Therefore, a reduction in microglia activity in the hippocampus can be favorable for long term outcome. This is supported by our other findings relevant to hippocampal function after intranasal insulin treatment. We found a significant improvement in memory recall in the Morris water maze as a result of intranasal insulin treatment. Additionally, we saw a significant increase in [¹⁸F]-FDG uptake in the hippocampus compared to baseline.

We also examined the effect of intranasal insulin on astrocyte activation as they are also implicated in long term negative outcome after brain injury. Reactive astrocytosis persists for up to a year following fluid percussion injury. (231) We found no significant difference in glial fibrillary acidic protein (GFAP), a marker of astrocytes, in the hippocampus of animals treated with intranasal insulin compared to intranasal saline after CCI. In vitro studies have shown that high doses of insulin can reduce IL-6 and IL-8 expression from activated astrocytes. (235) Future studies may examine additional doses to see if a similar response could be produced from astrocytes *in vivo*.

While our study supplies novel findings about the response of glial populations with intranasal insulin treatment after injury, one significant shortcoming of this work is a lack of neuronal pathological outcomes. Neuronal function was indirectly measured by MWM testing. We also assume that a reduction in Iba1 is beneficial for neuron function after trauma, as has been previously shown. (for review (140) However, histological assessment of markers of neuronal health (NeuN) or cell death (Fluoro Jade) would provide significant support to our research but were not conducted in the present study

due to technical difficulties. Neuronal response has been the primary focus of most previous intranasal insulin studies and findings support a role of insulin in promoting neuronal health. (8, 150, 191)

Activated microglia response to insulin *in vitro*

Our analysis of the specific effects of insulin on microglia *in vitro* revealed additional insight to the mechanism by which intranasal insulin reduces deficits after TBI. We found a significant reduction in NO and ROS following insulin treatment in activated BV2 microglia. The doses tested did not show a significant change in either M1 or M2 microglia polarization markers. An analysis of the cytokines released following insulin treatment showed a significant reduction in two chemokines, JE/MCP-1 and MIP-1A, but no significant reduction in other cytokines such as IL-1 α and IL-1 β . This significant reduction in chemokines may be related to observed reductions in microglia/macrophage observed in the hippocampus of animals treated with intranasal insulin. Reduced release of chemokines would result in less recruitment of microglia to the site after injury. (219) The reduction in NO and ROS production suggests that treatment with insulin reduced the inflammatory action of microglia but we did not observe a reduction in markers of M1 polarization markers. This indicates that a robust shift in polarization markers is not necessary to produce an anti-inflammatory effect.

This *in vitro* analysis of BV2s, a mouse microglia cell line, shows that some aspects of microglia inflammatory response are reduced with insulin treatment. These data supports previous findings in activated human primary microglia which produced significantly less MCP-1 with insulin treatment, one of the same chemokines we observed a change in our study. (235)

CONCLUSIONS AND FUTURE DIRECTIONS

TBI results in a complicated cascade of cellular events that no treatment, to date, has been able to adequately address. One aspect of the complicated etiology of TBI is the neurometabolic response. (84) After injury, cells utilize ATP-requiring membrane ionic pumps in an effort to normalize their environment. (84, 283) This hypermetabolic acute stage state is followed by a period of hypometabolism. (229) This hypometabolic state is the target of our treatment as it presents a period of increased cerebral vulnerability and associated with neuropsychological deficits. (174, 227)

Our study examined intranasal insulin administration following TBI and our data suggest a potential component of the etiology of the neurometabolic cascade that has not been previously identified. Our findings are graphically represented in Figure 13. After injury (lightning bolt), there is a significant increase in the activation of quiescent microglia (red cells), a decrease in glucose (blue box) uptake and neuronal cell death (green stars) (Fig. 13 A). These cellular responses manifest as deficits in memory and learning dysfunction. Our data shows that treatment with intranasal insulin significantly increased [¹⁸F]-FDG uptake in the hippocampus after CCI. We observed a significant reduction in microglia/macrophage number in the hippocampus. Collectively this resulted in improved memory function. Our in vitro examination of microglial response to insulin provided additional insight as to the mechanism by which intranasal insulin improved outcome after TBI. We found that insulin treatment significantly reduced NO and JE/MCP-1 and MIP-1A production (Fig. 13 B). This suggests that intranasal insulin reduces the number of microglia migrating to the lesion site, as evidence by the reduction

in IBA1 staining, and the microglia present produce less NO. Both of these factors would create an environment more amenable to neuronal repair.

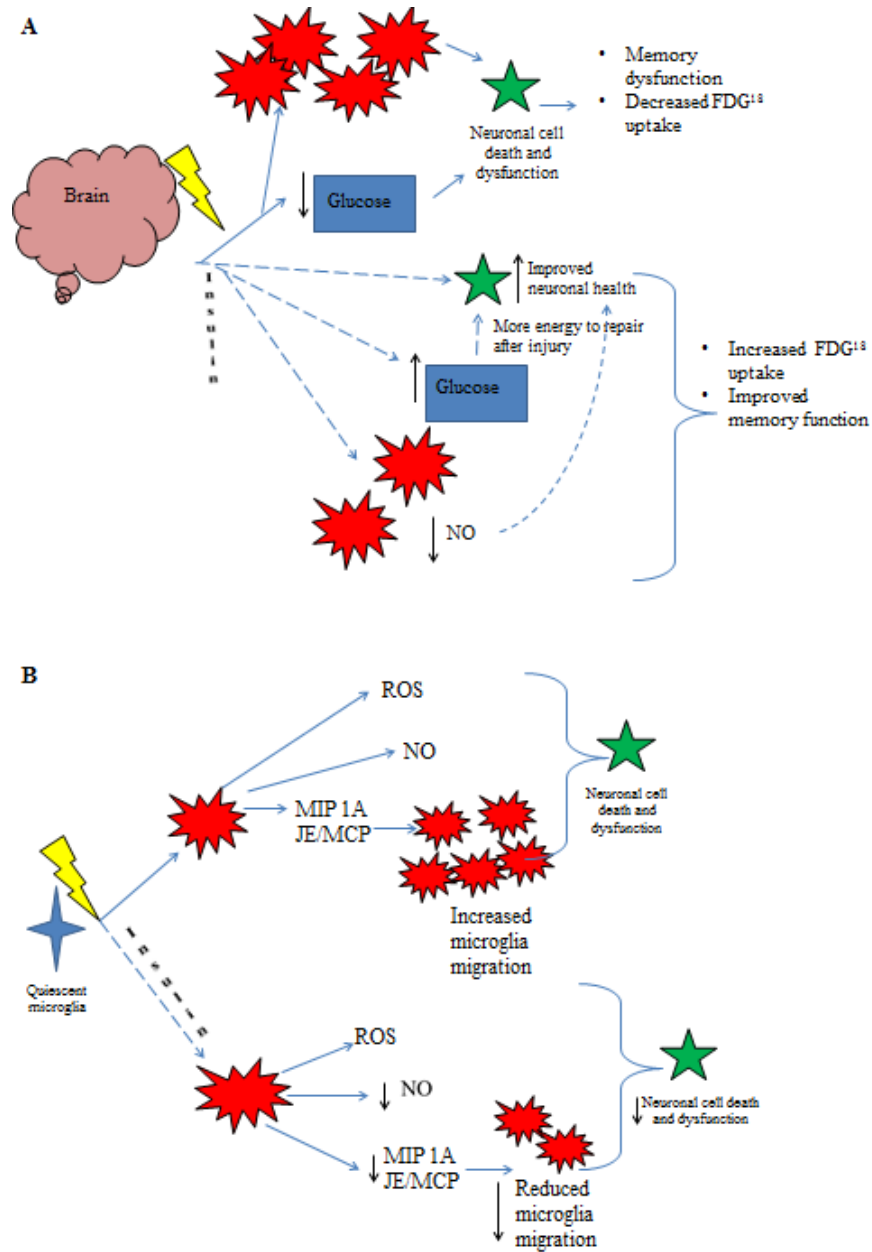


Figure 13: A graphical representation of the pathways examined in this dissertation.

This study provides a strong starting point for future studies to examine intranasal insulin treatment before progression into clinical trials. Future studies will examine the

effect of intranasal insulin on neuronal outcome after TBI. Additionally, a range of doses can be tested to establish the most effective dose. Our study examined a dose administered acutely after TBI; future work can examine the ability of intranasal insulin treatment to improve function when administered at later time points. Overall, the data presented in this dissertation provide valuable insight into the treatment of TBI by targeting the metabolic response.

Appendix 1: [¹⁸F]FDG-PET Combined with Diffusion MRI Enhances the Detection of Traumatic Brain Injury in Rats

Fiona Brabazon¹, Colin M. Wilson, M.A.^{2,3}, Dinesh K Shukla, PhD^{2,3}, Sanjeev Mathur, MD^{2,3}, Shalini Jaiswal, M.S.^{2,3}, Sara Bermudez, M.S.⁴, Kimberly R. Byrnes, PhD^{1,3,4}, Reed Selwyn, PhD^{2,3,5}

¹Neuroscience Program, Uniformed Services University of the Health Sciences, 4301 Jones Bridge Road, Bethesda, MD 20814

²Department of Radiology, Uniformed Services University of the Health Sciences, 4301 Jones Bridge Road, Bethesda, MD 20814

³Center for Neuroscience and Regenerative Medicine, Uniformed Services University of the Health Sciences, 4301 Jones Bridge Road, Bethesda, MD 20814

⁴Department of Anatomy, Physiology and Genetics, Uniformed Services University of the Health Sciences, 4301 Jones Bridge Road, Bethesda, MD 20814

⁵Department of Radiology, University of New Mexico, 1 University of New Mexico, Albuquerque, NM 87131

*Correspondence:

Reed Selwyn, PhD, DABR(D)

Department of Radiology, University of New Mexico

MSC10 5530

1 University of New Mexico

Albuquerque, NM 87131-0001

Phone: 505-272-4433

Email: RSelwyn@salud.unm.edu

Fiona Brabazon
Neuroscience Program
Room C2099
4301 Jones Bridge Road
Bethesda, MD 20814
301-295-3217 (telephone)
301-295-1786 (FAX)
fiona.brabazon@usuhs.edu

Colin M. Wilson
Department of Radiology
Room C1073
4301 Jones Bridge Road
Bethesda, MD 20814
301-319-0557 (telephone)
301-295-3893 (FAX)
colin.wilson.ctr@usuhs.edu

Dinesh Shukla
Department of Psychiatry
Maryland Psychiatric Research Center
UMB School of Medicine
55 Wade Ave
Catonsville, MD 21228
410-402-6028 (telephone)
dshukla@mprc.umaryland.edu

Sanjeev Mathur
Department of Radiology
Room C1073
4301 Jones Bridge Road
Bethesda, MD 20814
301-319-0557 (telephone)
301-295-3893 (FAX)
sa_mathur@yahoo.com

Shalini Jaiswal
Department of Radiology
Room G163
4301 Jones Bridge Road

Bethesda, MD 20814
301-295-5674 (telephone)
301-295-3893 (FAX)
shalini.jaiswal.ctr@usuhs.edu

Sara Bermudez
Department of Anatomy, Physiology and Genetics
Room C2099
4301 Jones Bridge Road
Bethesda, MD 20814
301-295-3217 (telephone)
301-295-1786 (FAX)
sara.bermudez.ctr@usuhs.edu

Kimberly R. Byrnes
Department of Anatomy, Physiology and Genetics
Room C2115
4301 Jones Bridge Road
Bethesda, MD 20814
301-295-3217 (telephone)
301-295-1786 (FAX)
kimberly.byrnes@usuhs.edu

ABSTRACT

Non-invasive measurements of brain metabolism using ^{18}F fluorodeoxyglucose ([^{18}F]-FDG) with positron emission tomography (PET) may provide important information about injury severity following traumatic brain injury (TBI). But there is growing interest in the potential of combining functional PET imaging with anatomical and functional magnetic resonance imaging (MRI). This study aimed to investigate the effectiveness of combining [^{18}F]-FDG-PET with diffusion MR imaging, with a particular focus on inflammation and the influence of glial alterations after injury, and correlating imaging results with pathology. Adult male Sprague Dawley rats underwent a moderate controlled cortical impact (CCI) injury followed by [^{18}F]-FDG-PET, MRI and histological evaluation. [^{18}F]-FDG uptake showed significant alterations in the corpus callosum, hippocampus and amygdala after TBI, demonstrating that a relatively ‘focal’ CCI injury can result in global alterations. Analysis of MRI T2 intensity and apparent diffusion coefficient (ADC) also showed significant alterations in these regions. Histology showed increased glial activation in the corpus callosum and hippocampus that was associated with increased [^{18}F]-FDG uptake and decreased ADC at early time points. Glial activation was not detected in the amygdala, which was the only region to show a reduction in both [^{18}F]-FDG uptake and ADC. Overall, [^{18}F]-FDG-PET detected glial activation but was confounded by cell death, while diffusion MRI consistently detected cell death but was confounded by glial activation. These results demonstrate that [^{18}F]-FDG-PET and diffusion MRI can be used together to improve the detection of complex alterations in brain function after TBI.

KEYWORDS

FDG PET, Brain Injury, Inflammation, Microglia, Astrocytes

INTRODUCTION

Traumatic brain injury (TBI) affects 2.5 million people in the United States each year and results in serious cognitive and physical deficits. (69, 213, 223) Brain injuries result in a series of downstream secondary events that include neuronal damage and glial activation in focal and diffuse regions. Better understanding of the role of glial activation in regional sensitivity to damage and methods to detect these glial changes may improve diagnosis and prognosis of TBI and improve therapeutic approaches.

One common preclinical model of TBI is the controlled cortical impact (CCI) injury, which results in a focal impact leading to local neuronal damage and glial activation, as well as diffuse injury. (38, 177) Specifically, the hippocampus, corpus callosum and amygdala, which have been suggested to be particularly sensitive to TBI, are affected in the CCI model. Clinically, damage to these regions is related to memory dysfunction, learning difficulties, motor skill deficit, depression and anxiety. Hippocampal damage is associated with learning and memory impairments after TBI, (47) while dysfunction of the amygdala has been linked to post traumatic stress disorder (PTSD). (53, 55, 246) Additionally, corpus callosum damage plays a significant role in hemispheric communication. (90) These regions have been shown to demonstrate significant neuronal and glial changes following TBI.

The pathological outcome after CCI has been examined in several studies and has demonstrated neuronal apoptosis that peaks at 24 hours post-injury followed by chronic glial activation. (38) Both neurons and glia play a significant role in the metabolic function of the brain. (262) Previous work in our laboratory has identified a strong correlation between depressed glucose uptake and delayed increases in regional astrocyte

activation; similarly, this depressed glucose uptake was observed in regions demonstrating axonal damage. (226)

Only one study has investigated the glucose uptake profile in the CCI model using non-invasive imaging of ^{18}F -fluorodeoxyglucose (^{18}F -FDG) with positron emission tomography (PET), investigating the influence of transplanted stem cells after TBI.(89) ^{18}F -FDG is a radiolabeled glucose analog that is transported into cells and phosphorylated but cannot be metabolized further; therefore, it accumulates within cells and then can be detected via PET imaging. (208) Clinical data and animal studies have shown that TBI results in a long-term reduction in cerebral glucose uptake and this phenomenon is more likely to present as injury severity increases (for review, see (34)).

Magnetic resonance imaging (MRI) is currently more widely used for evaluating TBI compared to ^{18}F -FDG - PET imaging. Following lateral fluid percussion TBI injury, T2-weighted MRI demonstrates hyperintense regions in the injured cortex at 24 hours post-injury, which is associated with edema, (129) while T2 imaging has identified regions containing microhemorrhages. (190) In the clinic, measures of apparent diffusion coefficient (ADC) have been associated with worsening outcomes. (137, 178) Vasogenic edema, which results from endothelial disruption, is generally indicated when both T2 and ADC values increase whereas cytotoxic edema, which is the accumulation of water in cells, is indicated when T2 increases but ADC decreases. (270) However, it is currently unclear if ^{18}F -FDG-PET can improve upon or be used synergistically with MRI to improve diagnostic and prognostic measures after TBI. Therefore, this study aimed to examine the capabilities and the sensitivity of multimodality imaging at detecting diffuse damage to the brain after a focal CCI, with a focus on glial activation in

brain regions suspected to be affected by TBI: the hippocampus, amygdala and corpus callosum.

MATERIALS AND METHODS

Study Design

The study was designed as a cross-sectional study with an acute (n=3) and 5 subacute-chronic cohorts (n=4/cohort). All cohorts obtained baseline PET/CT and MRI scans prior to injury and a second PET/CT scan at one of the following time points after moderate CCI injury: [¹⁸F]-FDG-PET at 1, 3, 7, 10, or 20 days and MRI at 2, 4, 8, 10 or 21 days. The acute cohort was scanned at baseline and again at 3 hours post injury ([¹⁸F]-FDG-PET) and 1 day post injury (MRI). Animals were euthanized 24 hours after post-injury scans and tissue was extracted for immunohistochemical analysis. A naive cohort (n=2) was evaluated for histological comparison only. Animal groups are defined in Table 2.

Table 2. Experimental groups and timepoints for Appendix 1

Group	n	Injury	[¹⁸ F]-FDG-PET scan day	MRI day	Histology
Naïve	2/historical controls	No surgery	None	None	7 days after arrival
3h	3	Moderate CCI	3h post-injury	24h post-injury	24h post-injury
24h	4	Moderate CCI	24h post-injury	48h post-injury	48h post-injury
3d	4	Moderate CCI	3d post-injury	4d post-injury	4d post-injury
7d	4	Moderate CCI	7d post-injury	8d post-injury	8d post-injury
11d	4	Moderate CCI	11d post-injury	10d post-injury	12d post-injury
20d	4	Moderate CCI	20d post-injury	21d post-injury	21d post-injury

Moderate Traumatic Brain Injury

Adult male Sprague Dawley rats (n = 25; 150 – 200g) were given free access to food and water and a 12h light/12h dark cycle. All animal procedures were approved by

the Uniformed Services University IACUC. CCI was performed as previously described. (31) Rats were anesthetized with isoflurane (4% induction, 2% maintenance), temperature was measured rectally and maintained at 36.5 – 37.5°C. The animal was placed in a standard rodent stereotaxic frame and positioned using ear and incisor bars. A 5mm craniotomy was performed over the left cortex at -2.5 mm lateral and -3.0 mm posterior from Bregma. Following the craniotomy, the CCI device (Impact One™, Leica Microsystems, Buffalo Grove, IL) with a 3mm impactor tip was placed in the center of the craniotomy site and a moderate injury was induced with 5 m/s speed, 200 msec dwell time and 2 mm deformation depth. (31) The skull flap removed for craniotomy was not replaced after injury.

PET/CT imaging

[¹⁸F]-FDG-PET/CT images were acquired using a Siemens Inveon Multimodality (Siemens Medical Solutions USA, Malvern, PA) scanner in the small-animal PET/CT facility of the Translational Imaging Core, Center for Neuroscience and Regenerative Medicine (CNRM). Animals were anesthetized with isoflurane (4% induction; 1.5-2% maintenance) and injected intravenously with 1–2 mCi (37–74 MBq) FDG. Subjects were maintained under anesthesia for the duration of the uptake and imaging session. Vital signs were continuously monitored. A three-bed CT scan was acquired for anatomical localization and attenuation correction. CT data were acquired (80 kVp, 500uA; exposure time 320 ms) with a bin of 4 using low magnification in ‘Rat Mode’ (CCD Readout – Transaxial 2944 and Axial 1920). CT data were reconstructed in real time using a modified-Feldkamp algorithm (bilinear interpolation, Shepp-Logan filter) and corrected for beam hardening. CT image dimensions were 352 x 352 x 536 with a

voxel size of 0.23 mm isotropic. PET data were acquired with a coincidence-timing window (Dt) of 3.432ns and energy window (DE) of 350-650keV in list mode for 30 minutes following a 45-minute uptake period. PET sinograms were reconstructed as a single, high-resolution static frame using a 3D-OSEM/MAP algorithm (2 OSEM iterations, 18 MAP iterations, requested resolution: 0.5 mm) with scatter, attenuation and decay corrections applied. The intrinsic resolution of the PET scanner is approximately 1.4 mm FWHM at the center of the field of view. PET image dimensions were 256 x 256 x 159 with a voxel size 0.39 x 0.39 x 0.80 mm.

MR Imaging

In vivo MR imaging was performed on a 7 Tesla small animal Bruker BioSpec 70/20 USR Superconducting Magnet System (Bruker-Biospin, Ettlingen, Germany) equipped with 650 mT/m gradient coils. Animals were anaesthetized with 1% isoflurane and placed in a magnetic resonance-compatible head holder. 2D multi-shot echo planar imaging (EPI) (repetition time/echo time=6250/26 ms; 8 segments) was used to acquire diffusion-weighted imaging (DWI) data with an unweighted ($b = 0$ s/mm²) image and 5 diffusion weighted images ($b = 100, 200, 400, 800, 1000$ s/mm²) using a Stejskal-Tanner diffusion preparation with parameters of $\Delta=9$ ms and $\delta=3.2$ ms; field-of-view=25.6×25.6 mm², matrix=256×256, slice thickness/gap=.95/.05mm and 3 nonlinear directions. Multi-echo 2D Rapid Acquisition with Relaxation Enhancement (RARE) sequence was used to acquire T2-weighted images (TR=10000 ms, TE=20, 60, 100, 120 ms, rare factor 4, field-of-view=25.6×25.6 mm², matrix=256×256, and slice thickness=1mm).

PET & MR Image Processing

Image post-processing and analyses of FDG-PET data were performed using VivoQuant™ software version 1.22patch2 (Invicro, LLC Boston, MA). T2 and ADC maps were generated using a non-linear with constant algorithm (Levenberg-Marquardt) and a linear (OLS) least squares estimations algorithm, respectively. FDG, T2 and ADC maps were resampled to match CT voxel size (0.23mm isotropic) and dimensions (352x352x536). For each subject, the T2-weighted image was manually registered with the CT image (6-parameter, rigid) and the generated transformation matrix was applied to the T2 map. The ADC map was manually registered with the CT image (6-parameter, rigid) and the scanner transformation matrix was applied to the PET image to produce a co-registered set of images - FDG, CT, T2 and ADC map. Coregistered images were uniformly cropped to a region surrounding the brain (170x170x240), which were manually reoriented (x,y,z-rotation) and automatically registered to a 14-region rat brain atlas using an algorithm that combines a rigid transformation of the data and scaling of the atlas. Quantitative output was obtained for left, right and combined hemisphere regions. For PET, the uptake concentration for each region of interest (ROI) was normalized to the uptake concentration of the entire atlas (whole brain normalization) for inter-subject comparison.

Histology

A 5mm segment of the brain encompassing the lesion epicenter was dissected following euthanasia and perfusion with 10% buffered formalin. Brain tissue was sectioned at 20µm and immunolabeled for microglia (Iba-1, 1:100, Wako Chemicals USA, Richmond, VA), astrocytes (GFAP, 2.5:1000 Abcam, Cambridge, MA) and neurons (NeuN, 5:1000, Millipore, Billerica, MA). Fluorescent secondary antibodies

(Alexa-Fluor Secondaries, Invitrogen, Grand Island, NY) were used to visualize primary antibodies. Images were then captured on a NanoZoomer system (Hamamatsu, Bridgewater, NJ) or an Olympus BX43 microscope (Olympus America, Center Valley, PA). Fluorescent immunohistochemistry was quantified in 5 – 8 brain sections per animal within the amygdala, corpus callosum and hippocampus as previously described using pixel density measurement in Scion Image (Scion Corporation, Frederick, MD). (62) Regions of interest were identified using the Inveon atlas from the FDG-PET scans as a guide (Fig. 14). Density measurements were obtained at a 20X magnification in the hippocampus and corpus callosum, producing a 0.358 mm² region of analysis, and a 10X magnification in the amygdala, producing a 1.4 mm² area of analysis.

Statistics

Immunohistochemistry pixel density values were compared to naive tissue with one-way ANOVA with Dunnett's post-test. Post-injury [¹⁸F]-FDG uptake and MRI measures was compared to baseline measures using two-way ANOVA with each comparison assessed with uncorrected Fisher's LSD post-test. All data is shown as mean +/- SEM. All statistical tests were performed using the GraphPad Prism Program, Version 5.0 for Windows (GraphPad Software, San Diego, CA). A *p* value < 0.05 was considered statistically significant.

RESULTS

The purpose of this study was to determine the effectiveness of evaluating TBI by combining [¹⁸F]-FDG-PET with MRI measurements and to validate these measures with

histological results. Globally, alterations in glucose uptake were detected acutely after injury and persisted to at least 20 days post-injury (dpi). Detailed regional analysis (Table 3) revealed distinct patterns of glucose uptake that may provide insight into the long term outcomes of TBI.

Table 3. Summary of observations based on region of interest (*p<0.05, **p<0.01, ***p<0.0001, ****p<0.00001).

Region	Histology	FDG	T2	ADC
Corpus Callosum	Acute: Not measured Subacute: Increase** GFAP (activation) Chronic: Return to baseline	Acute: No change Subacute: Increase** (activation) Chronic: Return to baseline	Acute: Not measured Subacute: Increase**** (edema) Chronic: Return to baseline	Acute: Not measured Subacute: Increase* @ 8 dpi (vasogenic) Chronic: Return to baseline
Hippocampus	Acute: Not measured Subacute: Elevated GFAP, IBA1 (activation) Chronic: Slightly elevated GFAP, IBA1 (activation)	Acute: Increase* (activation) Subacute: Return to baseline Chronic: Increase* (activation)	Acute: Not measured Subacute: Increase*** (edema) Chronic: Increase** (edema)	Acute: Not measured Subacute: Decrease** (dysfunction) followed by increase to baseline Chronic: Decrease* (dysfunction)
Amygdala	Acute: Not measured Subacute: Elevated GFAP followed by decrease. Decrease NeuN, IBA1 (dysfunction) Chronic: Elevated GFAP	Acute: Elevated (activation) Subacute: Decrease** (dysfunction) Chronic: Elevated (activation)	Acute: Not measured Subacute: Increase** (edema) Chronic: Elevated (edema)	Acute: Not measured Subacute: Decrease*** (dysfunction) followed by increase to baseline Chronic: Decrease* (dysfunction)

The corpus callosum showed increased [¹⁸F]-FDG uptake, increased T2, decreased ADC, and increased glial activation.

[¹⁸F]-FDG uptake in the ipsilateral corpus callosum was increased at 3 dpi compared to baseline (Fig. 15A). The uptake remained elevated through 11 dpi, before reducing at 20 days. [¹⁸F]-FDG uptake in the entire corpus callosum and the contralateral corpus callosum followed a similar pattern (Supplementary Fig. 19A). However, the uptake remained significantly elevated through 20 days in the contralateral hemisphere.

MRI T2 and ADC values were measured 24 hours after PET image acquisition (except for the 11 day group, which was performed 24 hours prior to PET due to scheduling conflicts). T2 measurements were elevated in comparison to baseline at days 8 and 10 in the ipsilateral corpus callosum (Fig. 15B). ADC values were also significantly elevated at 8 dpi in the ipsilateral corpus callosum (Fig. 15C), with a trend toward reduced ADC at days 1, 2, and 4. This bimodal response in ADC may indicate early cytotoxic edema followed by vasogenic edema at day 8. In the whole corpus callosum, T2 measurements were elevated in comparison to baseline at days 1, 2, 8, 10 and 20 and at days 1, 2, 8 and 10 in the contralateral corpus callosum (Supplementary Fig. 14A). ADC values were significantly reduced at 2 and 10 dpi in the contralateral corpus callosum (Supplementary Fig. 19).

Astrocytes were identified with an antibody against glial fibrillary acidic protein (GFAP; Fig. 15D), which was negligible in naïve corpus callosum and at 1 dpi. A significant increase in GFAP positive cells was observed that peaked by 4 dpi and remained slightly, though not significantly, elevated through 21 dpi. Microglia and macrophages were identified using an antibody against the Iba1 protein. Iba1 immunolabeling was observed in naïve tissue and was slightly elevated in the 3-hour post-injury group (1dpi; Fig. 15E). Iba1 expression peaked by 8 dpi, although

significance was not reached due to high variability within sample groups. While FDG uptake, T2 and ADC show elevation at the same time that histology demonstrated glial activation, changes in ADC may indicate other cellular processes such as endothelial dysfunction in the corpus callosum.

FDG uptake in the hippocampus is bimodal and is accompanied by elevated glial activity, increased T2 and decreased ADC.

FDG uptake was significantly elevated at 3 hours and 20 dpi in the ipsilateral hippocampus, but returned to baseline between days 1 and 10 (Fig. 16A). The entire hippocampus showed the same pattern, but the contralateral hippocampus only showed elevated FDG uptake at 20 dpi (Supplementary Fig. 19B).

Edema was identified by elevated T2 values at days 4, 8, 10 and 21 in the ipsilateral hippocampus (Fig. 16B). ADC values, on the other hand, were significantly decreased at days 2, 4 and 21 in the ipsilateral hippocampus (Fig. 16C). This finding may indicate cytotoxic edema at early time points with mixed edema (cytotoxic + vasogenic) at day 10. In the entire hippocampus, T2 values were elevated at days 2, 4, 8, 10 and 21 and at 2 and 4 dpi in the contralateral hippocampus. ADC values, on the other hand, were significantly decreased at all days except day 10 in the entire hippocampus and days 2, 4, and 8 in the contralateral hippocampus.

Similar to the corpus callosum, immunostaining for GFAP showed undetectable levels in naïve tissue and an elevation in labeling at 1 dpi that peaked at 4 dpi and persisted for 21 days (Fig. 16D). Quantitation of immunolabeling demonstrated marked elevations above the naïve tissue that did not reach statistical significance due to tissue variability.

Immunostaining for Iba1 was elevated in the hippocampus after injury (Fig. 16E). Iba1 was elevated within the 3-hour post-injury group, and remained elevated throughout the study period. Quantitation of Iba1 pixel density showed elevations that did not reach statistical significance. Considering the robust activation of microglia and astrocytes along with significant cytotoxic edema, [^{18}F]-FDG uptake profile could indicate mixed cellular response (activation + cell dysfunction) with competing effects on [^{18}F]-FDG uptake.

The amygdala shows a dramatic decrease in [^{18}F]-FDG uptake after CCI in addition to small alterations in glial responses.

The most pronounced changes in [^{18}F]-FDG uptake were observed in the amygdala. [^{18}F]-FDG uptake in the ipsilateral amygdala showed a trend toward elevation that did not reach significance at 3 hours, followed by a pronounced depression that was significant at 3 and 7 dpi (Fig 17A). The entire region and contralateral amygdala independently showed similar patterns (Supplementary Fig. 19C).

T2 values were found to be significantly elevated at 4 and 8 dpi time points in the ipsilateral amygdala (Fig. 17B). In contrast, ADC values paralleled [^{18}F]-FDG uptake, with significant reductions observed at 2, 4, 8 and 21 dpi (Fig. 17C). T2 and ADC values were found to follow the same patterns in the entire amygdala and contralateral amygdala as the ipsilateral amygdala (Supplementary Fig. 14C) and indicated cytotoxic edema.

GFAP expression clearly increased subacutely at 1 dpi, returned to baseline at 4 dpi, and increased chronically at 21 dpi; however, these changes did not reach statistical significance (Fig. 17D). There was no significant alteration in Iba1 immunolabeling in the amygdala after CCI injury but a slight depression was observed at 8 dpi (Fig. 17E).

Due to the pronounced [^{18}F]-FDG changes and lack of significant glial changes, we investigated the effect of CCI on amygdala neurons. The NeuN antibody recognizes a DNA binding protein in the nucleus, and was observed as a nuclear stain in tissue from naïve animals (Fig. 18). At 1 dpi, NeuN staining was still observed in the nucleus but staining was also observed in the cytoplasm. By 2 dpi and continuing through 4 dpi, NeuN staining in the amygdala was absent, although DAPI counterstain showed no marked reduction in cell presence. NeuN immunolabeling returned by 8 dpi, although the density of the stain and the nuclear localization were diminished. This lighter, cytoplasmic stain remained through 21 dpi. This suggests that neuronal damage without a significant increase in glial activation corresponds to a decrease in [^{18}F]-FDG uptake. This damage also corresponds with elevated T2 and decreased ADC (interpreted as cytotoxic edema) and would indicate cell death.

DISCUSSION

The research presented is a descriptive analysis of the effectiveness of measuring TBI outcomes with [^{18}F]-FDG-PET and MRI in distinct brain regions and correlating with histology. Analysis and interpretation of these data show a pattern of responses that are dependent on the glial and neuronal responsiveness of the region investigated. In summary, it appears that dysfunctional neurons lead to an acute elevation in [^{18}F]-FDG uptake followed by a delayed depression, while astrocyte and microglial activations lead to a broad increase in [^{18}F]-FDG uptake. If responses in both cell types (neurons and glia) are present, there appears to be a ‘canceling’ of effects and [^{18}F]-FDG uptake remains near baseline levels, such as the case in the hippocampus. T2 values were consistently elevated regardless of cellular composition and indicated non-specific edema

while ADC values were generally depressed, which indicated cytotoxic edema and cell dysfunction. In addition, elevated ADC values and vasogenic edema were noted at days 8 and 10 in the corpus callosum and hippocampus, respectively, possibly indicating a delayed disruption in the blood-brain-barrier.

Due to limited tissue availability, NeuN staining was not completed in the hippocampus and corpus callosum. However, previous studies have shown increased neuronal activity acutely after injury in the hippocampus and amygdala, (19) followed by neuronal dystrophy and apoptosis for approximately 2 weeks after injury. (4, 55, 115, 247) Our data contributes to this body of knowledge, demonstrating elevated glial responses in the neuron rich hippocampus and the neuron-free corpus callosum, but limited glial responses in the amygdala with acute loss of NeuN staining in this region. Corresponding with these cellular changes, we show a pattern of glucose uptake, T2 and ADC changes that, when taken together, indicate that these non-invasive imaging techniques are uniquely sensitive to alterations in cellular activation and dysfunction.

Our most surprising finding was evidence of a robust decrease in [^{18}F]-FDG uptake in the amygdala after injury. This structure, which is relatively distant from the injury site, showed a strong reduction in [^{18}F]-FDG uptake at 3 and 7 dpi before returning to baseline uptake levels by 10 dpi. T2 measures were elevated at this time point, accompanied by significant depression in ADC measures. Taken together, [^{18}F]-FDG and MRI demonstrate neuronal dysfunction without significant cellular activation. Research has shown that CCI results in a significant loss of interneurons in the amygdala at these same time points,(4, 247) and our NeuN data agree with these findings, suggesting marked damage to neurons resulting in loss of NeuN or alteration of NeuN staining.

Previous studies have shown that NeuN staining is lost or altered following neuronal damage. (9) Due to technical complications, it was not possible to quantify the NeuN positive cells, but qualitative analysis demonstrates that NeuN loss is associated with alterations in [¹⁸F]-FDG uptake and MRI measurements. Furthermore, acute elevation in [¹⁸F]-FDG uptake appears to predict chronic dysfunction in the amygdala as determined by histology, PET, and MRI.

The corpus callosum represents a region with altered glial responses without influence of neurons. Here we show delayed elevation in [¹⁸F]-FDG uptake in concert with variable or less robust T2 and ADC alterations. These data suggest that increased [¹⁸F]-FDG uptake is associated with glial activation, while T2 and ADC are less sensitive to these glial changes. Astrocyte and microglia labeling peaked or was markedly elevated at the same time point of increased [¹⁸F]-FDG uptake. This is similar to a 2003 study by Chen et al., demonstrating an acute increase in astrocyte response in the corpus callosum. (39) In clinical TBI, a number of studies have revealed periods of hyperglycolysis after moderate to severe TBI, particularly in regions near the injury epicenter. (19) Further, Wu et al. (275) demonstrated that white matter failed to show a reduced glucose uptake after TBI, while gray matter did show a reduction. However, to date, no study has investigated the cellular source of this hyperglycolysis after TBI. In this case, the lack of acute changes in [¹⁸F]-FDG uptake appears to indicate improved chronic outcomes as determined by histology, PET, and MRI.

The hippocampus region reflects both neuronal damage and glial activation, and exhibited a significant increase in [¹⁸F]-FDG uptake compared to baseline at the most acute, 3 hours post injury, and most chronic, 20 dpi, time points only. Studies have

shown that the hippocampus is vulnerable to CCI-mediated neuronal death, occurring as early as 24 hours post-injury and continuing for weeks after injury. (115, 142, 289) A 2003 study by Chen et al. showed very similar results to our current investigation, demonstrating an acute increase in astrocyte response in the ipsilateral hippocampus that returned to baseline levels by the conclusion of the study, despite minor differences in the injury parameters. (38) Astrocyte and microglia labeling peaked or was markedly elevated at the same time point of observed elevation of [^{18}F]-FDG uptake in this region. It is possible that neuronal death and damage and glial activation combine to mimic a baseline level of glucose uptake. However, T2 elevation and ADC depression appears to be more sensitive to neuronal response than glial response, as these measures were altered in a similar manner to the amygdala measures. Elevated T2 with reduced ADC is typically interpreted as cytotoxic edema. However, increased [^{18}F]-FDG uptake tends to denote increased cellularity and gliosis, not necessarily cytotoxic edema. In this case, T2, ADC, and FDG uptake parameters might signal an increase in cellularity rather than the traditional form of cytotoxic edema.

Altered glucose uptake patterns have been observed in a number of preclinical and clinical TBI models (for review, see (34)). More importantly, these uptake patterns are often correlated with functional impairments. We have previously shown that preclinical mild TBI, using a lateral fluid percussion model, resulted in an acute reduction in FDG uptake that slowly returned to baseline levels by 10 dpi. (226) That study previously utilized Siemens Inveon Research Workplace (Siemens Medical Solutions USA, Malvern, PA) software package with a hand-drawn ROI located in the ipsilateral cortex or subcortical tissue, including the corpus callosum, hippocampus and amygdala.

The progression to using the VivoQuant software provides the ability to utilize a template rat brain atlas, which allows for the analysis of more regions in a more concise and reproducible manner than hand-drawn ROI. It is possible that the reduced uptake observed in our initial study is similar to the reduction observed in the amygdala in the current study, demonstrating consistent alterations in glucose uptake across injury models and injury severities.

With the advent of clinical PET/MRI, there still remains and a strong need to demonstrate how the two imaging modalities can be used to increase our knowledge or provide a series of biomarkers to diagnose or follow treatment of TBI. In this study we show:

1) Based on histology, cell activation was identified in the corpus callosum and hippocampus but was limited in the amygdala. Based on NeuN staining, cell death was identified in the amygdala.

2) Based on [^{18}F]-FDG-PET alone, normalized [^{18}F]-FDG uptake provided a relatively consistent measure of cell activation or infiltration (corpus callosum) and cell dysfunction/death (amygdala) when each effect was observed in isolation. [^{18}F]-FDG-PET was sensitive to the injury but was unable to accurately reflect tissue response when the two effects (activation and dysfunction) were present simultaneously in the tissue (hippocampus).

3) Based on MRI measurements alone (T2 and ADC), cell death or cytotoxic edema was identified in all three regions. In addition, possible endothelial cell dysfunction could be identified as vasogenic edema in the corpus callosum and

hippocampus but was not detected in the amygdala. MRI was sensitive to the injury but had limited specificity for detecting the underlying pathology such as cell activation.

4) Based on the PET and MRI combined, cell activation and cell dysfunction were accurately identified in the corpus callosum and hippocampus, while cell dysfunction without cell activation was accurately identified in the amygdala.

Therefore, the combination of MRI with [¹⁸F]-FDG-PET significantly improves sensitivity to the underlying processes involved with the tissue response to TBI and. The clinical utility of acute and subacute PET/MRI should be further investigated in TBI.

ACKNOWLEDGEMENTS

This study was funded by the Department of Defense in the Center for Neuroscience and Regenerative Medicine. The opinions or assertions contained herein are the private ones of the author(s) and are not to be construed as official or reflecting the views of the DoD or the USUHS.

AUTHOR DISCLOSURE STATEMENT

No competing financial interests exist.

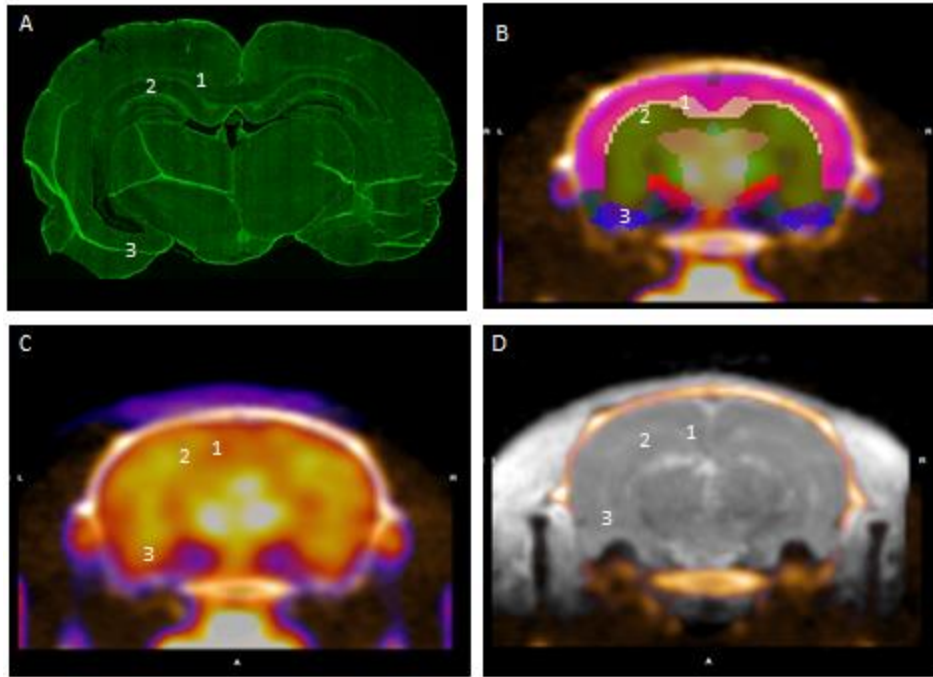


Figure 14. Location of regions of interest. Figure A depicts the regions analyzed for histology in a GFAP (green) stained section: 1) corpus callosum, 2) hippocampus, and 3) amygdala. These regions are analogous to those in the atlas produced by VivoQuant (B) for analysis of FDG-PET (C) and MRI (D) scans.

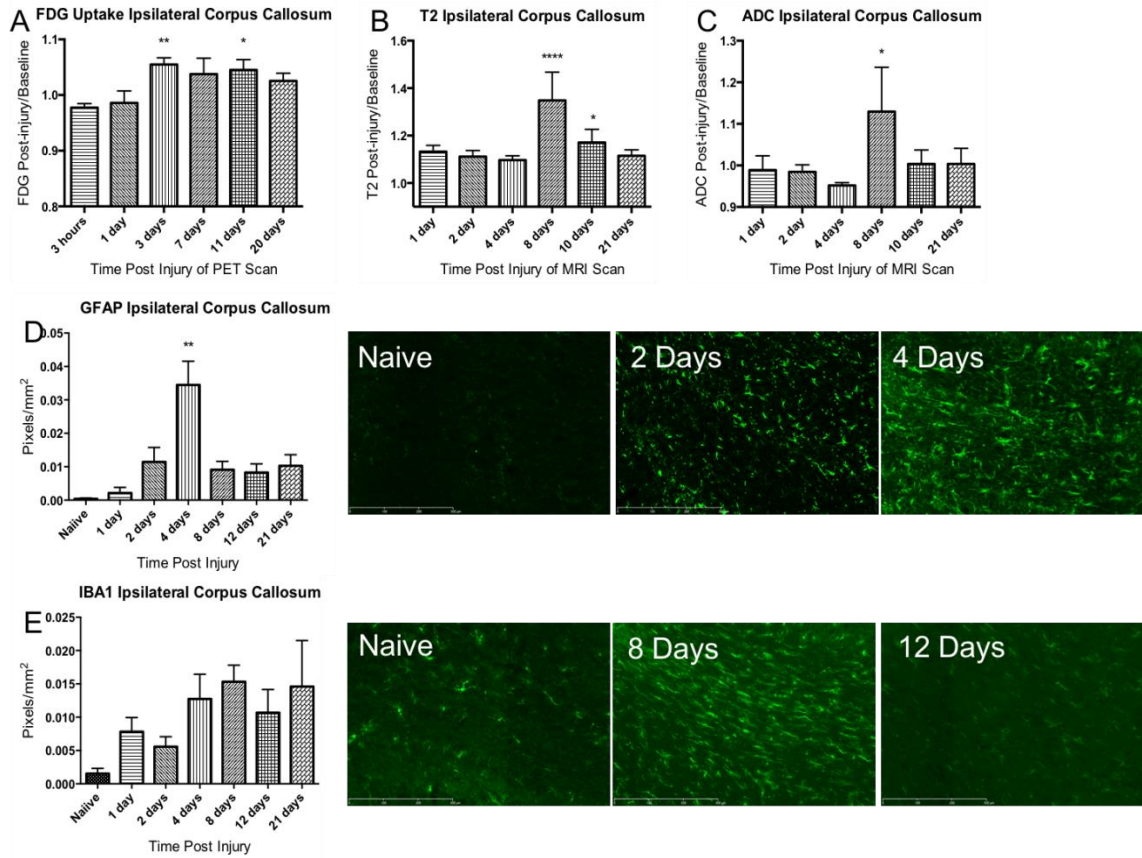


Figure 15. FDG uptake, T2, ADC values (A-C), normalized to baseline (1.0 = normal), and histology values (D-E) are presented for the ipsilateral corpus callosum. FDG uptake measurements showed a significant increase on 3 and 11 dpi (A). T2 values were elevated at days 8 and 10 in the ipsilateral corpus callosum (B). ADC values were significantly increased at 8 dpi in the corpus callosum (C). * $p < 0.05$, ** $p < 0.01$, *** $p < 0.0001$, **** $p < 0.00001$. Density of GFAP immunostaining was quantified (D), and showed a significant increase in the corpus callosum at 4 days. Representative images of astrocytes, visualized using GFAP antibody, in the corpus callosum in naïve, 2 and 4 dpi tissue. Density of Iba1 immunostaining was quantified (E) and showed no significant elevation after injury due to high variability in tissue. Representative images of microglia, visualized using Iba1 antibody, in the corpus callosum is shown in naïve and at 8 and 12 dpi. Tissue was collected 24 hours after terminal PET scan ** $p < 0.01$ vs naïve. Size bar = 300 μ m. Bars represent mean \pm SEM.

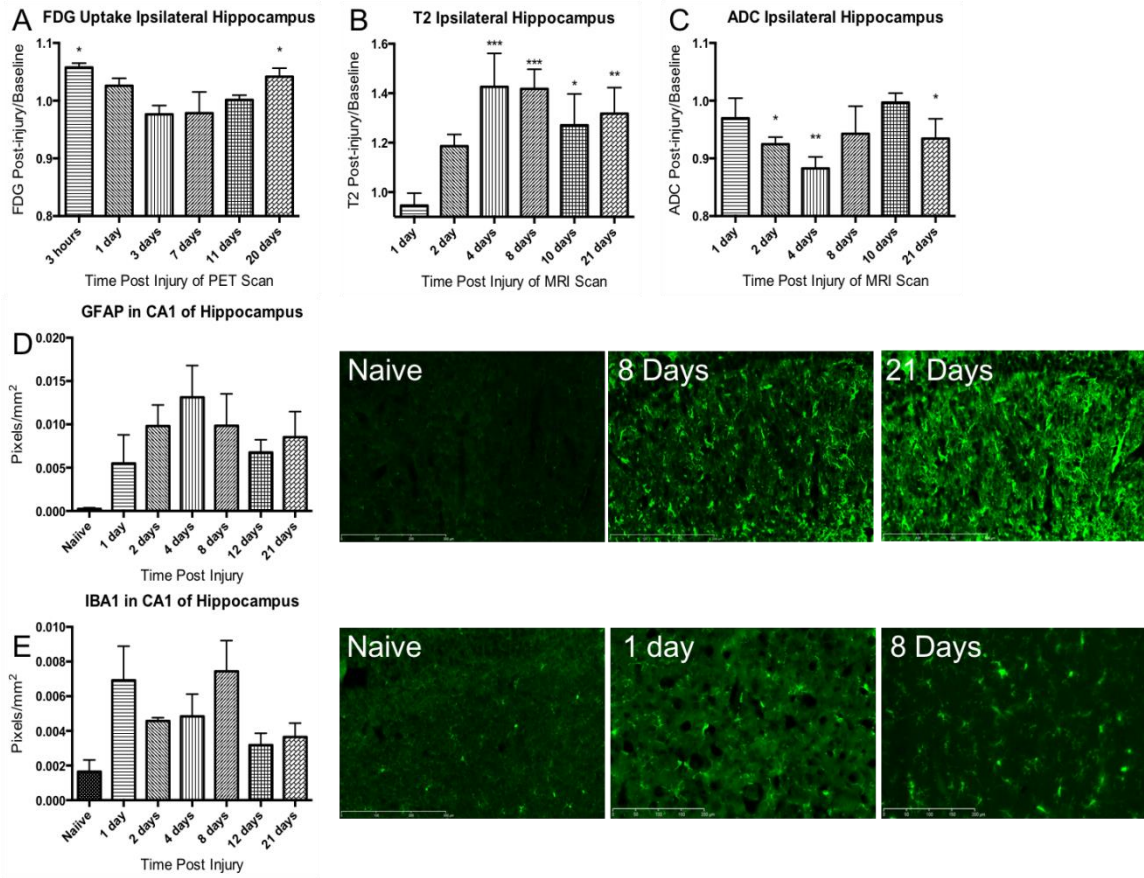


Figure 16. FDG uptake, T2, and ADC values (A-C), normalized to baseline (1.0 = normal), and histology values (D-E) in CA1 are presented for the ipsilateral hippocampus. FDG uptakes (A) were significantly increased from baseline at the acute (3 hours) and chronic stage (20 days) post injury in the ipsilateral hippocampus. In contrast, T2 values (B) were elevated at days 4, 8, 10 and 20 in ipsilateral hippocampus. ADC values (C) were significantly depressed at 2, 4 and 20 dpi in the ipsilateral hippocampus. * $p < 0.05$, ** $p < 0.01$, *** $p < 0.0001$, **** $p < 0.00001$. GFAP density was quantified and showed an overall increase in the hippocampus following CCI injury that did not reach significance (D). Representative images of astrocytes in CA1 of the hippocampus from naïve, 8 and 21 dpi tissue are shown. Microglia/macrophage activity was quantified and showed a slight but not significant increase in the hippocampus following CCI injury (E). Representative images of microglia in CA1 of the hippocampus are shown from naïve, 1 and 8 dpi tissue. Size bar = 300 μ m (D), 200 μ m (E).

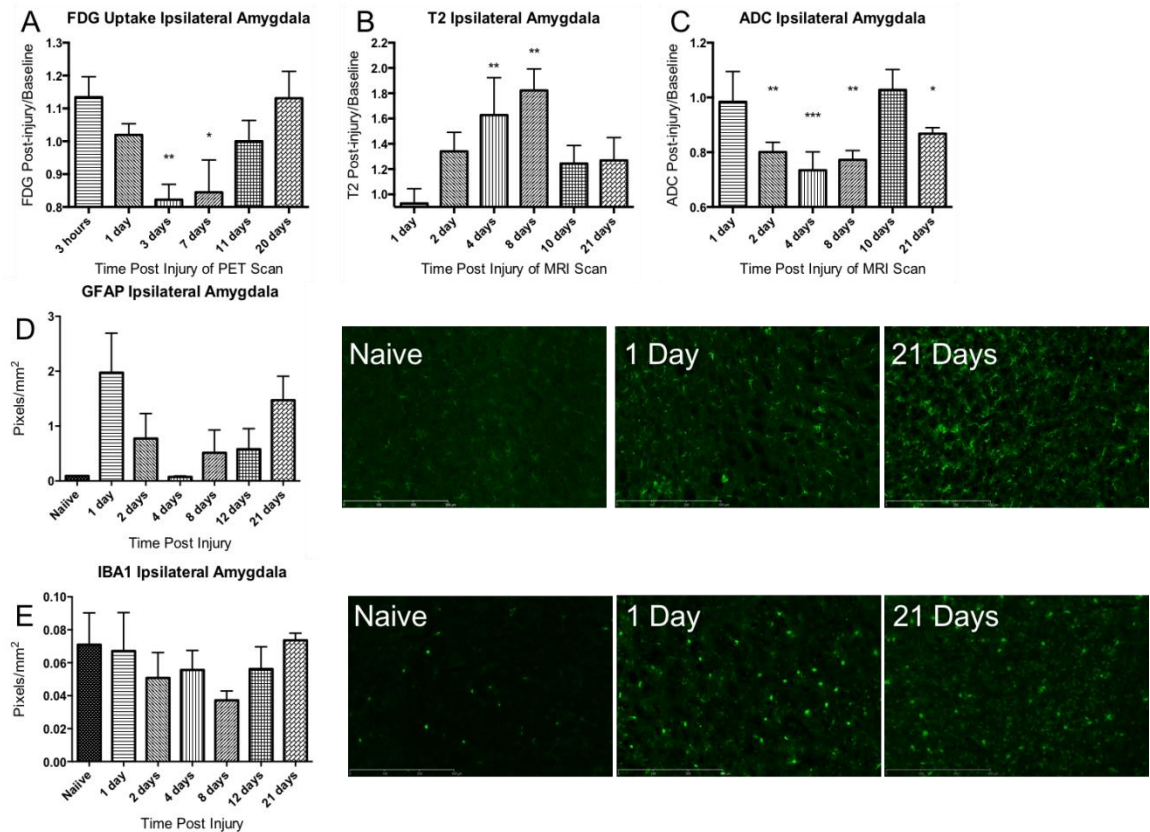


Figure 17. FDG uptake, T2, and ADC values (A-C), normalized to baseline (1.0 = normal), and histology values (D-E) are presented for the ipsilateral amygdala. FDG uptakes were significantly decreased compared to baseline at 3 and 7 dpi in the ipsilateral amygdala (A). T2 values were significantly elevated at 4 and 8 dpi (B). ADC values were significantly reduced at 2, 4, 8 and 21 dpi (C). * $p < 0.05$, ** $p < 0.01$, *** $p < 0.0001$, **** $p < 0.00001$. Density of GFAP immunostaining was quantified (D) and showed no significant change in astrocyte activity at any time point in comparison to naïve tissue. Representative images of astrocytes in the amygdala are shown for naïve, 1 and 21 dpi tissue. Iba1 immunostaining was quantified (E), and showed no significant change in microglia presence at any time point. Representative images of microglia in the amygdala are shown for naïve, 1 and 21 dpi tissue. Size bar = 300 μ m.

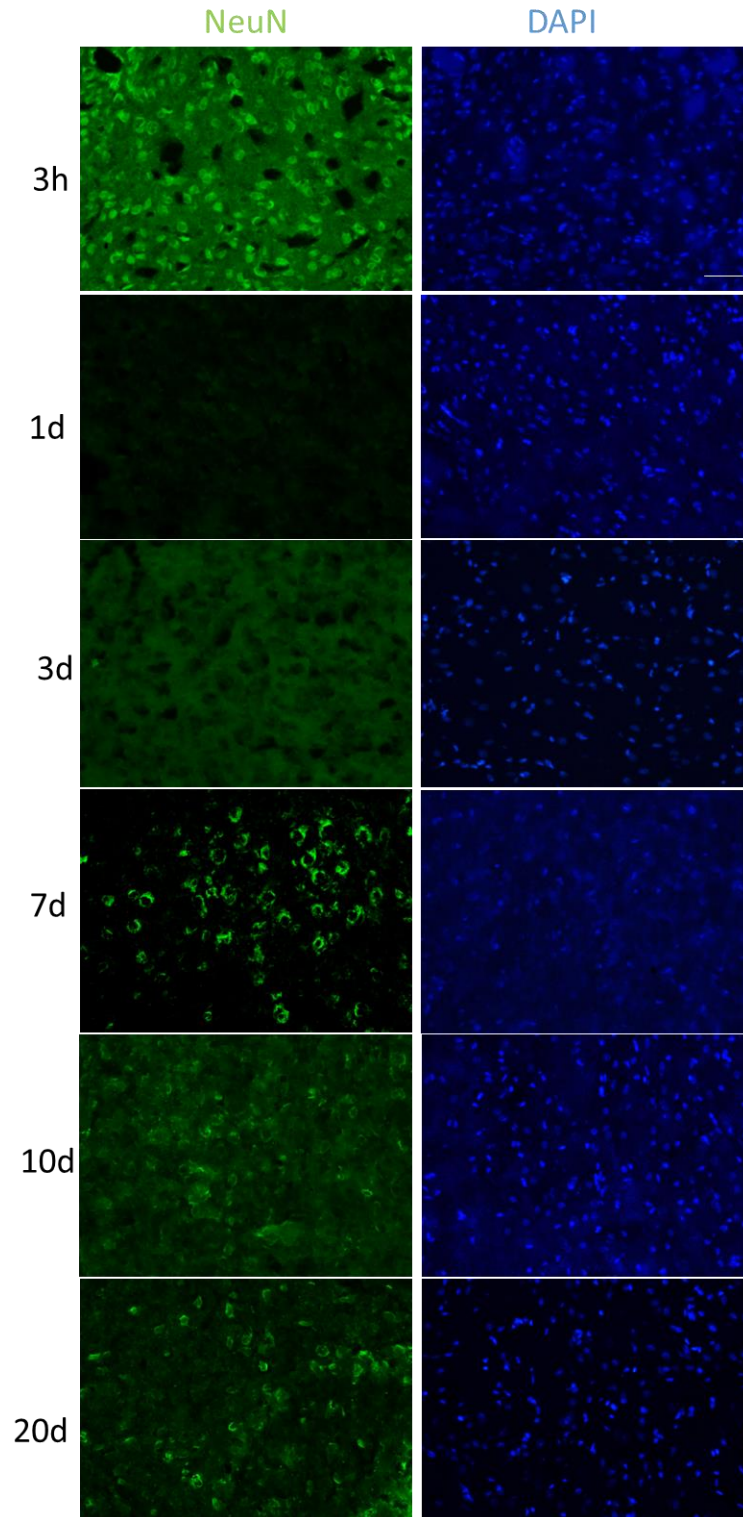
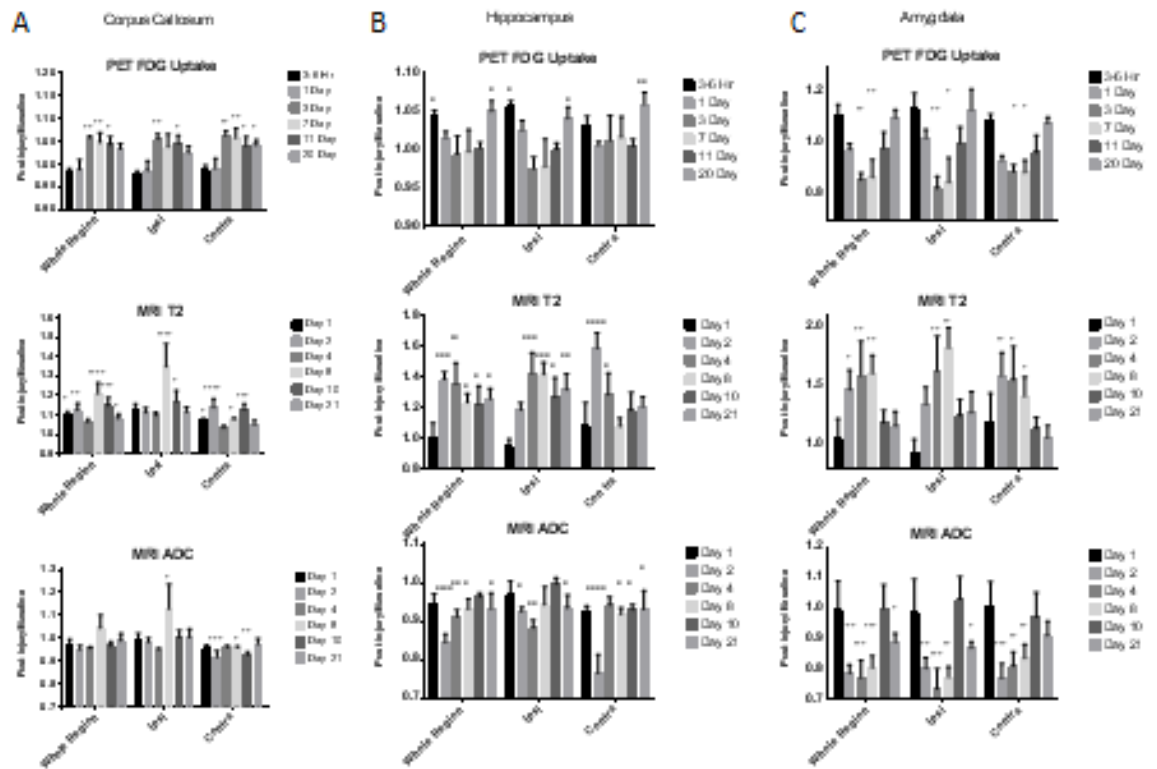


Figure 18. Representative images of neurons in the amygdala. NeuN immunolabeling was performed 24 hours after PET imaging at 1, 2, 4, 8, 12, and 21 dpi. NeuN in the amygdala is lost acutely with no change in DAPI staining at any time point but NeuN staining is partially recovered by 8 days. Bar = 50 μ m.



Supplementary Figure 19. FDG uptake, T2 and ADC values normalized to baseline values (post-injury/baseline, normal = 1.0) for the corpus callosum (A), hippocampus (B), and amygdala (C) for whole region as well as ipsilateral and contralateral regions. Statistical significance provided for two-way ANOVA without baseline normalization. * $p < 0.05$, ** $p < 0.01$, *** $p < 0.0001$, **** $p < 0.00001$.

REFERENCES

1. 2003. Report to Congress on Mild Traumatic Brain Injury in the United States: Steps to Prevent a Serious Public Health Problem. ed. NCFIPaC Centers for Disease Control and Prevention. Atlanta (GA):
2. 2011. Nonfatal traumatic brain injuries related to sports and recreation activities among persons aged ≤ 19 years--United States, 2001-2009. *MMWR Morb Mortal Wkly Rep* 60: 1337-42
3. Alexander AL, Lee JE, Lazar M, Field AS. 2007. Diffusion tensor imaging of the brain. *Neurotherapeutics* 4: 316-29
4. Almeida-Suhett CP, Prager EM, Pidoplichko V, Figueiredo TH, Marini AM, et al. 2014. Reduced GABAergic inhibition in the basolateral amygdala and the development of anxiety-like behaviors after mild traumatic brain injury. *PLoS One* 9: e102627
5. Anderova M, Kubinova S, Mazel T, Chvatal A, Eliasson C, et al. 2001. Effect of elevated K^{+} , hypotonic stress, and cortical spreading depression on astrocyte swelling in GFAP-deficient mice. *Glia* 35: 189-203
6. Annegers JF, Hauser WA, Coan SP, Rocca WA. 1998. A population-based study of seizures after traumatic brain injuries. *N Engl J Med* 338: 20-4
7. Apelt J, Mehlhorn G, Schliebs R. 1999. Insulin-sensitive GLUT4 glucose transporters are colocalized with GLUT3-expressing cells and demonstrate a chemically distinct neuron-specific localization in rat brain. *J Neurosci Res* 57: 693-705
8. Apostolatos A, Song S, Acosta S, Peart M, Watson JE, et al. 2012. Insulin promotes neuronal survival via the alternatively spliced protein kinase CdeltaII isoform. *J Biol Chem* 287: 9299-310
9. Aviles-Reyes RX, Angelo MF, Villarreal A, Rios H, Lazarowski A, Ramos AJ. 2010. Intermittent hypoxia during sleep induces reactive gliosis and limited neuronal death in rats: implications for sleep apnea. *J Neurochem* 112: 854-69
10. Baker H, Spencer RF. 1986. Transneuronal transport of peroxidase-conjugated wheat germ agglutinin (WGA-HRP) from the olfactory epithelium to the brain of the adult rat. *Exp Brain Res* 63: 461-73
11. Banerjee PN HW. 2008. Incidence and prevalence. In *Epilepsy a comprehensive textbook*, ed. LW Wilkins. Philadelphia, PA
12. Banks WA, Jaspan JB, Kastin AJ. 1997. Selective, physiological transport of insulin across the blood-brain barrier: novel demonstration by species-specific radioimmunoassays. *Peptides* 18: 1257-62

13. Barker S. 2007. Subdural and primary subarachnoid hemorrhages: a case study. *Neonatal Netw* 26: 143-51
14. Baumann CR. 2012. Traumatic brain injury and disturbed sleep and wakefulness. *Neuromolecular Med* 14: 205-12
15. Baura GD, Foster DM, Porte D, Jr., Kahn SE, Bergman RN, et al. 1993. Saturable transport of insulin from plasma into the central nervous system of dogs in vivo. A mechanism for regulated insulin delivery to the brain. *J Clin Invest* 92: 1824-30
16. Bedse G, Di Domenico F, Serviddio G, Cassano T. 2015. Aberrant insulin signaling in Alzheimer's disease: current knowledge. *Front Neurosci* 9: 204
17. Benedict C, Hallschmid M, Hatke A, Schultes B, Fehm HL, et al. 2004. Intranasal insulin improves memory in humans. *Psychoneuroendocrinology* 29: 1326-34
18. Berg JM TJ, Stryer L. 2002. Biochemistry. New York: W H Freeman
19. Bergsneider M, Hovda DA, Shalmon E, Kelly DF, Vespa PM, et al. 1997. Cerebral hyperglycolysis following severe traumatic brain injury in humans: a positron emission tomography study. *J Neurosurg* 86: 241-51
20. Bigler ED, Blatter DD, Johnson SC, Anderson CV, Russo AA, et al. 1996. Traumatic brain injury, alcohol and quantitative neuroimaging: preliminary findings. *Brain Inj* 10: 197-206
21. Bilotta F, Caramia R, Cernak I, Paoloni FP, Doronzio A, et al. 2008. Intensive insulin therapy after severe traumatic brain injury: a randomized clinical trial. *Neurocrit Care* 9: 159-66
22. Block ML, Zecca L, Hong JS. 2007. Microglia-mediated neurotoxicity: uncovering the molecular mechanisms. *Nat Rev Neurosci* 8: 57-69
23. Boche D, Perry VH, Nicoll JA. 2013. Review: activation patterns of microglia and their identification in the human brain. *Neuropathol Appl Neurobiol* 39: 3-18
24. Boje KM, Arora PK. 1992. Microglial-produced nitric oxide and reactive nitrogen oxides mediate neuronal cell death. *Brain Res* 587: 250-6
25. Born J, Lange T, Kern W, McGregor GP, Bickel U, Fehm HL. 2002. Sniffing neuropeptides: a transnasal approach to the human brain. *Nat Neurosci* 5: 514-6
26. Brandeis R, Brandys Y, Yehuda S. 1989. The use of the Morris Water Maze in the study of memory and learning. *Int J Neurosci* 48: 29-69
27. Brant AM, Jess TJ, Milligan G, Brown CM, Gould GW. 1993. Immunological analysis of glucose transporters expressed in different regions of the rat brain and central nervous system. *Biochem Biophys Res Commun* 192: 1297-302

28. Broadwell RD, Balin BJ. 1985. Endocytic and exocytic pathways of the neuronal secretory process and trans-synaptic transfer of wheat germ agglutinin-horseradish peroxidase in vivo. *J Comp Neurol* 242: 632-50
29. Brody DL, Holtzman DM. 2006. Morris water maze search strategy analysis in PDAPP mice before and after experimental traumatic brain injury. *Exp Neurol* 197: 330-40
30. Brown AM, Ransom BR. 2007. Astrocyte glycogen and brain energy metabolism. *Glia* 55: 1263-71
31. Budinich CS, Tucker LB, Lowe D, Rosenberger JG, McCabe JT. 2013. Short and long-term motor and behavioral effects of diazoxide and dimethyl sulfoxide administration in the mouse after traumatic brain injury. *Pharmacol Biochem Behav* 108: 66-73
32. Burant CF, Bell GI. 1992. Mammalian facilitative glucose transporters: evidence for similar substrate recognition sites in functionally monomeric proteins. *Biochemistry* 31: 10414-20
33. Byrnes KR, Stoica B, Loane DJ, Riccio A, Davis MI, Faden AI. 2009. Metabotropic glutamate receptor 5 activation inhibits microglial associated inflammation and neurotoxicity. *Glia* 57: 550-60
34. Byrnes KR, Wilson CM, Brabazon F, von Leden R, Jurgens JS, et al. 2014. FDG-PET imaging in mild traumatic brain injury: a critical review. *Front Neuroenergetics* 5: 13
35. Capruso DX, Levin HS. 1992. Cognitive impairment following closed head injury. *Neurol Clin* 10: 879-93
36. Carson MJ, Doose JM, Melchior B, Schmid CD, Ploix CC. 2006. CNS immune privilege: hiding in plain sight. *Immunol Rev* 213: 48-65
37. Cashion MF, Banks WA, Kastin AJ. 1996. Sequestration of centrally administered insulin by the brain: effects of starvation, aluminum, and TNF-alpha. *Horm Behav* 30: 280-6
38. Chen S, Pickard JD, Harris NG. 2003. Time course of cellular pathology after controlled cortical impact injury. *Exp Neurol* 182: 87-102
39. Chen Y, Swanson RA. 2003. Astrocytes and brain injury. *J Cereb Blood Flow Metab* 23: 137-49
40. Chen Y, Zhao Y, Dai CL, Liang Z, Run X, et al. 2014. Intranasal insulin restores insulin signaling, increases synaptic proteins, and reduces Abeta level and microglia activation in the brains of 3xTg-AD mice. *Exp Neurol* 261: 610-9

41. Chhor V, Le Charpentier T, Lebon S, Ore MV, Celador IL, et al. 2013. Characterization of phenotype markers and neuronotoxic potential of polarised primary microglia in vitro. *Brain Behav Immun* 32: 70-85
42. Chio CC, Lin MT, Chang CP. 2015. Microglial activation as a compelling target for treating acute traumatic brain injury. *Curr Med Chem* 22: 759-70
43. Chiu SL, Chen CM, Cline HT. 2008. Insulin receptor signaling regulates synapse number, dendritic plasticity, and circuit function in vivo. *Neuron* 58: 708-19
44. Chiu SL, Cline HT. 2010. Insulin receptor signaling in the development of neuronal structure and function. *Neural Dev* 5: 7
45. Claxton A, Baker LD, Hanson A, Trittschuh EH, Cholerton B, et al. 2015. Long-acting intranasal insulin detemir improves cognition for adults with mild cognitive impairment or early-stage Alzheimer's disease dementia. *J Alzheimers Dis* 44: 897-906
46. Cochran BH, Reffel AC, Stiles CD. 1983. Molecular cloning of gene sequences regulated by platelet-derived growth factor. *Cell* 33: 939-47
47. Colicos MA, Dixon CE, Dash PK. 1996. Delayed, selective neuronal death following experimental cortical impact injury in rats: possible role in memory deficits. *Brain Res* 739: 111-9
48. Conturo TE, Lori NF, Cull TS, Akbudak E, Snyder AZ, et al. 1999. Tracking neuronal fiber pathways in the living human brain. *Proc Natl Acad Sci U S A* 96: 10422-7
49. Cooney SJ, Bermudez-Sabogal SL, Byrnes KR. 2013. Cellular and temporal expression of NADPH oxidase (NOX) isotypes after brain injury. *J Neuroinflammation* 10: 155
50. Cooney SJ, Zhao Y, Byrnes KR. 2014. Characterization of the expression and inflammatory activity of NADPH oxidase after spinal cord injury. *Free Radic Res* 48: 929-39
51. Cornford EM, Hyman S, Cornford ME, Caron MJ. 1996. Glut1 glucose transporter activity in human brain injury. *J Neurotrauma* 13: 523-36
52. Craft S, Baker LD, Montine TJ, Minoshima S, Watson GS, et al. 2012. Intranasal insulin therapy for Alzheimer disease and amnesic mild cognitive impairment: a pilot clinical trial. *Arch Neurol* 69: 29-38
53. Davis M. 1997. Neurobiology of fear responses: the role of the amygdala. *J Neuropsychiatry Clin Neurosci* 9: 382-402

54. de la Monte SM. 2014. Type 3 diabetes is sporadic Alzheimers disease: mini-review. *Eur Neuropsychopharmacol* 24: 1954-60
55. Depue BE, Olson-Madden JH, Smolker HR, Rajamani M, Brenner LA, Banich MT. 2014. Reduced amygdala volume is associated with deficits in inhibitory control: a voxel- and surface-based morphometric analysis of comorbid PTSD/mild TBI. *Biomed Res Int* 2014: 691505
56. Deshmane SL, Kremlev S, Amini S, Sawaya BE. 2009. Monocyte chemoattractant protein-1 (MCP-1): an overview. *J Interferon Cytokine Res* 29: 313-26
57. Dhuria SV, Hanson LR, Frey WH, 2nd. 2010. Intranasal delivery to the central nervous system: mechanisms and experimental considerations. *J Pharm Sci* 99: 1654-73
58. Dineley KT, Jahrling JB, Denner L. 2014. Insulin resistance in Alzheimer's disease. *Neurobiol Dis* 72 Pt A: 92-103
59. Dixon CE, Clifton GL, Lighthall JW, Yaghmai AA, Hayes RL. 1991. A controlled cortical impact model of traumatic brain injury in the rat. *J Neurosci Methods* 39: 253-62
60. Dixon CE, Kochanek PM, Yan HQ, Schiding JK, Griffith RG, et al. 1999. One-year study of spatial memory performance, brain morphology, and cholinergic markers after moderate controlled cortical impact in rats. *J Neurotrauma* 16: 109-22
61. Dominik Weishaupt VDK, Borut Marincek, ed. 2008. *How does MRI work?: An Introduction to the Physics and Function of Magnetic Resonance Imaging*
62. Donnelly DJ, Gensel JC, Ankeny DP, van Rooijen N, Popovich PG. 2009. An efficient and reproducible method for quantifying macrophages in different experimental models of central nervous system pathology. *J Neurosci Methods* 181: 36-44
63. Duarte AI, Moreira PI, Oliveira CR. 2012. Insulin in central nervous system: more than just a peripheral hormone. *J Aging Res* 2012: 384017
64. Duhaime AC, Gean AD, Haacke EM, Hicks R, Wintermark M, et al. 2010. Common data elements in radiologic imaging of traumatic brain injury. *Arch Phys Med Rehabil* 91: 1661-6
65. Engelhardt JF, Sen CK, Oberley L. 2001. Redox-modulating gene therapies for human diseases. *Antioxid Redox Signal* 3: 341-6

66. Erbsloh F, Bernsmeier A, Hillesheim H. 1958. [The glucose consumption of the brain & its dependence on the liver]. *Arch Psychiatr Nervenkr Z Gesamte Neurol Psychiatr* 196: 611-26
67. Eriksson C, Van Dam AM, Lucassen PJ, Bol JG, Winblad B, Schultzberg M. 1999. Immunohistochemical localization of interleukin-1beta, interleukin-1 receptor antagonist and interleukin-1beta converting enzyme/caspase-1 in the rat brain after peripheral administration of kainic acid. *Neuroscience* 93: 915-30
68. Falkowska A, Gutowska I, Goschorska M, Nowacki P, Chlubek D, Baranowska-Bosiacka I. 2015. Energy Metabolism of the Brain, Including the Cooperation between Astrocytes and Neurons, Especially in the Context of Glycogen Metabolism. *Int J Mol Sci* 16: 25959-81
69. Faul M, Coronado V. 2015. Epidemiology of traumatic brain injury. *Handb Clin Neurol* 127: 3-13
70. Faul M XL, Wald MM, Coronado VG. 2010. Traumatic brain injury in the United States: emergency department visits, hospitalizations, and deaths. . *Atlanta (GA): Centers for Disease Control and Prevention, National Center for Injury Prevention and Control*
71. Feeney DM, Gonzalez A, Law WA. 1982. Amphetamine, haloperidol, and experience interact to affect rate of recovery after motor cortex injury. *Science* 217: 855-7
72. Finger TE, St Jeor VL, Kinnamon JC, Silver WL. 1990. Ultrastructure of substance P- and CGRP-immunoreactive nerve fibers in the nasal epithelium of rodents. *J Comp Neurol* 294: 293-305
73. Florian C, Mons N, Rouillet P. 2006. CREB antisense oligodeoxynucleotide administration into the dorsal hippocampal CA3 region impairs long- but not short-term spatial memory in mice. *Learn Mem* 13: 465-72
74. Fox GB, Fan L, LeVasseur RA, Faden AI. 1998. Effect of traumatic brain injury on mouse spatial and nonspatial learning in the Barnes circular maze. *J Neurotrauma* 15: 1037-46
75. Franco MC, Ye Y, Refakis CA, Feldman JL, Stokes AL, et al. 2013. Nitration of Hsp90 induces cell death. *Proc Natl Acad Sci U S A* 110: E1102-11
76. Frey WH, 2nd. 2013. Intranasal insulin to treat and protect against posttraumatic stress disorder. *J Nerv Ment Dis* 201: 638-9
77. Fridman EA, Beattie BJ, Broft A, Laureys S, Schiff ND. 2014. Regional cerebral metabolic patterns demonstrate the role of anterior forebrain mesocircuit dysfunction in the severely injured brain. *Proc Natl Acad Sci U S A* 111: 6473-8

78. Frolich L, Blum-Degen D, Bernstein HG, Engelsberger S, Humrich J, et al. 1998. Brain insulin and insulin receptors in aging and sporadic Alzheimer's disease. *J Neural Transm (Vienna)* 105: 423-38
79. Frolich L, Blum-Degen D, Riederer P, Hoyer S. 1999. A disturbance in the neuronal insulin receptor signal transduction in sporadic Alzheimer's disease. *Ann N Y Acad Sci* 893: 290-3
80. Gallagher M, Burwell R, Burchinal M. 2015. Severity of spatial learning impairment in aging: Development of a learning index for performance in the Morris water maze. *Behav Neurosci* 129: 540-8
81. Ganguly A, Devaskar SU. 2008. Glucose transporter isoform-3-null heterozygous mutation causes sexually dimorphic adiposity with insulin resistance. *Am J Physiol Endocrinol Metab* 294: E1144-51
82. Gehring TV, Luksys G, Sandi C, Vasilaki E. 2015. Detailed classification of swimming paths in the Morris Water Maze: multiple strategies within one trial. *Sci Rep* 5: 14562
83. Giza CC, Hovda DA. 2001. The Neurometabolic Cascade of Concussion. *J Athl Train* 36: 228-35
84. Giza CC, Hovda DA. 2014. The new neurometabolic cascade of concussion. *Neurosurgery* 75 Suppl 4: S24-33
85. Goldman D, Song X, Kitai R, Casadevall A, Zhao ML, Lee SC. 2001. *Cryptococcus neoformans* induces macrophage inflammatory protein 1alpha (MIP-1alpha) and MIP-1beta in human microglia: role of specific antibody and soluble capsular polysaccharide. *Infect Immun* 69: 1808-15
86. Goodman JC, Cherian L, Bryan RM, Jr., Robertson CS. 1994. Lateral cortical impact injury in rats: pathologic effects of varying cortical compression and impact velocity. *J Neurotrauma* 11: 587-97
87. Gordon S, Taylor PR. 2005. Monocyte and macrophage heterogeneity. *Nat Rev Immunol* 5: 953-64
88. Gross H, Kling A, Henry G, Herndon C, Lavretsky H. 1996. Local cerebral glucose metabolism in patients with long-term behavioral and cognitive deficits following mild traumatic brain injury. *J Neuropsychiatry Clin Neurosci* 8: 324-34
89. Guan J, Zhu Z, Zhao RC, Xiao Z, Wu C, et al. 2013. Transplantation of human mesenchymal stem cells loaded on collagen scaffolds for the treatment of traumatic brain injury in rats. *Biomaterials* 34: 5937-46

90. Hagelthorn KM, Brown WS, Amano S, Asarnow R. 2000. Normal development of bilateral field advantage and evoked potential interhemispheric transmission time. *Dev Neuropsychol* 18: 11-31
91. Hallschmid M, Benedict C, Schultes B, Fehm HL, Born J, Kern W. 2004. Intranasal insulin reduces body fat in men but not in women. *Diabetes* 53: 3024-9
92. Hamlin GP, Cernak I, Wixey JA, Vink R. 2001. Increased expression of neuronal glucose transporter 3 but not glial glucose transporter 1 following severe diffuse traumatic brain injury in rats. *J Neurotrauma* 18: 1011-8
93. Hamm RJ, Dixon CE, Gbadebo DM, Singha AK, Jenkins LW, et al. 1992. Cognitive deficits following traumatic brain injury produced by controlled cortical impact. *J Neurotrauma* 9: 11-20
94. Hanson LR, Frey WH, 2nd. 2008. Intranasal delivery bypasses the blood-brain barrier to target therapeutic agents to the central nervous system and treat neurodegenerative disease. *BMC Neurosci* 9 Suppl 3: S5
95. Harkins JM, Moustaid-Moussa N, Chung YJ, Penner KM, Pestka JJ, et al. 2004. Expression of interleukin-6 is greater in preadipocytes than in adipocytes of 3T3-L1 cells and C57BL/6J and ob/ob mice. *J Nutr* 134: 2673-7
96. Hauser WA, Annegers JF, Kurland LT. 1993. Incidence of epilepsy and unprovoked seizures in Rochester, Minnesota: 1935-1984. *Epilepsia* 34: 453-68
97. Havrankova J, Roth J, Brownstein M. 1978. Insulin receptors are widely distributed in the central nervous system of the rat. *Nature* 272: 827-9
98. Heni M, Hennige AM, Peter A, Siegel-Axel D, Ordelheide AM, et al. 2011. Insulin promotes glycogen storage and cell proliferation in primary human astrocytes. *PLoS One* 6: e21594
99. Heni M, Wagner R, Kullmann S, Veit R, Mat Husin H, et al. 2014. Central insulin administration improves whole-body insulin sensitivity via hypothalamus and parasympathetic outputs in men. *Diabetes* 63: 4083-8
100. Henn A, Lund S, Hedtjarn M, Schrattenholz A, Porzgen P, Leist M. 2009. The suitability of BV2 cells as alternative model system for primary microglia cultures or for animal experiments examining brain inflammation. *ALTEX* 26: 83-94
101. Hergan K, Schaefer PW, Sorensen AG, Gonzalez RG, Huisman TA. 2002. Diffusion-weighted MRI in diffuse axonal injury of the brain. *Eur Radiol* 12: 2536-41
102. Hinojosa AE, Garcia-Bueno B, Leza JC, Madrigal JL. 2011. CCL2/MCP-1 modulation of microglial activation and proliferation. *J Neuroinflammation* 8: 77

103. Hoekman JD, Ho RJ. 2011. Enhanced analgesic responses after preferential delivery of morphine and fentanyl to the olfactory epithelium in rats. *Anesth Analg* 113: 641-51
104. Hong EG, Ko HJ, Cho YR, Kim HJ, Ma Z, et al. 2009. Interleukin-10 prevents diet-induced insulin resistance by attenuating macrophage and cytokine response in skeletal muscle. *Diabetes* 58: 2525-35
105. Hopkins DF, Williams G. 1997. Insulin receptors are widely distributed in human brain and bind human and porcine insulin with equal affinity. *Diabet Med* 14: 1044-50
106. Hoskison MM, Moore AN, Hu B, Orsi S, Kobori N, Dash PK. 2009. Persistent working memory dysfunction following traumatic brain injury: evidence for a time-dependent mechanism. *Neuroscience* 159: 483-91
107. Hoyer S. 2004. Glucose metabolism and insulin receptor signal transduction in Alzheimer disease. *Eur J Pharmacol* 490: 115-25
108. Hoyt DB, Holcomb J, Abraham E, Atkins J, Sopko G. 2004. Working Group on Trauma Research Program summary report: National Heart Lung Blood Institute (NHLBI), National Institute of General Medical Sciences (NIGMS), and National Institute of Neurological Disorders and Stroke (NINDS) of the National Institutes of Health (NIH), and the Department of Defense (DOD). *J Trauma* 57: 410-5
109. Huang CC, Lee CC, Hsu KS. 2004. An investigation into signal transduction mechanisms involved in insulin-induced long-term depression in the CA1 region of the hippocampus. *J Neurochem* 89: 217-31
110. Humphreys I, Wood RL, Phillips CJ, Macey S. 2013. The costs of traumatic brain injury: a literature review. *Clinicoecon Outcomes Res* 5: 281-7
111. Jagoda AS. 2010. Mild traumatic brain injury: key decisions in acute management. *Psychiatr Clin North Am* 33: 797-806
112. James DE, Brown R, Navarro J, Pilch PF. 1988. Insulin-regulatable tissues express a unique insulin-sensitive glucose transport protein. *Nature* 333: 183-5
113. Janus C. 2004. Search strategies used by APP transgenic mice during navigation in the Morris water maze. *Learn Mem* 11: 337-46
114. Jauch-Chara K, Friedrich A, Rezmer M, Melchert UH, H GS-E, et al. 2012. Intranasal insulin suppresses food intake via enhancement of brain energy levels in humans. *Diabetes* 61: 2261-8
115. Kabadi SV, Stoica BA, Loane DJ, Byrnes KR, Hanscom M, et al. 2012. Cyclin D1 gene ablation confers neuroprotection in traumatic brain injury. *J Neurotrauma* 29: 813-27

116. Kanda H, Tateya S, Tamori Y, Kotani K, Hiasa K, et al. 2006. MCP-1 contributes to macrophage infiltration into adipose tissue, insulin resistance, and hepatic steatosis in obesity. *J Clin Invest* 116: 1494-505
117. Karelina K, Sarac B, Freeman LM, Gaier KR, Weil ZM. 2016. Traumatic Brain Injury and Obesity Induce Persistent Central Insulin Resistance. *Eur J Neurosci*
118. Kline AE, Massucci JL, Dixon CE, Zafonte RD, Bolinger BD. 2004. The therapeutic efficacy conferred by the 5-HT(1A) receptor agonist 8-Hydroxy-2-(di-n-propylamino)tetralin (8-OH-DPAT) after experimental traumatic brain injury is not mediated by concomitant hypothermia. *J Neurotrauma* 21: 175-85
119. Kotapka MJ, Graham DI, Adams JH, Gennarelli TA. 1992. Hippocampal pathology in fatal non-missile human head injury. *Acta Neuropathol* 83: 530-4
120. Kreutzberg GW. 1996. Microglia: a sensor for pathological events in the CNS. *Trends Neurosci* 19: 312-8
121. Kumar A, Alvarez-Croda DM, Stoica BA, Faden AI, Loane DJ. 2015. Microglial/Macrophage Polarization Dynamics following Traumatic Brain Injury. *J Neurotrauma*
122. Kumar A, Chen SH, Kadiiska MB, Hong JS, Zielonka J, et al. 2014. Inducible nitric oxide synthase is key to peroxynitrite-mediated, LPS-induced protein radical formation in murine microglial BV2 cells. *Free Radic Biol Med* 73: 51-9
123. Kurland D, Hong C, Aarabi B, Gerzanich V, Simard JM. 2012. Hemorrhagic progression of a contusion after traumatic brain injury: a review. *J Neurotrauma* 29: 19-31
124. Lazarov O, Hollands C. 2016. Hippocampal neurogenesis: Learning to remember. *Prog Neurobiol*
125. Lee B, Newberg A. 2005. Neuroimaging in traumatic brain imaging. *NeuroRx* 2: 372-83
126. Leino RL, Gerhart DZ, van Bueren AM, McCall AL, Drewes LR. 1997. Ultrastructural localization of GLUT 1 and GLUT 3 glucose transporters in rat brain. *J Neurosci Res* 49: 617-26
127. LeMay DR, Gehua L, Zelenock GB, D'Alecy LG. 1988. Insulin administration protects neurologic function in cerebral ischemia in rats. *Stroke* 19: 1411-9
128. Leo P, McCrea M. 2016. Epidemiology.
129. Lescot T, Fulla-Oller L, Po C, Chen XR, Puybasset L, et al. 2010. Temporal and regional changes after focal traumatic brain injury. *J Neurotrauma* 27: 85-94

130. Levin BE, Dunn-Meynell AA, Routh VH. 2001. Brain glucosensing and the K(ATP) channel. *Nat Neurosci* 4: 459-60
131. Ley EJ, Srour MK, Clond MA, Barnajian M, Tillou A, et al. 2011. Diabetic patients with traumatic brain injury: insulin deficiency is associated with increased mortality. *J Trauma* 70: 1141-4
132. Li H, Liu B, Huang J, Chen H, Guo X, Yuan Z. 2013. Insulin inhibits lipopolysaccharide-induced nitric oxide synthase expression in rat primary astrocytes. *Brain Res* 1506: 1-11
133. Li J, Gu L, Feng DF, Ding F, Zhu G, Rong J. 2012. Exploring temporospatial changes in glucose metabolic disorder, learning, and memory dysfunction in a rat model of diffuse axonal injury. *J Neurotrauma* 29: 2635-46
134. Li L, Zuo Z. 2009. Isoflurane preconditioning improves short-term and long-term neurological outcome after focal brain ischemia in adult rats. *Neuroscience* 164: 497-506
135. Li W, Long JA, Watts LT, Jiang Z, Shen Q, et al. 2014. A quantitative MRI method for imaging blood-brain barrier leakage in experimental traumatic brain injury. *PLoS One* 9: e114173
136. Li Y, Rinne JO, Mosconi L, Pirraglia E, Rusinek H, et al. 2008. Regional analysis of FDG and PIB-PET images in normal aging, mild cognitive impairment, and Alzheimer's disease. *Eur J Nucl Med Mol Imaging* 35: 2169-81
137. Li YH, Wang JB, Li MH, Li WB, Wang D. 2012. Quantification of brain edema and hemorrhage by MRI after experimental traumatic brain injury in rabbits predicts subsequent functional outcome. *Neurol Sci* 33: 731-40
138. Licinio J, Prolo P, McCann SM, Wong ML. 1999. Brain iNOS: current understanding and clinical implications. *Mol Med Today* 5: 225-32
139. Lighthall JW. 1988. Controlled cortical impact: a new experimental brain injury model. *J Neurotrauma* 5: 1-15
140. Loane DJ, Byrnes KR. 2010. Role of microglia in neurotrauma. *Neurotherapeutics* 7: 366-77
141. Loane DJ, Kumar A. 2016. Microglia in the TBI brain: The good, the bad, and the dysregulated. *Exp Neurol* 275 Pt 3: 316-27
142. Loane DJ, Kumar A, Stoica BA, Cabatbat R, Faden AI. 2014. Progressive neurodegeneration after experimental brain trauma: association with chronic microglial activation. *J Neuropathol Exp Neurol* 73: 14-29

143. Lochhead JJ, Thorne RG. 2012. Intranasal delivery of biologics to the central nervous system. *Adv Drug Deliv Rev* 64: 614-28
144. Lochhead JJ, Wolak DJ, Pizzo ME, Thorne RG. 2015. Rapid transport within cerebral perivascular spaces underlies widespread tracer distribution in the brain after intranasal administration. *J Cereb Blood Flow Metab* 35: 371-81
145. Lu D, Qu C, Goussev A, Jiang H, Lu C, et al. 2007. Statins increase neurogenesis in the dentate gyrus, reduce delayed neuronal death in the hippocampal CA3 region, and improve spatial learning in rat after traumatic brain injury. *J Neurotrauma* 24: 1132-46
146. Lumeng CN, Bodzin JL, Saltiel AR. 2007. Obesity induces a phenotypic switch in adipose tissue macrophage polarization. *J Clin Invest* 117: 175-84
147. Maas AI, Stocchetti N, Bullock R. 2008. Moderate and severe traumatic brain injury in adults. *Lancet Neurol* 7: 728-41
148. Maher F, Vannucci SJ, Simpson IA. 1994. Glucose transporter proteins in brain. *FASEB J* 8: 1003-11
149. Mahler B, Carlsson S, Andersson T, Adelow C, Ahlbom A, Tomson T. 2015. Unprovoked seizures after traumatic brain injury: A population-based case-control study. *Epilepsia* 56: 1438-44
150. Maimaiti S, Anderson KL, DeMoll C, Brewer LD, Rauh BA, et al. 2016. Intranasal Insulin Improves Age-Related Cognitive Deficits and Reverses Electrophysiological Correlates of Brain Aging. *J Gerontol A Biol Sci Med Sci* 71: 30-9
151. Man HY, Lin JW, Ju WH, Ahmadian G, Liu L, et al. 2000. Regulation of AMPA receptor-mediated synaptic transmission by clathrin-dependent receptor internalization. *Neuron* 25: 649-62
152. Mantych GJ, James DE, Chung HD, Devaskar SU. 1992. Cellular localization and characterization of Glut 3 glucose transporter isoform in human brain. *Endocrinology* 131: 1270-8
153. Marin-Teva JL, Cuadros MA, Martin-Oliva D, Navascues J. 2011. Microglia and neuronal cell death. *Neuron Glia Biol* 7: 25-40
154. Marks JL, Porte D, Jr., Stahl WL, Baskin DG. 1990. Localization of insulin receptor mRNA in rat brain by in situ hybridization. *Endocrinology* 127: 3234-6
155. Mathias JL, Alvaro PK. 2012. Prevalence of sleep disturbances, disorders, and problems following traumatic brain injury: a meta-analysis. *Sleep Med* 13: 898-905

156. McAllister TW, Sparling MB, Flashman LA, Guerin SJ, Mamourian AC, Saykin AJ. 2001. Differential working memory load effects after mild traumatic brain injury. *Neuroimage* 14: 1004-12
157. McEwen BS, Reagan LP. 2004. Glucose transporter expression in the central nervous system: relationship to synaptic function. *Eur J Pharmacol* 490: 13-24
158. McGregor K, Pentland B. 1997. Head injury rehabilitation in the U.K.: an economic perspective. *Soc Sci Med* 45: 295-303
159. McKee AC, Daneshvar DH. 2015. The neuropathology of traumatic brain injury. *Handb Clin Neurol* 127: 45-66
160. McNett M. 2007. A review of the predictive ability of Glasgow Coma Scale scores in head-injured patients. *J Neurosci Nurs* 39: 68-75
161. Meaney DF, Ross DT, Winkelstein BA, Brasko J, Goldstein D, et al. 1994. Modification of the cortical impact model to produce axonal injury in the rat cerebral cortex. *J Neurotrauma* 11: 599-612
162. Mergenthaler P, Lindauer U, Dienel GA, Meisel A. 2013. Sugar for the brain: the role of glucose in physiological and pathological brain function. *Trends Neurosci* 36: 587-97
163. Mill JF, Chao MV, Ishii DN. 1985. Insulin, insulin-like growth factor II, and nerve growth factor effects on tubulin mRNA levels and neurite formation. *Proc Natl Acad Sci U S A* 82: 7126-30
164. Moen KG, Skandsen T, Folvik M, Brezova V, Kvistad KA, et al. 2012. A longitudinal MRI study of traumatic axonal injury in patients with moderate and severe traumatic brain injury. *J Neurol Neurosurg Psychiatry* 83: 1193-200
165. Moloney AM, Griffin RJ, Timmons S, O'Connor R, Ravid R, O'Neill C. 2010. Defects in IGF-1 receptor, insulin receptor and IRS-1/2 in Alzheimer's disease indicate possible resistance to IGF-1 and insulin signalling. *Neurobiol Aging* 31: 224-43
166. Morgello S, Uson RR, Schwartz EJ, Haber RS. 1995. The human blood-brain barrier glucose transporter (GLUT1) is a glucose transporter of gray matter astrocytes. *Glia* 14: 43-54
167. Morris JK, Burns JM. 2012. Insulin: an emerging treatment for Alzheimer's disease dementia? *Curr Neurol Neurosci Rep* 12: 520-7
168. Morris R. 1984. Developments of a water-maze procedure for studying spatial learning in the rat. *J Neurosci Methods* 11: 47-60

169. Mosconi L. 2005. Brain glucose metabolism in the early and specific diagnosis of Alzheimer's disease. FDG-PET studies in MCI and AD. *Eur J Nucl Med Mol Imaging* 32: 486-510
170. Mowery NT, Gunter OL, Guillaumondegui O, Dossett LA, Dortch MJ, et al. 2009. Stress insulin resistance is a marker for mortality in traumatic brain injury. *J Trauma* 66: 145-51; discussion 51-3
171. Muhic M, Vardjan N, Chowdhury HH, Zorec R, Kreft M. 2015. Insulin and Insulin-like Growth Factor 1 (IGF-1) Modulate Cytoplasmic Glucose and Glycogen Levels but Not Glucose Transport across the Membrane in Astrocytes. *J Biol Chem* 290: 11167-76
172. Myer DJ, Gurkoff GG, Lee SM, Hovda DA, Sofroniew MV. 2006. Essential protective roles of reactive astrocytes in traumatic brain injury. *Brain* 129: 2761-72
173. Nakamura Y, Si QS, Kataoka K. 1999. Lipopolysaccharide-induced microglial activation in culture: temporal profiles of morphological change and release of cytokines and nitric oxide. *Neurosci Res* 35: 95-100
174. Nakashima T, Nakayama N, Miwa K, Okumura A, Soeda A, Iwama T. 2007. Focal brain glucose hypometabolism in patients with neuropsychologic deficits after diffuse axonal injury. *AJNR Am J Neuroradiol* 28: 236-42
175. Narayan RK, Michel ME, Ansell B, Baethmann A, Biegon A, et al. 2002. Clinical trials in head injury. *J Neurotrauma* 19: 503-57
176. Nathan C, Xie QW. 1994. Nitric oxide synthases: roles, tolls, and controls. *Cell* 78: 915-8
177. Newcomb JK, Zhao X, Pike BR, Hayes RL. 1999. Temporal profile of apoptotic-like changes in neurons and astrocytes following controlled cortical impact injury in the rat. *Exp Neurol* 158: 76-88
178. Newcombe V, Chatfield D, Outtrim J, Vowler S, Manktelow A, et al. 2011. Mapping traumatic axonal injury using diffusion tensor imaging: correlations with functional outcome. *PLoS One* 6: e19214
179. Nichols JN, Deshane AS, Niedzielko TL, Smith CD, Floyd CL. 2016. Greater neurobehavioral deficits occur in adult mice after repeated, as compared to single, mild traumatic brain injury (mTBI). *Behav Brain Res* 298: 111-24
180. Nimmerjahn A, Kirchhoff F, Helmchen F. 2005. Resting microglial cells are highly dynamic surveillants of brain parenchyma in vivo. *Science* 308: 1314-8
181. O'Connell MT, Seal A, Nortje J, Al-Rawi PG, Coles JP, et al. 2005. Glucose metabolism in traumatic brain injury: a combined microdialysis and [18F]-2-

- fluoro-2-deoxy-D-glucose-positron emission tomography (FDG-PET) study. *Acta Neurochir Suppl* 95: 165-8
182. Odegaard JI, Ricardo-Gonzalez RR, Goforth MH, Morel CR, Subramanian V, et al. 2007. Macrophage-specific PPARgamma controls alternative activation and improves insulin resistance. *Nature* 447: 1116-20
 183. Oertel M, Kelly DF, McArthur D, Boscardin WJ, Glenn TC, et al. 2002. Progressive hemorrhage after head trauma: predictors and consequences of the evolving injury. *J Neurosurg* 96: 109-16
 184. Oldendorf WH. 1971. Brain uptake of radiolabeled amino acids, amines, and hexoses after arterial injection. *Am J Physiol* 221: 1629-39
 185. Olefsky JM, Glass CK. 2010. Macrophages, inflammation, and insulin resistance. *Annu Rev Physiol* 72: 219-46
 186. Onyszchuk G, Al-Hafez B, He YY, Bilgen M, Berman NE, Brooks WM. 2007. A mouse model of sensorimotor controlled cortical impact: characterization using longitudinal magnetic resonance imaging, behavioral assessments and histology. *J Neurosci Methods* 160: 187-96
 187. Orihuela R, McPherson CA, Harry GJ. 2015. Microglial M1/M2 polarization and metabolic states. *Br J Pharmacol*
 188. Osier ND, Korpon JR, Dixon CE. 2015. Controlled Cortical Impact Model.
 189. Ott V, Lehnert H, Staub J, Wonne K, Born J, Hallschmid M. 2015. Central nervous insulin administration does not potentiate the acute glucoregulatory impact of concurrent mild hyperinsulinemia. *Diabetes* 64: 760-5
 190. Palacios EM, Sala-Llonch R, Junque C, Roig T, Tormos JM, et al. 2013. Resting-state functional magnetic resonance imaging activity and connectivity and cognitive outcome in traumatic brain injury. *JAMA Neurol* 70: 845-51
 191. Pang Y, Lin S, Wright C, Shen J, Carter K, et al. 2016. Intranasal insulin protects against substantia nigra dopaminergic neuronal loss and alleviates motor deficits induced by 6-OHDA in rats. *Neuroscience* 318: 157-65
 192. Pardridge WM, Boado RJ, Farrell CR. 1990. Brain-type glucose transporter (GLUT-1) is selectively localized to the blood-brain barrier. Studies with quantitative western blotting and in situ hybridization. *J Biol Chem* 265: 18035-40
 193. Park SJ, Hur JW, Kwon KY, Rhee JJ, Lee JW, Lee HK. 2009. Time to recover consciousness in patients with diffuse axonal injury : assessment with reference to magnetic resonance grading. *J Korean Neurosurg Soc* 46: 205-9

194. Parwaresch MR, Wacker HH. 1984. Origin and kinetics of resident tissue macrophages. Parabiosis studies with radiolabelled leucocytes. *Cell Tissue Kinet* 17: 25-39
195. Payne J, Maher F, Simpson I, Mattice L, Davies P. 1997. Glucose transporter Glut 5 expression in microglial cells. *Glia* 21: 327-31
196. Pekny M, Nilsson M. 2005. Astrocyte activation and reactive gliosis. *Glia* 50: 427-34
197. Perel P, Arango M, Clayton T, Edwards P, Komolafe E, et al. 2008. Predicting outcome after traumatic brain injury: practical prognostic models based on large cohort of international patients. *BMJ* 336: 425-9
198. Peters A, Schweiger U, Pellerin L, Hubold C, Oltmanns KM, et al. 2004. The selfish brain: competition for energy resources. *Neurosci Biobehav Rev* 28: 143-80
199. Peterson TC, Maass WR, Anderson JR, Anderson GD, Hoane MR. 2015. A behavioral and histological comparison of fluid percussion injury and controlled cortical impact injury to the rat sensorimotor cortex. *Behav Brain Res* 294: 254-63
200. Plum L, Schubert M, Bruning JC. 2005. The role of insulin receptor signaling in the brain. *Trends Endocrinol Metab* 16: 59-65
201. Polito A, Brouland JP, Porcher R, Sonnevile R, Siami S, et al. 2011. Hyperglycaemia and apoptosis of microglial cells in human septic shock. *Crit Care* 15: R131
202. Prins ML, Alexander D, Giza CC, Hovda DA. 2013. Repeated mild traumatic brain injury: mechanisms of cerebral vulnerability. *J Neurotrauma* 30: 30-8
203. Radi R. 2004. Nitric oxide, oxidants, and protein tyrosine nitration. *Proc Natl Acad Sci U S A* 101: 4003-8
204. Radi R, Beckman JS, Bush KM, Freeman BA. 1991. Peroxynitrite oxidation of sulfhydryls. The cytotoxic potential of superoxide and nitric oxide. *J Biol Chem* 266: 4244-50
205. Rangel-Castilla L, Gopinath S, Robertson CS. 2008. Management of intracranial hypertension. *Neurol Clin* 26: 521-41, x
206. Rassovsky Y, Levi Y, Agranov E, Sela-Kaufman M, Sverdlik A, Vakil E. 2015. Predicting long-term outcome following traumatic brain injury (TBI). *J Clin Exp Neuropsychol* 37: 354-66

207. Reger MA, Watson GS, Green PS, Baker LD, Cholerton B, et al. 2008. Intranasal insulin administration dose-dependently modulates verbal memory and plasma amyloid-beta in memory-impaired older adults. *J Alzheimers Dis* 13: 323-31
208. Reivich M, Kuhl D, Wolf A, Greenberg J, Phelps M, et al. 1979. The [18F]fluorodeoxyglucose method for the measurement of local cerebral glucose utilization in man. *Circ Res* 44: 127-37
209. Renner DB, Svitak AL, Gallus NJ, Ericson ME, Frey WH, 2nd, Hanson LR. 2012. Intranasal delivery of insulin via the olfactory nerve pathway. *J Pharm Pharmacol* 64: 1709-14
210. Roe C, Sveen U, Alvsaker K, Bautz-Holter E. 2009. Post-concussion symptoms after mild traumatic brain injury: influence of demographic factors and injury severity in a 1-year cohort study. *Disabil Rehabil* 31: 1235-43
211. Ruff RM, Iverson GL, Barth JT, Bush SS, Broshek DK. 2009. Recommendations for diagnosing a mild traumatic brain injury: a National Academy of Neuropsychology education paper. *Arch Clin Neuropsychol* 24: 3-10
212. Runge JW. 1993. The cost of injury. *Emerg Med Clin North Am* 11: 241-53
213. Rutland-Brown W, Langlois JA, Thomas KE, Xi YL. 2006. Incidence of traumatic brain injury in the United States, 2003. *J Head Trauma Rehabil* 21: 544-8
214. Ryu BR, Ko HW, Jou I, Noh JS, Gwag BJ. 1999. Phosphatidylinositol 3-kinase-mediated regulation of neuronal apoptosis and necrosis by insulin and IGF-I. *J Neurobiol* 39: 536-46
215. Saatman KE, Duhaime AC, Bullock R, Maas AI, Valadka A, Manley GT. 2008. Classification of traumatic brain injury for targeted therapies. *J Neurotrauma* 25: 719-38
216. Schechter R, Sadiq HF, Devaskar SU. 1990. Insulin and insulin mRNA are detected in neuronal cell cultures maintained in an insulin-free/serum-free medium. *J Histochem Cytochem* 38: 829-36
217. Schechter R, Whitmire J, Wheet GS, Beju D, Jackson KW, et al. 1994. Immunohistochemical and in situ hybridization study of an insulin-like substance in fetal neuron cell cultures. *Brain Res* 636: 9-27
218. Scheff SW, Baldwin SA, Brown RW, Kraemer PJ. 1997. Morris water maze deficits in rats following traumatic brain injury: lateral controlled cortical impact. *J Neurotrauma* 14: 615-27

219. Schilling M, Strecker JK, Schabitz WR, Ringelstein EB, Kiefer R. 2009. Effects of monocyte chemoattractant protein 1 on blood-borne cell recruitment after transient focal cerebral ischemia in mice. *Neuroscience* 161: 806-12
220. Schneider CA, Rasband WS, Eliceiri KW. 2012. NIH Image to ImageJ: 25 years of image analysis. *Nat Methods* 9: 671-5
221. Schulingkamp RJ, Pagano TC, Hung D, Raffa RB. 2000. Insulin receptors and insulin action in the brain: review and clinical implications. *Neurosci Biobehav Rev* 24: 855-72
222. Scoville WB, Milner B. 1957. Loss of recent memory after bilateral hippocampal lesions. *J Neurol Neurosurg Psychiatry* 20: 11-21
223. Selassie AW, Zaloshnja E, Langlois JA, Miller T, Jones P, Steiner C. 2008. Incidence of long-term disability following traumatic brain injury hospitalization, United States, 2003. *J Head Trauma Rehabil* 23: 123-31
224. Selhorst JB, Gudeman SK, Butterworth JFt, Harbison JW, Miller JD, Becker DP. 1985. Papilledema after acute head injury. *Neurosurgery* 16: 357-63
225. Selkoe DJ. 1989. Amyloid beta protein precursor and the pathogenesis of Alzheimer's disease. *Cell* 58: 611-2
226. Selwyn R, Hockenbury N, Jaiswal S, Mathur S, Armstrong RC, Byrnes KR. 2013. Mild traumatic brain injury results in depressed cerebral glucose uptake: An (18)FDG PET study. *J Neurotrauma* 30: 1943-53
227. Selwyn RG, Cooney SJ, Khayrullina G, Hockenbury N, Wilson CM, et al. 2016. Outcome after Repetitive Mild Traumatic Brain Injury Is Temporally Related to Glucose Uptake Profile at Time of Second Injury. *J Neurotrauma*
228. Shah K, Desilva S, Abbruscato T. 2012. The role of glucose transporters in brain disease: diabetes and Alzheimer's Disease. *Int J Mol Sci* 13: 12629-55
229. Shiga T, Ikoma K, Katoh C, Ioyama H, Matsuyama T, et al. 2006. Loss of neuronal integrity: a cause of hypometabolism in patients with traumatic brain injury without MRI abnormality in the chronic stage. *Eur J Nucl Med Mol Imaging* 33: 817-22
230. Simpson IA, Cushman SW. 1986. Hormonal regulation of mammalian glucose transport. *Annu Rev Biochem* 55: 1059-89
231. Smith DH, Chen XH, Pierce JE, Wolf JA, Trojanowski JQ, et al. 1997. Progressive atrophy and neuron death for one year following brain trauma in the rat. *J Neurotrauma* 14: 715-27

232. Smith DH, Lowenstein DH, Gennarelli TA, McIntosh TK. 1994. Persistent memory dysfunction is associated with bilateral hippocampal damage following experimental brain injury. *Neurosci Lett* 168: 151-4
233. Smith DH, Okiyama K, Thomas MJ, Claussen B, McIntosh TK. 1991. Evaluation of memory dysfunction following experimental brain injury using the Morris water maze. *J Neurotrauma* 8: 259-69
234. Song J, Li P, Chaudhary N, Gemmete JJ, Thompson BG, et al. 2015. Correlating Cerebral (18)FDG PET-CT Patterns with Histological Analysis During Early Brain Injury in a Rat Subarachnoid Hemorrhage Model. *Transl Stroke Res* 6: 290-5
235. Spielman LJ, Bahniwal M, Little JP, Walker DG, Klegeris A. 2015. Insulin Modulates In Vitro Secretion of Cytokines and Cytotoxins by Human Glial Cells. *Curr Alzheimer Res* 12: 684-93
236. Stein M, Keshav S, Harris N, Gordon S. 1992. Interleukin 4 potently enhances murine macrophage mannose receptor activity: a marker of alternative immunologic macrophage activation. *J Exp Med* 176: 287-92
237. Stephens JM, Lee J, Pilch PF. 1997. Tumor necrosis factor-alpha-induced insulin resistance in 3T3-L1 adipocytes is accompanied by a loss of insulin receptor substrate-1 and GLUT4 expression without a loss of insulin receptor-mediated signal transduction. *J Biol Chem* 272: 971-6
238. Stevens RB, Sutherland DE, Ansite JD, Saxena M, Rossini TJ, et al. 1997. Insulin down-regulates the inducible nitric oxide synthase pathway: nitric oxide as cause and effect of diabetes? *J Immunol* 159: 5329-35
239. Streit WJ, Walter SA, Pennell NA. 1999. Reactive microgliosis. *Prog Neurobiol* 57: 563-81
240. Sullivan KA, Edmed SL, Allan AC, Karlsson LJ, Smith SS. 2015. Characterizing self-reported sleep disturbance after mild traumatic brain injury. *J Neurotrauma* 32: 474-86
241. Sun M, Deng B, Zhao X, Gao C, Yang L, et al. 2015. Isoflurane preconditioning provides neuroprotection against stroke by regulating the expression of the TLR4 signalling pathway to alleviate microglial activation. *Sci Rep* 5: 11445
242. Szymusiak R, McGinty D. 2008. Hypothalamic regulation of sleep and arousal. *Ann N Y Acad Sci* 1129: 275-86
243. Tajiri Y, Mimura K, Umeda F. 2005. High-sensitivity C-reactive protein in Japanese patients with type 2 diabetes. *Obes Res* 13: 1810-6

244. Takemori K, Ito H, Suzuki T. 2000. Effects of inducible nitric oxide synthase inhibition on cerebral edema in severe hypertension. *Acta Neurochir Suppl* 76: 335-8
245. Tanaka M, Sawada M, Yoshida S, Hanaoka F, Marunouchi T. 1995. Insulin prevents apoptosis of external granular layer neurons in rat cerebellar slice cultures. *Neurosci Lett* 199: 37-40
246. Tanev KS, Pentel KZ, Kredlow MA, Charney ME. 2014. PTSD and TBI comorbidity: scope, clinical presentation and treatment options. *Brain Inj* 28: 261-70
247. Taylor AN, Tio DL, Sutton RL. 2013. Restoration of neuroendocrine stress response by glucocorticoid receptor or GABA(A) receptor antagonists after experimental traumatic brain injury. *J Neurotrauma* 30: 1250-6
248. Teasdale G, Jennett B. 1974. Assessment of coma and impaired consciousness. A practical scale. *Lancet* 2: 81-4
249. Terzioglu B, Ekinici O, Berkman Z. 2015. Hyperglycemia is a predictor of prognosis in traumatic brain injury: Tertiary intensive care unit study. *J Res Med Sci* 20: 1166-71
250. Thorne RG, Emory CR, Ala TA, Frey WH, 2nd. 1995. Quantitative analysis of the olfactory pathway for drug delivery to the brain. *Brain Res* 692: 278-82
251. Thorne RG, Frey WH, 2nd. 2001. Delivery of neurotrophic factors to the central nervous system: pharmacokinetic considerations. *Clin Pharmacokinet* 40: 907-46
252. Thorne RG, Pronk GJ, Padmanabhan V, Frey WH, 2nd. 2004. Delivery of insulin-like growth factor-I to the rat brain and spinal cord along olfactory and trigeminal pathways following intranasal administration. *Neuroscience* 127: 481-96
253. Tremblay ME, Stevens B, Sierra A, Wake H, Bessis A, Nimmerjahn A. 2011. The role of microglia in the healthy brain. *J Neurosci* 31: 16064-9
254. Uehara Y, Nipper V, McCall AL. 1997. Chronic insulin hypoglycemia induces GLUT-3 protein in rat brain neurons. *Am J Physiol* 272: E716-9
255. Uemura E, Greenlee HW. 2006. Insulin regulates neuronal glucose uptake by promoting translocation of glucose transporter GLUT3. *Exp Neurol* 198: 48-53
256. Unger J, McNeill TH, Moxley RT, 3rd, White M, Moss A, Livingston JN. 1989. Distribution of insulin receptor-like immunoreactivity in the rat forebrain. *Neuroscience* 31: 143-57
257. Vakil E. 2005. The effect of moderate to severe traumatic brain injury (TBI) on different aspects of memory: a selective review. *J Clin Exp Neuropsychol* 27: 977-1021

258. van den Berghe G, Wouters P, Weekers F, Verwaest C, Bruyninckx F, et al. 2001. Intensive insulin therapy in critically ill patients. *N Engl J Med* 345: 1359-67
259. van der Heide LP, Ramakers GM, Smidt MP. 2006. Insulin signaling in the central nervous system: learning to survive. *Prog Neurobiol* 79: 205-21
260. van der Horn HJ, Spikman JM, Jacobs B, van der Naalt J. 2013. Postconcussive complaints, anxiety, and depression related to vocational outcome in minor to severe traumatic brain injury. *Arch Phys Med Rehabil* 94: 867-74
261. Vannucci SJ, Koehler-Stec EM, Li K, Reynolds TH, Clark R, Simpson IA. 1998. GLUT4 glucose transporter expression in rodent brain: effect of diabetes. *Brain Res* 797: 1-11
262. Vannucci SJ, Maher F, Simpson IA. 1997. Glucose transporter proteins in brain: delivery of glucose to neurons and glia. *Glia* 21: 2-21
263. Vespa P, Bergsneider M, Hattori N, Wu HM, Huang SC, et al. 2005. Metabolic crisis without brain ischemia is common after traumatic brain injury: a combined microdialysis and positron emission tomography study. *J Cereb Blood Flow Metab* 25: 763-74
264. Vik A, Nag T, Fredriksli OA, Skandsen T, Moen KG, et al. 2008. Relationship of "dose" of intracranial hypertension to outcome in severe traumatic brain injury. *J Neurosurg* 109: 678-84
265. Vorhees CV, Williams MT. 2006. Morris water maze: procedures for assessing spatial and related forms of learning and memory. *Nat Protoc* 1: 848-58
266. Wang D, Pascual JM, Yang H, Engelstad K, Mao X, et al. 2006. A mouse model for Glut-1 haploinsufficiency. *Hum Mol Genet* 15: 1169-79
267. Watson GS, Craft S. 2003. The role of insulin resistance in the pathogenesis of Alzheimer's disease: implications for treatment. *CNS Drugs* 17: 27-45
268. Weisberg SP, McCann D, Desai M, Rosenbaum M, Leibel RL, Ferrante AW, Jr. 2003. Obesity is associated with macrophage accumulation in adipose tissue. *J Clin Invest* 112: 1796-808
269. Weiss JM, Downie SA, Lyman WD, Berman JW. 1998. Astrocyte-derived monocyte-chemoattractant protein-1 directs the transmigration of leukocytes across a model of the human blood-brain barrier. *J Immunol* 161: 6896-903
270. Werner C, Engelhard K. 2007. Pathophysiology of traumatic brain injury. *Br J Anaesth* 99: 4-9
271. Whiting MD, Baranova AI, Hamm RJ. 2006. Cognitive Impairment following Traumatic Brain Injury.

272. Whiting MD, Hamm RJ. 2008. Mechanisms of anterograde and retrograde memory impairment following experimental traumatic brain injury. *Brain Res* 1213: 69-77
273. Wilde EA, Hunter, Bigler ED. 2012. Pediatric traumatic brain injury: neuroimaging and neurorehabilitation outcome. *NeuroRehabilitation* 31: 245-60
274. Wink DA, Kasprzak KS, Maragos CM, Elespuru RK, Misra M, et al. 1991. DNA deaminating ability and genotoxicity of nitric oxide and its progenitors. *Science* 254: 1001-3
275. Wu HM, Huang SC, Hattori N, Glenn TC, Vespa PM, et al. 2004. Subcortical white matter metabolic changes remote from focal hemorrhagic lesions suggest diffuse injury after human traumatic brain injury. *Neurosurgery* 55: 1306-15; discussio 16-7
276. Wu Z, Li S, Lei J, An D, Haacke EM. 2010. Evaluation of traumatic subarachnoid hemorrhage using susceptibility-weighted imaging. *AJNR Am J Neuroradiol* 31: 1302-10
277. Xiong KL, Zhu YS, Zhang WG. 2014. Diffusion tensor imaging and magnetic resonance spectroscopy in traumatic brain injury: a review of recent literature. *Brain Imaging Behav* 8: 487-96
278. Xu H, Barnes GT, Yang Q, Tan G, Yang D, et al. 2003. Chronic inflammation in fat plays a crucial role in the development of obesity-related insulin resistance. *J Clin Invest* 112: 1821-30
279. Yang M, Guo Q, Zhang X, Sun S, Wang Y, et al. 2009. Intensive insulin therapy on infection rate, days in NICU, in-hospital mortality and neurological outcome in severe traumatic brain injury patients: a randomized controlled trial. *Int J Nurs Stud* 46: 753-8
280. Yang Y, Ma D, Wang Y, Jiang T, Hu S, et al. 2013. Intranasal insulin ameliorates tau hyperphosphorylation in a rat model of type 2 diabetes. *J Alzheimers Dis* 33: 329-38
281. Yang Z, Wang J, Yu Y, Li Z. 2016. Gene silencing of MCP-1 prevents microglial activation and inflammatory injury after intracerebral hemorrhage. *Int Immunopharmacol* 33: 18-23
282. Yealy DM, Hogan DE. 1991. Imaging after head trauma. Who needs what? *Emerg Med Clin North Am* 9: 707-17
283. Yoshino A, Hovda DA, Kawamata T, Katayama Y, Becker DP. 1991. Dynamic changes in local cerebral glucose utilization following cerebral conclusion in rats: evidence of a hyper- and subsequent hypometabolic state. *Brain Res* 561: 106-19

284. Young B, Ott L, Dempsey R, Haack D, Tibbs P. 1989. Relationship between admission hyperglycemia and neurologic outcome of severely brain-injured patients. *Ann Surg* 210: 466-72; discussion 72-3
285. Yu S. 2006. Review of F-FDG Synthesis and Quality Control. *Biomed Imaging Interv J* 2: e57
286. Zafar SN, Iqbal A, Farez MF, Kamatkar S, de Moya MA. 2011. Intensive insulin therapy in brain injury: a meta-analysis. *J Neurotrauma* 28: 1307-17
287. Zemva J, Schubert M. 2014. The role of neuronal insulin/insulin-like growth factor-1 signaling for the pathogenesis of Alzheimer's disease: possible therapeutic implications. *CNS Neurol Disord Drug Targets* 13: 322-37
288. Zhao W, Chen H, Xu H, Moore E, Meiri N, et al. 1999. Brain insulin receptors and spatial memory. Correlated changes in gene expression, tyrosine phosphorylation, and signaling molecules in the hippocampus of water maze trained rats. *J Biol Chem* 274: 34893-902
289. Zhou H, Chen L, Gao X, Luo B, Chen J. 2012. Moderate traumatic brain injury triggers rapid necrotic death of immature neurons in the hippocampus. *J Neuropathol Exp Neurol* 71: 348-59